Identification of decisive molecular interactions regulating resistance to apoptosis in tumour cells

A thesis submitted to the National University of Ireland in fulfilment of the requirement for the degree of

Doctor of Philosophy

By

Paul John Lawson O' Reilly

BSc. (Hons)

Discipline of Biochemistry, School of Natural Sciences, National University of Ireland, Galway

Thesis supervisor: Dr Eva Szegezdi

July 1st 2014

Table of Contents

Declaration of work....4
Acknowledgements....5
Abbreviations....6
Chapter 1: General Introduction....11
1.1 Cancer....12
1.2 Signal Transduction of Cell Death....13
1.2.1 Apoptosis....14
1.2.2 Anoikis....18
1.2.3 Mitotic catastrophe....18
1.2.4 Pyroptosis....18
1.2.5 Paraptosis....19
1.2.6 Necrotic-like Cell Death....19
1.2.7 Autophagic Cell Death....21
1.2.8 Necrosis....22
1.3 TRAIL....23
1.3.1 The Physiological Role of TRAIL....26
1.3.2 TRAIL-induced Apoptosis....28
1.3.3 Ion Channels and Apoptosis....33
1.3.4 TRAIL Resistance....36
1.3.5 TRAIL Induced Pro-survival Signalling....43
1.3.6 Future prospects for TRAIL....49
1.4 Machine learning techniques....52
1.4.1 Supervised machine learning....53
1.4.2 Unsupervised machine learning....57
1.5 Aims and Objectives....59
1.6 Summary of Contents....60
Chapter 2: Correlation between Potassium Channel Expression and Sensitivity to Drug-induced Cell Death in Tumour Cell Lines....62
Abstract....63
2.1 Introduction....64
2.2 Materials and Methods....68
2.3 Results....73
2.4 Discussion....84

2.5 Future perspectives 87
Chapter 3: Co-acting gene matrices predict TRAIL responsiveness of tumour cells with high accuracy 88
Abstract 89
3.1 Introduction 90
3.2 Materials and Methods 93
3.3 Results 95
3.4 Discussion 103
3.5 Future perspectives 107
Chapter 4: Crosstalk between the death inducing signalling complex and mitochondria is the major determinant of TRAIL-mediated apoptosis 108
Abstract 109
4.1 Introduction 110
4.2 Materials and Methods 112
4.3 Results 123
4.4 Discussion 152
4.5 Future perspectives 155
Chapter 5: General Discussion 156
Bibliography 162

Declaration of work

The work presented in Chapter 1 was a collaborative project with the group of Dr. Ildiko Szabo (Leanza et al, 2014). The specifics of my contribution are outlined below

Figure 1: I downloaded the raw DNA microarray data files from the NIH cell-miner database and carried out background correction/normalization. I generated the graphs seen in figure 1A. The correlation analysis seen in figure 1B was carried out by Anne Doyle and me.

Figure 3: I determined the effects of staurosporine on cell survival using MTT and Annexin V (Fig. 3A and Fig. 3C). In addition the correlation analysis seen in figure 3B and figure 3D were carried out by Anne Doyle and me.

Figure 4: Anne Doyle and I carried out the correlation analysis seen in figure 4B and figure 4D

Figure 5: I quantified the expression levels of the Bcl-2 family proteins and XIAP using Western blotting following by densitometry. Correlation analysis was carried out by Anne Doyle and me.

All of the work presented in chapter 2 and 3 are my own.

Acknowledgements

This thesis would not be possible without the guidance and support of my supervisor Dr. Eva Szegezdi. For her numerous hours of work and dedication I am forever grateful. I would be remiss to not thank the members of the TRAIL group; Anna, Tamas, Mairead (NEDD) and Grainne for their support, regular tea breaks and more importantly for their friendship. To Tamas and Grainne especially I extend my sincere appreciation for all their help along the way.

I would like to say a big thank you to Dr. Enda O' Connell, Dr. Alessandro Natoni, Aoife O' Reilly, Dr. Chris Linehan and Prof. Cathal Seoige for their help and instruction.

I would like to acknowledge science foundation Ireland (SFI) who funded my PhD.

I have an amazing, close, loud and loving family. To my Grandfather, aunts, uncles, cousins and brothers thank you for a loving home. I want to wish my mama Sandra a happy 70th birthday, you as much as anyone previous listed deserve recognition for being generally awesome.

Finally I would like to express my love for my mother Paula and my girlfriend Fiona the two women who have inspired me to pursue my dreams and aspirations both past and present.

Abbreviations

3-MA	3-methyladenine
4-AP	4-Aminopyridine
AICD	Activation induced cell death
ALL	Acute lymphoblastic leukaemia
AML	Acute myeloid leukaemia
ANT	Adenine nucleotide translocator
APAF-1	Apoptotic protease activating factor-1
APC	Adenomatous polyposis coli
ASM	Acid sphingomyelinase
AUC	Area under the receiver operator curve
AVD	Apoptosis volume decrease
Bad	Bcl-2 antagonist of cell death
Bak	Bcl-2 antagonist killer
Bax	Bcl-2 associated X protein
Bcl-2	B-cell lymphoma-2
Bcl-XL	B-cell lymphoma extra large
BCR	B-cell receptor
BH	Bcl-2 homology
BID	BH3-interacting death domain agonist
BIM	Bcl2-interacting mediator of cell death
BIR	Baculovirus inhibitor of apoptosis protein repeat
CARD	Caspase activation and recruitment domain
CARP1	Caspases-8 and -10-associated RING finger protein 1
CART	Classification and regression tree

Caspase	Cysteine aspartate specific proteases
CDKI	Cyclin dependent kinase inhibitor
c-FLIP	Cellular FLICE like inhibitory protein
CI	Combination index
c-IAP-1/-2	Cellular inhibitor of apoptosis proteins-1/-2
CisPL	Cisplatin
CLL	Chronic lymphoblastic leukaemia
CLZM	Clofazimine
CRD	Cysteine rich domain
CRM	C2-ceramide
CrmA	cytokine response modifier A
DcR1	Decoy receptor 1
DcR2	Decoy receptor 2
DD	Death domain
DED	Death effector domain
DISC	Death inducing signalling complex
Dox	Doxycycline
DR3	Death receptor 3
DR4	Death receptor 4
DR5	Death receptor 5
DR6	Death receptor 6
EDAR	Ectodysplasin-A receptor
EGFR	Epithelial growth factor receptor
ERK	Extracellular-signal-regulated kinase
ETOP	Etoposide
FADD	Fas associated death domain
FOX	Forkhead box

GALNT14	Polypeptide N-acetylgalactosaminyltransferase 14
GI	Gini importance
GPI	Glycosylphosphatidylinositol
HDAC	Histone deacetylase
HER-2	Human epithelial receptor-2
IAP	Inhibitor of apoptosis proteins
IBM	IAP-binding motif
IFN-α	Interferon alpha
IFN-β	Interferon beta
IFN-γ	Interferon gamma
IKK	Inhibitor of kappa kinase
IL-12	Interleukin-12
IL-2	Interleukin-2
JNK	c-Jun N-terminal kinase
Kv	Potassium voltage-gated channel
LPS	Lipopolysaccharide
LT	Lymphotoxin
MAPK	Mitogen-activated protein kinase
Mcl-1	Induced myeloid leukaemia cell differentiation protein Mcl-1
MDR	Multi-drug resistance
MEF	Mouse embryonic fibroblast
MLKL	Mixed lineage kinase domain-like protein
MMR	Miss-match repair
MOMP	Mitochondrial outer membrane permeabilization
MS	Multiple sclerosis
mtKV	Potassium voltage-gated channel in mitochondria

MTT	2-(4, 5-dimethyltriazol-2-yl)-2, 5-diphenyl tetrazolium bromide
NEMO	NF-kappa-B essential modulator
NF-κB	Nuclear factor kappa-light-chain-enhancer of activated B cells
NOD	Non-obese diabetic
Noxa	Phorbol-12-myristate-13-acetate-induced protein 1
NSCLC	Non-small cell lung cancer
OMM	Outer mitochondrial membrane
OPG	Osteoprotegerin
$p75^{NTR}$	Low affinity nerve growth factor receptor
PAMP	Pathogen associated molecular pattern
PIDD	p53-induced protein with death domain
PKB/AKT	Protein kinase B
PLAD	Pre-ligand assembly domain
PRR	Pattern recognition receptor
PTP	Permeability transition pores
Puma	p53 up-regulated modulator of apoptosis
QQQ	Triple quadruple mass spectrometer
QTOF	Quadruple-time of flight mass spectrometer
RAIDD	receptor-interacting protein (RIP)-associated ICH-1/CED-3 homologous protein with a death domain
RGC	Rat retinal ganglion cells
RING	Really interesting new gene
RIP1	Receptor interacting protein kinase 1
RIP3	Receptor interacting protein kinase 3
ROS	Reactive oxygen species
QTOF-MS	Quadruple-time of flight mass spectrometry

SCLC	Small cell lung cancer
Smac/Diablo	Second mitochondria-derived activator of caspases
SRM	Selective reaction monitoring
STS	Staurosporine
tBID	Truncated BH3-interacting death domain agonist
TEA	Tetraethylammonium
Tet-ON	Tetracycline inducible system
TL1A	TNF-like protein A1
TLR	Toll like receptor
TNF	Tumour necrosis factor
TNFR1	Tumour necrosis factor receptor 1
TNFRSF	TNF receptor super family
TPP	Trans protein pipeline
TRADD	Tumour necrosis factor receptor type 1-associated DEATH domain protein
TRAF-2	TNF receptor-associated factor-2
TRAIL	Tumour necrosis factor related apoptosis inducing ligand
TWEAK	TNF related weak inducer of apoptosis
UBA	Ubiquitin associated domain
VDAC	Voltage-dependent anion-selective channel protein
XIAP	X-linked inhibitor of apoptosis proteins

Chapter 1: General Introduction

1.1 Cancer

Cancer is a group of diseases in which mutated/aberrant cells divide in an uncontrolled fashion and are capable of invading other tissues via the blood or lymphatic system. In a seminal publication 14 years ago Weinberg and colleagues outlined the six common characteristics shared by all cancers of which more than 100 types are known. The hallmarks of cancerous cells which distinguish them from normal tissue are; self-sufficiency in growth signals, reduced sensitivity to growth suppressors, evasion of apoptosis, sustained angiogenesis, metastatic potential and limitless reproductive potential. In light of the advances made in cancer research since then the list has been expanded to include two more characteristics which are; deregulated cellular energetics and avoidance of immune destruction (Hanahan & Weinberg, 2011).

In regards to anticancer therapy consideration must be given to the risk-benefit of treatment and expected quality of life. The conventional chemotherapeutic drugs and exposure to radiation preferentially target and kill rapidly dividing cells but not solely cancerous cells. Rapidly dividing normal cells such as bone marrow cells, hair follicles and the cells lining the intestinal lumen also die. This leads to the numerous noxious side effects associated with chemotherapy/radiation treatments. Examples of such toxicity include nausea, hair loss, anaemia, bone marrow toxicity, impaired wound healing, damage to the gastrointestinal epithelium and sterility. Advances in the genetic and molecular characterization of cancers have enhanced our capabilities to develop novel therapies which target a particular tumour driving protein or gene associated with cancer causation or progression. These drugs are expected to have much lower toxicity due to their higher specificity against cancer cells. One of the first of a bevy of targeted regimes, Trastuzumab, specifically and drastically improves breast cancer patient survival in cohorts overexpressing the human epithelial receptor-2 (HER-2). Other such therapies include epidermal growth factor receptor (EGFR) inhibitors (gefitinib), tyrosine kinase inhibitor (imatinib mesylate) and the inhibitor of BRAF (vemurafenib).

The aberrant molecules these drugs target drive cell survival and proliferation. Tumour cells are often addicted to these pro-survival pathways and their inhibition is either sufficient in itself to kill tumour cells or to sensitize tumour cells to other cytotoxic agents. This would allow the use of the conventional chemotherapeutics at a much lower concentration thus reducing toxicity.

Therefore research which delineates the regulation of cell death signal transduction pathways and how these pathways are intertwined with cell cycle regulation, metabolism, cellular stress etc. are essential for both the development of therapeutics with low toxicity and for the identification of which treatment is the most effective against a given tumour.

1.2 Signal Transduction of Cell Death

Cell death has been reportedly observed as early as 1841. For an extended period it was thought to be a passive process (Glucksmann, 1951). This notion was rebuked when studies of silkworms and tadpoles showed cell death occurred at particular moments during development. This suggests that the cell death process may in fact be an active and regulated process (Lockshin & Williams, 1965; Tata, 1966). Cells that die during development exhibit a distinct ultrastructure. Cells displaying these unique morphological changes were termed apoptotic. Apoptosis may be defined as a programmed process of self-destruction. Physiologically apoptosis eliminates damaged, diseased, superfluous or unwanted cells (removal of self-recognising immune cells). Defects in apoptosis can lead to cancer, neurodegenerative disease and immune-deficiency (Li & Yuan, 2008; Thompson, 1995; Yuan & Yankner, 2000). In addition to apoptosis other forms of regulated cell death have been described. Therefore the manner in which a cell dies can be classified into subtypes depending on morphological changes, enzymatic requirements and whether or not the process is immunogenic. These subtypes are regulated (apoptosis, necrotic-like cell death, autophagic cell death, mitotic catastrophe, paraptosis and pyroptosis) and accidental (necrosis) cell death.

1.2.1 Apoptosis

In 1972 Kerr and colleagues described a morphologically distinct form of cell death which they termed apoptosis. During apoptosis cells underwent shrinkage, nuclear condensation and fragmentation, membrane blebbing and loss of adhesion to neighbouring cells as well as the surrounding substrata. Ultimately the cells break up into membrane bound vesicles known as apoptotic bodies (Wyllie et al, 1980). The induction and execution of apoptosis was found to be dependent on a family of proteolytic enzymes known as caspases (cysteine aspartate specific proteases).

Apoptosis can occur via two pathways; the extrinsic and intrinsic.

The extrinsic apoptotic pathway is mediated through a family of transmembrane proteins known as the death receptors. Damage to the cell by toxins, oxidative stress, viral infection and radiation triggers the intrinsic apoptotic pathway where the death signal originates from the mitochondria (details of the two pathways are described under section 1.3.2).

Regardless of their differences the overarching commonality of both pathways is their convergence and reliance upon caspase activation

1.2.1.1 Caspases

In 1993 Horvitz and colleagues discovered that the ced-3 gene was necessary for developmental cell death in *Caenorhabditis elegans* (Yuan et al, 1993). Its homologue in humans was described shortly after as the interleukin-1β-converting enzyme which has since been renamed caspase-1 (Nicholson et al, 1995). Caspases were originally thought to be integral for inflammation or apoptosis but not both. It is now known that caspases are centrally positioned during apoptosis, inflammation and differentiation (Frisch, 2008; Lamkanfi et al, 2007). Substantial progress has been made in elucidating their function, structure, activation and regulation.

Currently there are 12 identified members of the family in humans which can be grouped according to their known roles in apoptosis (caspase-2, -3, -6, -7, -8, -9 and -10), inflammation (caspase-1, -4, -5 and -12 although the caspase-12 gene is mutated in the majority of the human population coding for a pseudo-caspase) or differentiation (caspase-14) (Denecker et al, 2007). Caspase-1, -11 and -12 are reputedly involved during the inflammatory response in mice. The caspases involved in apoptosis are divided into two types based upon their biological function; initiators of apoptosis (this may be further subdivided into extrinsic (caspase-8 and -10) and intrinsic initiators (caspase-2 and -9)) and effectors of apoptosis (caspase -3,-6 and -7). Regardless of their predominant physiological role all caspases function in signalling pathways by the cleavage of specific substrates immediately after aspartate residues (Timmer & Salvesen, 2007).

All family members are produced in an inactive state as a single chain zymogen with N-terminal pro-domains and a highly conserved catalytic domain which consist of two subunits; one large (α, ~ 20 kDa) and one small (β, ~10 kDa). Both subunits contain residues required for the caspases enzymatic activity. Specifically the α-subunit possesses the catalytic residues (Cys and His) and the β forms the substrate binding grove. Generation of the active form requires limited proteolysis in the linker region connecting the large and small catalytic domain subunits. This is immediately followed by the removal of the N-terminal pro-domain. The released catalytic subunits form a hetero-dimeric enzyme consisting of two p20 and two p10 subunits (Pop & Salvesen, 2009).

Caspases are found in monomeric or dimeric form. Initiators of apoptosis are found as monomers that require dimerization for activation while the effector caspases are produced as inactive dimers. Within the N-terminal region of the initiator caspases there is a domain for the recruitment and activation of caspases. Two such domains exist in the caspases; these domains are the death effector domain (DED) and the caspase activation and recruitment domain (CARD). The DED domain is found in caspase -8 and -10 and is essential for their recruitment to the death receptor complex thus forming the so-called death inducing signalling complex (DISC) one of the

aforementioned caspase-activation platforms (Boatright et al, 2003). Likewise caspase-9's CARD domain is required for the formation of a caspase activation platform known as the apoptosome (Shiozaki et al, 2002). Caspase-2 was the most recent apoptosis-inducing caspase for which an activation platform has been identified. Approximately 12 years ago it was shown that similarly to caspase-8,-9 and -10, caspase-2 was also activated in a high molecular weight protein complex (Read et al, 2002). Some 2 years later a screen for protein interactions of death domain containing proteins identified p53-induced protein with death domain (PIDD) as a binding partner of receptor-interacting protein (RIP)-associated ICH-1/CED-3 homologous protein with a death domain (RAIDD). RAIDD had long been known to bind to caspase-2. Thus the PIDDosome was described as a 700 kDa structure formed upon activation of PIDD by heat shock or DNA damage resulting in the activation of caspase-2 (Tinel & Tschopp, 2004).

As previously mentioned the effector caspases are expressed as inactive dimers that require cleavage via the initiator caspases or granzyme B in order to become active. The process of dimerization occurs shortly after synthesis. A linker separates the α and the β subunits of the catalytic domain and proteolysis of this leads to the formation of the active catalytic site (Pop & Salvesen, 2009).

The inflammatory caspases are typically activated by pattern recognition receptors (PRR). Upon ligand binding PRRs trigger the formation of a protein complex similar to the apoptosome in the cytosol. Nucleotide-binding domain leucine repeat-containing (NLR) proteins polymerize upon the receipt of activation stimuli by their NACHT domain. Thereafter, apoptosis associated speck-like protein containing a CARD (ASC) protein is incorporated along with pro-caspase-1 to the complex thus forming the inflammasome. Pro-caspase-1 is activated by induced proximity within the inflammasome. Activation by induced proximity describes the process by which caspases in close proximity cleave and activates each other. Active caspase-1 cleaves pro-IL-1β and pro-IL-18 triggering their secretion (Davis et al, 2011; Ting et al, 2008). The exact function of the inflammasome is dependent on its composition which can vary depending on the NLRs

present in the complex. Which NLRs are present is influenced by the stimulus involved. It must be noted that the exact mechanism for activation of the inflammasome in a number of scenarios remains unknown (Davis et al, 2011). Finally excessive activation of inflammasome can end in pyroptosis a non-apoptotic form of cell death characterised by plasma membrane rupture and release of pro-inflammatory cytokines (Cookson & Brennan, 2001; Fink & Cookson, 2006).

The engagement of the caspase cascade if unchecked commits the cell to death because of this caspase activation is tightly controlled. Examples of such include expression as inactive precursors and dependence on stimuli induced activation complexes. There are 3 other stratagems employed by the cell to insure tight regulation of the induction of apoptosis. Firstly cells express the endogenous x-linked inhibitor of apoptosis proteins (XIAP) protein which inhibits caspase-9, -3, and -7. Specifically XIAP can inhibit active caspase-3 and -7 and prevent the activation of caspase-9 (Suzuki et al, 2001). This mechanism has been utilised by viruses expressing proteins like XIAP that target the substrate binding cleft of the caspases. In this way they can inhibit caspase activity. Examples of such are cytokine response modifier A (CrmA) and p35/p49 produced by cowpox and baculoviruses respectively (Lannan et al, 2007; Ray et al, 1992). Secondly the use of proteins that possess similar pro-domains as the initiator caspases can prevent caspase activation by excluding them from their activation platform. An example of which is cellular FADD-like interleukin-1β–converting enzyme (FLICE)-like inhibitory protein (c-FLIP) which inhibits the activation of pro-caspase-8 (Safa, 2012). Finally the ubiquitination of active caspases by the inhibitor of apoptosis proteins (IAP) through their Really Interesting New Gene (RING) domain increases their proteasomal turnover (Choi et al, 2009).

1.2.2 Anoikis

When a cell becomes detached from the surrounding extracellular matrix (ECM) or adheres to an inappropriate location, they undergo a form of apoptotic cell death known as anoikis (Frisch & Francis, 1994; Meredith et al, 1993). Physiologically anoikis is important in regulating migration, proliferation and cell survival (Frisch & Ruoslahti, 1997; Reddig & Juliano, 2005). The ability to induce cell death upon detachment implicates anoikis as the primary defense against metastasis preventing re-adhesion elsewhere to new a matrix. Indeed when anoikis was inhibited by the activation of TrkB a neurotrophic tyrosine kinase receptor there was an increase in tumour growth and metastatic rate in mice (Douma et al, 2004).

1.2.3 Mitotic catastrophe

Cells which are unable to complete cell division and which subsequently die in mitosis are said to have under gone mitotic catastrophe. Morphologically this form of cell death is typified by the formation of large cells with multiple micronuclei and decondensed chromatin. Studies have associated mitotic catastrophe and apoptosis however the link between the two is tentative. On one hand some groups report caspase activation, cytochrome *c* release and apoptotic morphology during mitotic catastrophe (Castedo et al, 2004a; Castedo et al, 2004b; Jordan et al, 1996; Merritt et al, 1997). On the other mitotic catastrophe has been shown to occur despite over expression of the B-cell lymphoma-2 (Bcl-2) protein (Lock & Stribinskiene, 1996).

1.2.4 Pyroptosis

Pyroptosis is a form of cell death associated with inflammation that occurs upon activation of intracellular PRRs the NOD-like receptors (NLR). Pyroptosis has been described in monocytes, macrophages and dendritic cells infected with a range of pathogens (Bergsbaken et al, 2009). Pyroptosis is uniquely dependent upon caspase-1. Morphological traits include cell swelling, pore formation, plasma membrane rupture and DNA fragmentation (Brennan & Cookson, 2000; Fink & Cookson, 2006).

1.2.5 Paraptosis

This form of cell death is characterized by cytoplasmic vacuolization and mitochondrial swelling. Induced by insulin-like growth factor receptor 1 this pathway is considered independent of caspases as their inhibition could not protect the cells from death. Furthermore over expression of the anti-apoptotic B-cell lymphoma extra-large (Bcl-XL) protein could not prevent cell death. Interestingly despite the lack of response upon inhibition of the caspases and the overexpression of Bcl-XL this mode of cell death can be inhibited by mutation in the catalytic domain of pro-caspase-9. Furthermore this pathway does not require an apoptotically active form of caspase-9 as mutations in the residues required for activation could not inhibit paraptotic cell death (Sperandio et al, 2000).

1.2.6 Necrotic-like Cell Death

When it was discovered that tumour necrosis factor (TNF) could produce two morphologically distinct forms of cell death one of them resembling necrosis the following question arose. Is necrosis entirely an unregulated process? (Laster et al, 1988). Since then irrefutable evidence has been put forward describing regulated necrotic cell death deemed necrotic-like cell death or necroptosis. Currently there is no evidence to suggest necrosis is always regulated. Therefore the description of necroptosis does not preclude the existence of unregulated necrotic cell death. Rather they may be seen currently as separate cell death modalities that share common morphological characteristics but divergent biochemical traits. Necroptosis has been shown to be induced by the ligation of the death receptors TNF receptor 1 (TNFR1), FAS, death receptor 4 (DR4) and death receptor 5 (DR5) by their endogenous ligands TNF, FasL and tumour necrosis factor related apoptosis inducing ligand (TRAIL) respectively (Holler et al, 2000; Jouan-Lanhouet et al, 2012; Vercammen et al, 1998a; Vercammen et al, 1998b). The death receptors primarily induce apoptotic cell death however in instances where caspases are inhibited or their activity is low the necroptotic pathway may be engaged culminating in cell death that exhibits necrotic morphology. Common morphological features include swelling organelles, cellular swelling (oncosis), plasma membrane permeabilization, dilation of the

nuclear membrane and the absence of chromatin condensation (Yuan & Kroemer, 2010). It has become apparent that pattern recognition receptors (PRR) can also trigger necroptosis although the exact mechanism has yet to be described. For example the toll-like receptor 4 (TLR4) has been shown to induce cell death in macrophages after activation by lipopolysaccharides (LPS) (Ma et al, 2005). The study showed LPS induced caspase-8 activation however inhibition of caspase-8 did not cause a reduction in the loss of mitochondrial transmembrane potential and resulted in necrotic cell death. The knockdown of RIP1 did halt the loss of mitochondrial transmembrane potential and protected the cells against LPS insult. Other studies have shown that viral dsRNA could induce caspase-8 and FADD dependent cell death (apoptosis) and caspase-8 and FADD independent cell death (necroptosis) in the Jurkat cell line. Furthermore treatment of murine L929sA cells with dsRNA resulted in necroptosis (Kalai et al, 2002).

The most detailed information available for this mode of cell death is for TNFR1-mediated necroptosis. A number of initiators and effectors of this pathway have been elucidated in the last decade. These include receptor interacting protein kinase 1 (RIP1), receptor interacting protein kinase 3 (RIP3) (Cho et al, 2009; He et al, 2009; Holler et al, 2000; Hsu et al, 1996), IAPs, ubiquitin E3 ligases and deubiquitylating enzymes, pro-apoptotic Bcl-2 family members (Hitomi et al, 2008) and reactive oxygen species (ROS) (Goossens et al, 1999). While recent studies contend it (Wong et al, 2010), the general perception is that necroptotic cell death is RIP-1 dependent and requires caspase inhibition (Vercammen et al, 1998a). Specifically RIP1 and RIP3 form a complex known as the necrosome upon stimulation by TNF in cells where there is an absence of functional caspase-8 (Declercq et al, 2009). The exact mechanism used by this complex to execute cell death is presently unclear. The mixed lineage kinase domain-like protein (MLKL) is downstream of RIP3 and it is thought to regulate $Ca2^{+}$ influx an early event in necroptosis which may lead to plasma membrane rupture (Cai et al, 2014). In addition the generation of ROS has been proposed as a mechanism of necroptotic cell death (Kim et al, 2007; Schulze-Osthoff et al, 1992).

In pathology it is known that a large proportion of cells dying *in vivo* due to ischemia or reperfusion, viral or bacterial infection or chemical trauma show signs of necrotic cell death some of which display the biochemical traits indicative of necroptosis (Vanlangenakker et al, 2008).

1.2.7 Autophagic Cell Death

Autophagy is a degradative process used during times of severe nutrient deprivation, for the removal of miss-folded proteins and damaged organelles (Fimia & Piacentini, 2010). Autophagy is traditionally considered a survival mechanism whose inhibition has potential as an anti-tumour therapy. New studies have however described cell death mediated by autophagy (Yu et al, 2004). While it is conceivable that prolonged autophagy could result in cell death whether or not autophagy drives cell death or is merely an associated morphological feature is a contentious point. Recently evidence has been provided to suggest that autophagic like cell death occurs as an alternative to apoptosis in a manner similar to necroptosis. It was shown that mouse embryonic fibroblasts (MEFs) which lacked Bcl-2 associated X protein (Bax) and Bcl-2 antagonist killer (Bak) underwent a form of cell death distinct from apoptosis after treatment with a multitude of apoptotic inducers. This cell death was typified by non-apoptotic characteristics such as positive staining with propidium iodide and extensive double membrane vesicles. These vesicles were confirmed as autophagosomes in the cytoplasm. This non-apoptotic cell death could be prevented through the inhibition of autophagosome formation by the addition of 3-methyladenine (3-MA) or wortmannin. Alongside the extensive cytoplasmic vacuolization described earlier autophagic cell death may be discerned morphologically by a lack of chromatin condensation (Kroemer et al, 2009; Shimizu et al, 2004).

1.2.8 Necrosis

Necrosis is a form of accidental or unregulated cell death which occurs upon the exposure of the cell to physical stress, extremes in temperature and oxygen deprivation. Necrosis shares the same morphological traits as the previously described necrotic –like cell death (Kroemer et al, 2009).

1.3 TRAIL

TRAIL was identified as a member of the TNF family of cytokines in 1995 based on its high sequence homology with TNF and FasL (Pitti et al, 1996; Wiley et al, 1995). The aforementioned family consists of approximately 20 members which can bind to over 30 different receptors. The death ligands form a subfamily within the TNF ligand superfamily. The death ligands are FasL, TNF, TNF-like protein A1 (TL1A), ectodysplasin, lymphotoxin (LT) α, LTβ, TNF-like weak inducer of apoptosis (TWEAK) and TRAIL. TRAIL is of particular interest because of its ability to induce apoptotic cell death selectively in transformed cells only.

TRAIL is expressed endogenously as a type II transmembrane protein on the surface of immune cells. In particular TRAIL is expressed on monocytes, dendritic cells, natural killer cells and T-cells activated by interferons or interleukin-2 (IL-2) (Almasan & Ashkenazi, 2003; Bouralexis et al, 2005; Takeda et al, 2001a). The extracellular domain of TRAIL can be removed by proteolytic cleavage by cysteine proteases to produce a soluble protein (Wajant et al, 2001). Soluble TRAIL is a homotrimeric molecule in which the monomers interact in a head to tail manner to form a homotrimer (Fig. 1.1). The presence of a zinc atom in the zinc-binding site located in the trimerization interface is essential for the stability of the TRAIL trimer and ultimately efficacy (Fig. 1.1). This binding site consists of three cysteine residues located at position 230 in their respective monomer and a chloride ion (Cha et al, 1999b; Hymowitz et al, 2000).

TRAIL induces apoptosis through binding to the death receptors; death receptor 4 (DR4, TRAIL-R1) (Pan et al, 1997b) and death receptor 5 (DR5, TRAIL-R2, KILLER or TRICK2) (Chaudhary et al, 1997; Pan et al, 1997a; Schneider et al, 1997a; Walczak et al, 1997; Wu et al, 1997). The death receptors are part of the TNF receptor superfamily (TNFRSF). There are eight death receptors in total. They are p75 neurotrophin receptor (p75NTR), FAS, TNFR1, ectodysplasin-A receptor (EDAR), death receptor 3 (DR3), DR4, DR5 and death receptor 6 (DR6) (Chaudhary et al, 1997; Chinnaiyan et al, 1996; Nagata & Golstein, 1995; Pan et al, 1997a; Pan et al, 1997b; Schneider et al, 1997a; Walczak et al, 1997).

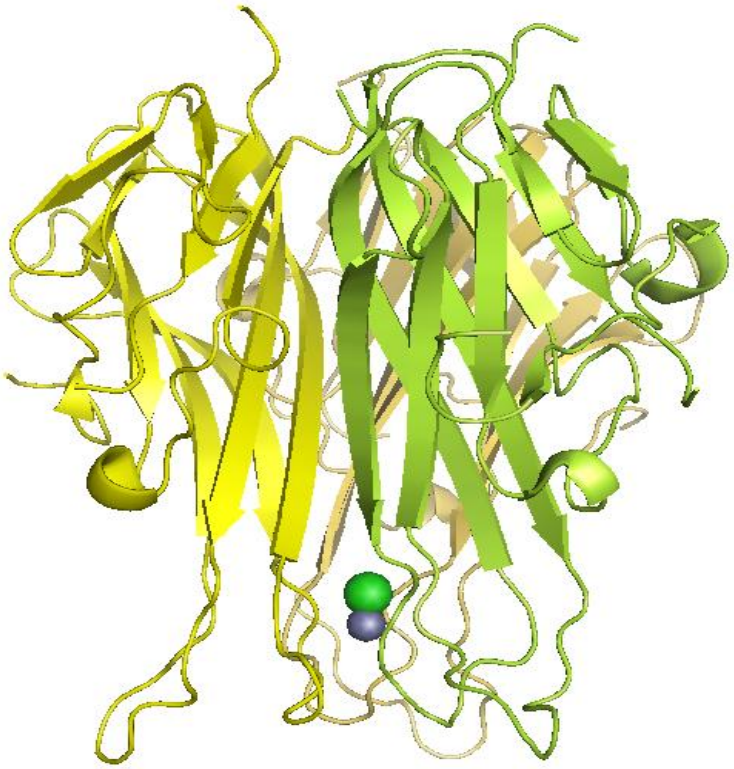

Figure 1.1: Depiction of the TRAIL homotrimer (Hymowitz et al, 2000); the zinc atom is depicted in blue and the chloride ion in green.

TNFRSF members have cysteine rich domains (CRDs) on the extracellular portion which are essential for interaction with their ligands. The number of CRDs present varies across the 8 members. DR4 and DR5 both have 3 CRD domains for example. The first CRD domain of DR4 and DR5 is incomplete but highly conserved. Recently it has been re-envisioned as a pre-ligand assembly domain (PLAD) involved in ligand-independent interactions between TRAIL receptors (Clancy et al, 2005). Meanwhile the complete second and third CRD domains are important for ligand binding (Cha et al, 1999a; Hymowitz et al, 1999; Mongkolsapaya et al, 1999).

Another common feature maintained across TNFRSF members is the intracellular death domain (DD). The DD is ~ 80 amino acids in length and plays a central role in the recruitment of scaffold proteins required for apoptosis (Ashkenazi & Dixit, 1998; Nagata, 1997). Upon activation the members of the TNFRSF recruit adapter proteins into large protein complexes which engage signalling pathways such as apoptosis, inflammation or differentiation. These adapter proteins are cytoplasmic

proteins which possess a DD. Recruitment to the activated TNFRSF member is by homotypic interaction of the DDs in the receptor and adapter protein. Currently there are approximately 30 cytoplasmic proteins with DDs known. Of these 30 only 4 have been consistently shown to be recruited to TNFRSF members these are EDARADD, fas associated death domain (FADD), tumour necrosis factor receptor type-1 associated DEATH domain protein (TRADD) and RIP1 (Sessler et al, 2013).

TRAIL can bind to three other receptors; decoy receptor 1 (DcR1, TRAIL-R3) (Degli-Esposti et al, 1997b; Mongkolsapaya et al, 1998; Pan et al, 1997a), decoy receptor 2 (DcR2, TRAIL-R4) (Degli-Esposti et al, 1997a; Marsters et al, 1997; Pan et al, 1997a) and osteoprotegerin (OPG) (Emery et al, 1998). DcR1 lacks a cytoplasmic tail and is instead anchored to the plasma membrane by glycosylphosphatydlinositol (GPI). DcR2 has a truncated non-functional DD that is missing approximately two thirds of the sequence seen in other TNFRSF members. OPG has least homology with the other four TRAIL receptors, is soluble and does not possess a DD (Emery et al, 1998; LeBlanc & Ashkenazi, 2003). While all three receptors have CRD domains and therefore are able to bind TRAIL none can initiate apoptosis (Ashkenazi & Dixit, 1998; Ashkenazi & Dixit, 1999). The affinity of TRAIL to OPG is relatively low (lowest of the five receptors). The binding of TRAIL to the decoy receptors can sequester TRAIL away from the death receptors and thus prevent the initiation of the apoptotic pathway. (Emery et al, 1998; LeBlanc & Ashkenazi, 2003). While TRAIL is expressed on specialised cells the 5 TRAIL receptors are almost ubiquitously expressed in all cell types (Daniels et al, 2005).

1.3.1 The Physiological Role of TRAIL

The majority of original research on TRAIL has focused on the assessment of its potential as an anti-cancer therapeutic. A number of groups however have devoted time to uncovering the physiological role of TRAIL. Initial experiments showed that TRAIL$^{-/-}$ mice developed normally with no defects or infertility observed. Similar results were seen for TRAIL-R$^{-/-}$ mice. Therefore TRAIL is considered to have minimal importance during embryonic development (Cretney et al, 2002; Diehl et al, 2004; Finnberg et al, 2005; Sedger et al, 2002).

TRAIL is a cytokine and as such might be expected to play a role in the immune system. Studies showed that certain immune cells could be stimulated to express TRAIL. For example monocytes treated with LPS or type I/II interferons increased the production of soluble as well as membrane bound TRAIL. The addition of interferon alpha (IFNα) or interferon beta (IFNβ) to dendritic cells and interferon gamma (IFNγ) to natural killer cells also induced TRAIL expression. In all instances induction of TRAIL correlated with enhanced cytotoxicity towards cancerous cells (Ehrlich et al, 2003; Halaas et al, 2000; Kemp et al, 2003; Liu et al, 2001; Takeda et al, 2001b). Further establishing the role of TRAIL in the immune system Zheng, S. J. and colleagues showed reduced apoptosis in TRAIL$^{-/-}$ mice that were more susceptible to listeria monocytogenes infection (Zheng et al, 2004). Knocking out the TRAIL receptor in mice resulted in resistance to infection by the murine cytomegalovirus however similar effects were not observed with a number of other pathogens (Diehl et al, 2004). The pathogens that TRAIL-R$^{-/-}$ mice did not become more resistant to did however elicit an increase in the expression of interleukin-12 (IL-12) and IFNγ from DC and NK cells. Stimulation of different toll-like receptors (TLRs) in the same study resulted in the increased expression of IL-12 and IFNα in dendritic cells and macrophages (Diehl et al, 2004). TRAIL is expressed on the surface of naive T-cells and this expression is increased in CD4+ and CD8+ cells after activation. Naive T-cells express the TRAIL receptors but are resistant to TRAIL-induced apoptosis. Upon activation both CD4+ and CD8+ become

sensitive to TRAIL suggesting a role for TRAIL in activation induced cell death (AICD) which is traditionally believed to be mediated by FasL (Bosque et al, 2005; Martinez-Lorenzo et al, 1998). These data suggest that TRAIL plays a role in both the innate and adaptive immune response.

Naturally, following on from the role of TRAIL in the regulation of the immune response there are reports of a role for TRAIL in autoimmune diseases. Deficiency of TRAIL or its receptor (there is only one TRAIL death receptor in mice) did not result in the spontaneous onset of autoimmune disease. However TRAIL has been shown to inhibit a number of autoimmune diseases in animal models. For example the development of type I diabetes in non-obese diabetic (NOD) mice was compounded upon inhibition of TRAIL signalling and the overexpression of TRAIL increased allograft survival time in the pancreatic islets of streptozotocin-induced diabetic rats (Dirice et al, 2009; Lamhamedi-Cherradi et al, 2003).

Furthermore TRAIL$^{-/-}$ mice develop worse cases of collagen induced arthritis than the wild-types (Song et al, 2000). Conversely there is a body of work indicating that inhibition of TRAIL can improve disease state in patients with multiple sclerosis (MS). MS is a disease that is characterised by the infiltration of immune cells into the central nervous system (CNS) resulting in neuroinflammation and the subsequent destruction of the myelin sheath on the proximal axons. The detrimental role of TRAIL in this system has been attributed to the induction of cell death in oligodendrocytes and neurons (Aktas et al, 2005). Generally speaking it seems TRAIL expression regulates autoimmune diseases such as diabetes, rheumatoid arthritis, scleroderma and psoriasis. This regulation is probably through regulating immune cell function/activity (Azab et al, 2012; Dirice et al, 2009; Lamhamedi-Cherradi et al, 2003; Peternel et al, 2011).

Evidence for the role of TRAIL in immune surveillance of tumour cells was provided by the Walczak and the Ashkenazi groups (Ashkenazi et al, 1999; Walczak et al, 1999). These studies showed that addition of soluble TRAIL reduced tumour volume in xenograft mouse models. Furthermore knocking out TRAIL or neutralisation of TRAIL with antibodies potentiated tumour

growth and increased metastatic rate in mice (Cretney et al, 2002; Takeda et al, 2001b). In addition TRAIL deficient mice displayed increased incidence of lymphoma (Zerafa et al, 2005). TRAIL-R$^{-/-}$ mice also suffered from increased number of metastases (Grosse-Wilde et al, 2008). These findings indicate a central role for TRAIL in tumour immune surveillance. However, contradicting these studies, it has been shown that deficiency in TRAIL-R in mice with mutated adenomatous polyposis coli did not affect intestinal tumour development (Yue et al, 2005). Likewise exogenous TRAIL was unable to abrogate tumour growth in a mouse mammary carcinoma model (Zerafa et al, 2005).

1.3.2 TRAIL-induced Apoptosis

Cell suicide or apoptosis may be executed along the extrinsic or intrinsic pathways. Originally both pathways were considered separate insofar as their convergence occurred solely upon the effector caspases. It is now known TRAIL triggers extrinsic apoptosis through binding the death receptors DR4 and DR5 and may engage the intrinsic or mitochondrial pathway through caspase-8 mediated cleavage of the BH3-only Bcl-2 family member BH3 interacting-domain death agonist (Bid) (Fig. 1.2).

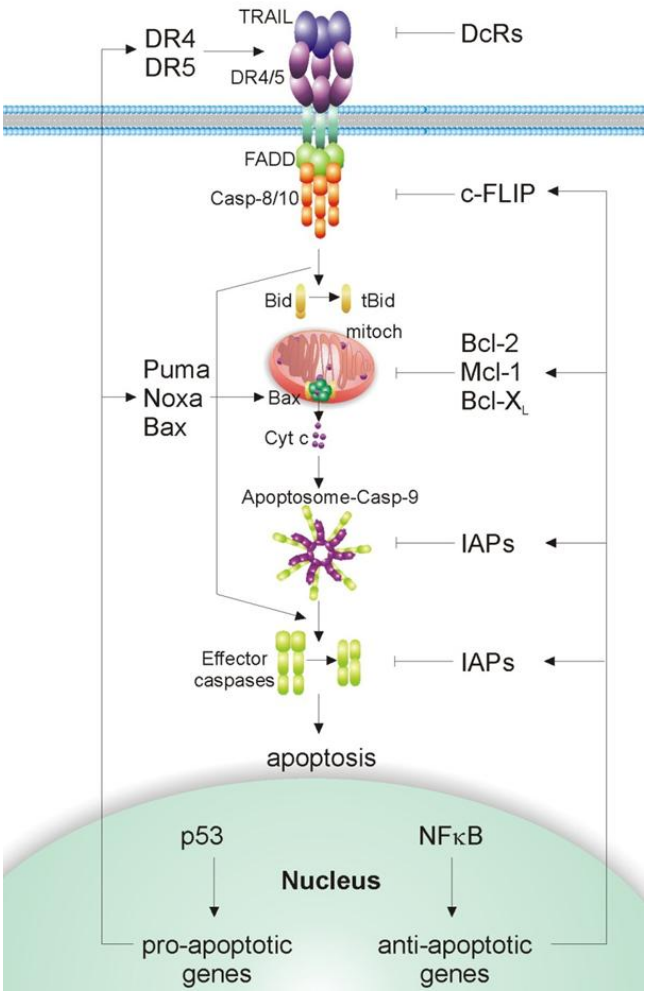

Figure 1.2: Schematic of TRAIL induced apoptosis (Mahalingam et al, 2011). The death receptors DR4 and DR5 trimerize after binding TRAIL. This facilitates the recruitment of FADD and pro-caspase-8. This protein complex is known as the DISC. Pro-caspase-8 is autoactivation within the DISC and released into the cytoplasm where it then cleaves and activates the effector caspases. Caspase-8 may also cleave the BH3-only Bcl-2 family member Bid engaging the intrinsic apoptotic pathway. Apoptosis may be inhibiting at multiple levels; c-FLIP at the level of the DISC, Bcl-2 at the level of the mitochondria and effector caspases may be inhibited by the IAPs.

1.3.2.1 Extrinsic Apoptosis

As previously mentioned the death receptors are expressed almost ubiquitously in the plasma membrane in the human body. Ligation of the death receptors by their cognate ligand induces conformational change and activation of the receptor allowing for the recruitment of the adaptor protein Fas associated death domain (FADD) to the DD of the receptor via homotypic interactions between the DDs. FADD also possesses a death effector domain (DED) which binds the DED present in pro-caspase-8. This protein complex is known as the DISC and it is here where caspase-8

undergoes autoactivation via induced proximity. When active caspase-8 is released from the DISC it moves to the cytoplasm where it cleaves and activates caspase-3, -6 and -7 resulting in cell death (Green, 2000; Kischkel et al, 2000).

1.3.2.2 The Intrinsic Apoptosis Pathway

Intrinsic or mitochondrial apoptosis is engaged by intracellular stressors such as oxidative stress, radiation and DNA damage. The signalling pathway initiated by these stimuli culminates in mitochondrial outer membrane permeabilization (MOMP). MOMP results in the release of pro-apoptotic proteins, such as cytochrome *c*, Endonuclease G and second mitochondria-derived activator of caspases (Smac) from the intermembrane space. Cytochrome *c* release brings about the assembly the apoptosome. In addition to cytochrome *c* the apoptosome also contains apoptosis protease activating factor-1 (APAF-1), dATP and pro-caspase-9. Caspase-9 is cleaved and activated within the apoptosome complex.

This pathway is controlled by the Bcl-2 family of proteins. There are three subtypes of Bcl-2 family members which tightly regulate MOMP (Fig. 1.3) (Decaudin et al, 1998; Green & Kroemer, 2004).

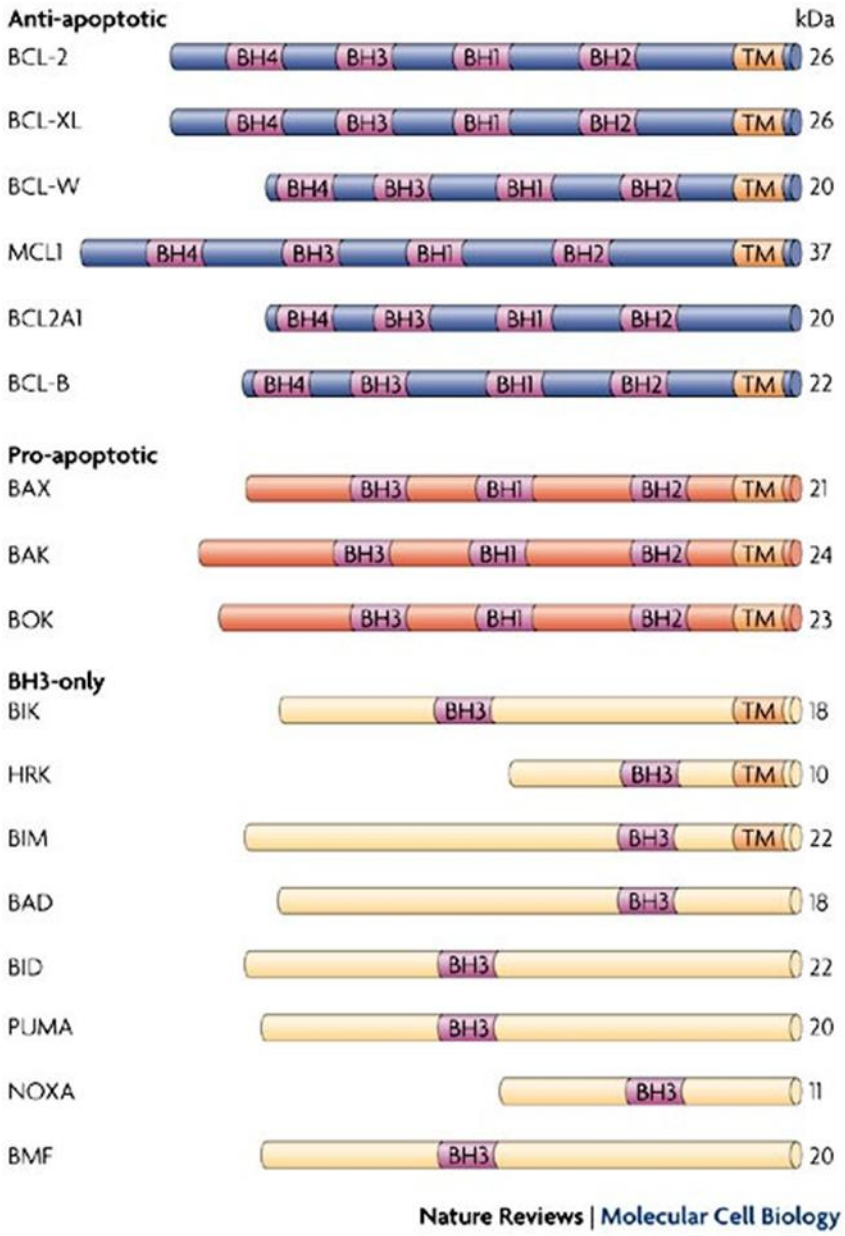

Figure 1.3: The structure of the Bcl-2 family members. The Bcl-2 family of proteins play a crucial role in regulation of apoptosis. The do this through their ability to regulate mitochondrial cytochrome c release. The family consists of three subtypes which are outlined here

Anti-apoptotic Bcl-2 family members contain four of the Bcl-2 homology (BH) domains (Fig. 1.3). Usually integrated into the outer mitochondrial membrane (OMM), these Bcl-2 family members may also be found in the nuclear and endoplasmic reticulum membranes as well as the cytosol. Prominent members of this subfamily include Bcl-2, Bcl-XL and induced myeloid leukaemia cell differentiation protein Mcl-1 (Mcl-1). These

proteins function by directly inhibiting the pro-apoptotic family members thus preserving OMM integrity by preventing MOMP (Chipuk et al, 2010).

The pro-apoptotic family members consist of multi-domain effectors and the BH3-only proteins (Fig. 1.3). The multi domain activators Bax and Bak possess 3 BH domains. Upon activation Bax/Bak homo-oligomerize into a lipidic pore in the OMM in order to promote MOMP. There is mounting evidence to suggest this event in dependent upon the interaction of Bax with mitochondrial ion channels (Chipuk et al, 2010; Szabo et al, 2011).

The BH3-only proteins can be further subdivided into two groups based on their binding profiles; do they interact with anti-apoptotic Bcl-2 family members, the multi-domain activators or both. Those BH3-only family members which only bind the anti-apoptotic family members are known as sensitizers examples of which include Bcl-2 antagonist of cell death (Bad) and Phorbol-12-myristate-13-acetate-induced protein 1 (Noxa). BH3-only proteins which bind to both the anti-apoptotic and pro-apoptotic are known as direct activators, these include Bid and Bcl-2 interacting mediator of cell death (Bim) (Chipuk et al, 2010)

Active caspase-8 produced by the extrinsic apoptotic pathway can cleave Bid into truncated Bid (tBid) which triggers MOMP and therefore activates the intrinsic apoptotic pathway (Korsmeyer et al, 2000) (Fig. 1.2). In this way TRAIL induced apoptosis can employ extrinsic and intrinsic apoptotic pathways in parallel.

Cells are differentiated based on which pathways are required for TRAIL-induced apoptosis. A cell which undergoes cell death by the classical extrinsic pathway without the requirement of the intrinsic pathway are said to be type I cells. Type II cells are those in which insufficient activation of caspase-8 occurs, possibly because of ineffective DISC formation, requiring the engagement of the mitochondrial pathway to serve as an amplification loop.

1.3.3 Ion Channels and Apoptosis

Intrinsic apoptosis via the mitochondria requires MOMP, the release of cytochrome *c* and caspase-9 activation. MOMP can occur via the formation of so called "megachannels" formed by Bax and Bak oligomers or as a consequence of mitochondrial membrane depolarisation brought about by the permeability transition pore (PTP). The PTP channel has been found to span across the inner and outer mitochondrial membrane. It permits the transit of solutes up to 1.5 kDa in size. The PTP is believed to be constituted by the adenine nucleotide translocator (ANT), the voltage dependent anion channel (VDAC), translocator protein and cyclophilin-D (Elrod & Molkentin, 2013). The involvement of VDAC is contended as knockdown has been reported to be unable to prevent MOMP (Baines et al, 2007).

Alongside VDAC other ion channels found on the plasma and mitochondrial membranes have been found to regulate apoptosis. Voltage-gated potassium channels for example have recently emerged as mediators of apoptotic cell death in various cell types. A crucial role for these K^+ potassium channels in the control of cell growth and cell death has been indicated in the literature.

Voltage-gated potassium channels (Kv) have four subunits. Each subunit contains six transmembrane sections (S1-S6) which surround a central pore (Pongs, 1993). The Kv family is a large family with 80 potassium channel genes described thus far. In the plasma membrane of excitable cells they control resting membrane potential by regulating outward potassium flux. Mutations in Kv channels in the excitable tissues such as the brain and the heart have been associated with epilepsy and arrhythmia (Partemi et al, 2013). In non-excitable cells such as the pancreatic islets, epithelial cells and the immune system these channels influence a number of processes from secretion to proliferation.

In relation to apoptosis the Kv channels mediate loss of water termed as apoptotic volume decrease (AVD). AVD typically precedes mitochondrial outer membrane permeabilization. Importantly the drastic decrease in intracellular K^+ resulting from AVD has been reported to facilitate the

activation of caspase-3 and endonuclease activity (Lang et al, 2004; Wang, 2004; Yu, 2003). Keeping this in mind, treatment with potassium channel blockers such as TEA and 4-AP has been shown to block apoptosis in several cell types (Wang et al, 2000; Wei et al, 2003; Yu et al, 1997). One of the first voltage-gated channels to be reportedly modulated during apoptosis and shown to contribute to the increased K^+ efflux seen during AVD in lymphocytes was Kv1.3 (Storey et al, 2003; Szabo et al, 1996; Valencia-Cruz et al, 2009). The knockdown or absence of this channel resulted in resistance to apoptosis (Bock et al, 2002; Szabo et al, 2008). Similar results have been observed for Kv1.1 in cerebellar granular neurons (Hu et al, 2008b). The down-regulation of Kv1.5 in pulmonary arterial hypertension reduced the amount of observed cell death while over-expression in smooth muscle cells potentiated the induction of apoptosis (Brevnova et al, 2004; Krick et al, 2001; Yuan et al, 1998). Interestingly the expression of K1.1 has been shown to reduce the severity of glutamate induced hippocampal cell death. Activation of the potassium channel by cromakalim prevented apoptosis in these cells (Shen et al, 2009).

The potassium channels do not reside solely in the plasma membrane. They may also be found in the mitochondrial membrane. The mitochondrial located Kv1.3 known as mtKv1.3 has been reported as directly interacting with the Bcl-2 family member Bax. Bax is unable to induce mitochondrial outer membrane permeabilization in the absence of mtKv1.3. This was shown by the inability of a mutant BaxK128E unable to associate with Kv1.3 to induce apoptosis in $Bax^{-/-}$ MEFs (Fig. 1.4). Interaction of Bax with other potassium channels has also been described which may provide a more in-depth and complete explanation as to the contribution of potassium channels in the apoptotic process (Szabo et al, 2008; Szabo et al, 2005; Szabo et al, 2011).

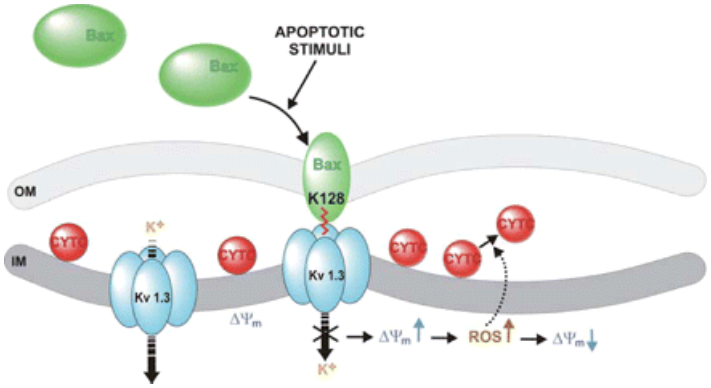

Figure 1.4: Proposed mechanism of action of the mitochondrial Kv1.3 potassium channel during apoptosis (Szabo et al, 2011). The Kv1.3 channel is inhibited by Bax which interacts via lysine 128 with the channel pore. This causes hyperpolarization of the inner mitochondrial membrane (IMM) which results in ROS generation and cytochrome c release.

1.3.4 TRAIL Resistance

During their development cancerous cells alter or disengage pivotal sections of the molecular machinery required for apoptosis in order to evade the immune system. Concurrently studies show 50-60% of tumour cell lines are resistant to TRAIL. Determining the causes of resistance to TRAIL may lead to the identification of novel treatment regimens which can circumvent this blockade of apoptosis. Abrogation of the apoptotic signal can occur at multiple levels of the pathway

1.3.4.1 Regulation of Death Receptors

The activation of the death receptors is the apical point in TRAIL induced apoptosis. Therefore if inadequate amounts of death receptors are expressed on the cell surface or if the receptors are expressed in a non-functional state then TRAIL will be unable to induce apoptosis. Deficient trafficking of the DR4 receptor in colon cancer cell lines for example has been shown to cause TRAIL resistance (Fisher et al, 2001; Jin et al, 2004; Pai et al, 1998). In addition epigenetic silencing of DR4 in ovarian cancer cell lines has been shown to confer resistance to TRAIL (Horak et al, 2005).

Some studies have suggested the amount of the death receptors relative to each other is important in determining whether or not a cell line is sensitive to TRAIL. The death receptor DR5 binds TRAIL with a higher affinity than DR4 at physiological conditions (Truneh et al, 2000). TRAIL has been shown to signal primarily through DR4 in human keratinocytes which express both of the death receptors (Leverkus et al, 2003). In addition DR4 and DR5 may or may not respond to particular preparations of TRAIL. For example it has been shown that cross-linked and non-cross-linked TRAIL can induce apoptosis through the DR4 receptor while DR5 will activate only upon the addition of cross-linked TRAIL (Wajant et al, 2001). These data suggest there may be a bias towards signalling through a particular death receptor and that the extent of cell death observed depends on the relative expression of DR4 and DR5, cell type and the formulation of TRAIL used. Furthermore Wagner and colleagues reported in 2007 that the post-translational modification status of the death receptors plays an integral role

in their function. Specifically they show that O-glycosylation of the death receptor promotes ligand-stimulated clustering of the receptors which is essential for efficient DISC formation. There was a strong association observed between the expression of the peptidyl O-glycosyltransferase (GALNT14) and TRAIL sensitivity (Wagner et al, 2007).

Redistribution of death receptors (DR4, DR5, Fas and TNFR1) into plasma membrane microdomains enriched in cholesterol and glycosphingolipids known as lipid rafts is thought to enhance signalling from death receptors (Delmas et al, 2004; Muppidi et al, 2004). Lipid rafts are formed when sphingomyelin which is found in the outer leaflet of the plasma membrane is hydrolysed by acid sphingomyelinase (ASM) thereby releasing ceramide which form platforms or microdomains. Colon cancer cell lines could be sensitized to TRAIL via pre-treatment with resveratol, a natural phenol, which induced DR4 and DR5 redistribution into lipid rafts (Delmas et al, 2004). Several other drugs and therapeutics have been reported to instigate redistribution of receptors into lipid rafts with an associated increase in sensitivity to TRAIL (Psahoulia et al, 2007). Additionally incorporation of death receptors into lipid rafts can be regulated post-translationally by S-palmitoylation (Rossin et al, 2009).

1.3.4.2 Decoy Receptors

Literature exists correlating the expression of the two decoy receptors, DcR1 and DcR2, with resistance to TRAIL. Overexpression of DcR2 in acute myeloid leukaemia (AML), breast, lung and prostate cancer cell lines was observed to contribute largely to TRAIL resistance (Aydin et al, 2007; Koksal et al, 2008; Riccioni et al, 2005; Sanlioglu et al, 2005). Of all the TRAIL receptors only DcR1 resides in lipid rafts prior to binding TRAIL. Merino and colleagues have thus concluded that DcR1 primarily confers resistance to TRAIL by binding and sequestering it in lipid rafts away from the death receptors (Merino et al, 2006). Meanwhile DcR2 forms heterodimers with DR5. This allows for DISC formation but prevents activation of pro-caspase-8 (Merino et al, 2006). Whether or not the DcR2-DR5 heterodimer forms as a result of TRAIL or PLAD interactions remains unclear. Activation of the protein kinase B pathway (PKB, AKT) through

DcR2 in a TRAIL independent manner resulting in increased survival and rate of proliferation in HELA cells has been reported (Lalaoui et al, 2011).

It was observed that genotoxic insult and radiation treatment could increase the expression of DR5 and thus these approaches appeared to be promising regimes for sensitizing cells to TRAIL. DcR2 expression has however been shown to increase after exposure to ionizing radiation also (Chinnaiyan et al, 2000; Sreekumar et al, 2001).

Decoy receptors are expressed on the surface of some cancer cells as well as certain non-transformed cells such as peripheral blood lymphocytes, kidney, liver and spleen (Daniels et al, 2005; LeBlanc & Ashkenazi, 2003; Pan et al, 1997a; Sheridan et al, 1997). The role decoy receptors play in the rise of resistance to TRAIL in transformed cells is uncontested. There is evidence to suggest that the resistance of non-transformed cells to TRAIL is not a result of decoy receptor expression as the inhibition of these receptors will not sensitise non-transformed cells to TRAIL.

1.3.4.3 Caspase-8

Downregulation of caspase-8 expression can account for resistance to TRAIL induced apoptosis. The deletion of chromosome 2q33, which contains caspase-8 and-10, has been observed in a number of cancer cell lines (Fernandes-Alnemri et al, 1996; Nishizuka et al, 1998; Otsuka et al, 1996; Park et al, 2002). The rate at which caspase-8 is degraded would seem an important determinant in TRAIL sensitivity. Until the discovery of caspase-8 and -10 associated RING protein 1 (CARP-1) and CARP-2 little was known about this subject. The IAP like RING domain that is present in both CARP-1 and -2 can polyubiquitinate active DED containing caspases targeting them for destruction via the proteasome. CARPs are overexpressed in a number of cancer cell lines and therefore may cause resistance to TRAIL through the removal of active caspase-8 (McDonald & El-Deiry, 2004; Sasaki et al, 2002). By tagging active caspase-8 for removal, CARPs are thought to act downstream of the DISC. However in addition to the aforementioned role it seems CARPs possess phospholipid-binding activity and thus they may localise to the plasma membrane.

The c-FLIP protein is one of the prominent inhibitors of caspase-8 activation and therefore one of the foremost causes of TRAIL resistance (Micheau, 2003). Three isoforms of c-FLIP are known (Irmler et al, 1997). The c-$FLIP_L$ isoform is highly homologous with caspase-8 possessing a caspase-like domain and a tandem DED. Through its DED c-$FLIP_L$ can bind to FADD. Once bound to FADD c-$FLIP_L$ forms a heterodimer with caspase-8 resulting in limited proteolysis to p43-c-FLIP and p41/43 caspase-8. No further processing of these fragments can occur and therefore they remain bound to the DISC preventing the propagation of the apoptotic signal (Micheau et al, 2002). The c-$FLIP_S$ and c-$FLIP_R$ isoforms possess DEDs but do not possess a caspase-like domain. Recruitment of these isoforms into the DISC prevents caspase dimerization and competitively antagonizes caspase-8 activation (Chang et al, 2006; Micheau et al, 2002). The half-life of c-FLIP isoforms is short. Several studies have taken advantage of this, sensitizing colon cancer cell lines by the addition of protein synthesis

inhibitors such as actinomycin D or cycloheximide (Hernandez et al, 2001a; Hernandez et al, 2001b)

1.3.4.4 Bcl-2 family

The three-dimensional structure of Bcl-2 proteins is globular consisting of six to seven amphipathic α-helices encompassing two hydrophobic α-helices. The majority of family members have a hydrophobic c-terminus, of approximately 20 residues, which allows for insertion into the nuclear, mitochondrial and endoplasmic reticulum membranes. In addition the BH1-3 domains form a hydrophobic pocket. Interaction between this pocket and the hydrophobic C-terminus of Bax can render Bax soluble allowing for its distribution in the cytosol (Chipuk et al, 2010).

While it is accepted that Bax and Bak are essential for MOMP and the progression of intrinsic apoptotic cell death exactly how the Bcl-2 family members interact with and regulate each other is undecided. Currently there are two schools of thought. The direct activation model postulates that the BH3- only proteins bind to Bax or Bak recruiting them into the OMM where they can oligomerize and cause MOMP. Thus far only Bid, Bim and p53 up-regulated modulator of apoptosis (Puma) have been reported to have this effect. The other BH3-only proteins may inhibit the anti-apoptotic Bcl-2 proteins resulting in the release of the BH3- only activators who then go on to activate Bax and Bak (Merino et al, 2009; Wong & Puthalakath, 2008).

The alternative is the indirect model in which the role of the BH3-only proteins is to bind and neutralize the anti-apoptotic Bcl-2 proteins (Mcl-1, Bcl-XL and Bcl-2) and replace the multi-domain pro-apoptotic Bax, Bak (Merino et al, 2009; Wong & Puthalakath, 2008).

Following apoptotic stimuli BH3-only proteins such as Bid induce a conformational change in Bax which results in its relocation to the OMM. In contrast to Bax, Bak is constitutively found in the OMM where it is inhibited by the anion channel VDAC2, Mcl-1 and Bcl-XL. Once activated by BH3-only proteins Bax and Bak homo-oligomerize and form a pore (megachannel) which causes MOMP.

Although TRAIL does not always require the amplification loop to induce apoptosis resistance can arise at the level of the mitochondria. In colon cancer cell lines deficient in mismatch repair (MMR) resistance to TRAIL results due to mutations in Bax. Other studies have shown in fibroblasts that TRAIL can induce apoptosis in Bax deficient or Bak deficient cells, but not in Bax/Bak double knockout cells (Kandasamy et al, 2003). Overexpression of anti-apoptotic Bcl-2 family members has also been correlated with TRAIL resistance. For example, Bcl-2 is overexpressed in neuroblastoma, glioblastoma and breast cancer cell lines resistant to TRAIL whereas Bcl-XL is highly expressed in some TRAIL-resistant pancreatic adenocarcinoma cell lines (Fulda et al, 2002; Hinz et al, 2000).

1.3.4.5 IAP family

Beyond the mitochondria the activation and/or the activity of caspase-3 and -9 may be regulated by inhibitor of apoptosis proteins (IAPs). IAP family members, of which there are 8 (XIAP, c-IAP1, c-IAP2, NAIP, Survivin, ILP2, Bruce and ML-IAP), are characterized by their baculovirus IAP repeat (BIR) domains. Additionally the majority of IAP proteins also have ubiquitin associated domain (UBA) and a RING domain (Fulda & Vucic, 2012).

BIR domains are integral in binding and inhibiting the activity of caspases (Eckelman et al, 2006). The RING domain has been shown to have ubiquitin ligase activity polyubiquitinating active caspases resulting in their degradation by the proteasome (Lorick et al, 1999).

The best-studied IAP, XIAP, is found as a homotrimer. The RING domain of XIAP has been found to be important for trimerization but trimerization is not required for the inhibition of caspases activity (Gao et al, 2007). XIAP has three BIR domains each playing a role in the inhibition of caspase activity/activation. The BIR2 and the linker region between BIR2 and BIR1 of XIAP are required for the inhibition of active caspases such as caspase-3 and -7. Specifically the linker region blocks the active site of the aforementioned caspases. In addition the BIR2 domain interacts with the small N-terminal regions of partially processed caspase-3 and -7 preventing further cleavage (Huang et al, 2001; Riedl et al, 2001; Scott et al, 2005; Suzuki et al, 2001). The inhibition of caspase-9 by XIAP is mediated by the BIR3 domain which binds to caspase-9 preventing its dimerization and thus activation (Shiozaki et al, 2003; Srinivasula et al, 2001). Inhibition of IAPs can sensitize cells to apoptotic stimuli. For example Smac/DIABLO a pro-apoptotic protein released from mitochondria upon MOMP binds to the BIR3 and BIR2 domains of XIAP via its IAP-binding motif (IBM) which prevents binding and inhibition of caspase-3,-7 and -9 (Vaux & Silke, 2003). Furthermore Smac3, a Smac/DIABLO splice variant, has been shown to reduce inhibition of apoptosis by XIAP. It does this by accelerating XIAP auto-ubiquitination and proteasomal degradation (Fu et al, 2003). Similar to Smac, OMI/HtrA2 blocks XIAP via their IBM.

Moreover OMI/HtrA2 is a serine protease and can cleave XIAP (Hunter et al, 2007).

While c-IAP1 and c-IAP2 do not physically bind caspases in a manner akin to XIAP they can regulate caspase activity through their E3 ligase activity targeting caspase-3, -7 and -8 for proteasomal degradation. The predominant role of c-IAP1 and c-IAP2 are as positive regulators of receptor mediated NF-κB activation. As such they ultimately play a role in regulating the expression of a number of anti-apoptotic proteins such as c-FLIP which can confer resistance to TRAIL (Eckelman & Salvesen, 2006; Varfolomeev & Vucic, 2008).

1.3.5 TRAIL Induced Pro-survival Signalling

TRAIL has emerged as a promising anticancer therapy as a result of its unique ability to induce apoptosis selectively in cancerous cell only. Unfortunately TRAIL exhibits non-canonical signalling through various pro-survival pathways such as nuclear factor kappa b (NF-κB), mitogen activated protein kinase (MAPK), c-Jun N-terminal kinases (JNKs), extracellular signal regulated kinase (ERK) and protein kinase B (PKB, AKT). The events associated with these non-canonical pathways are poorly understood. Immunoprecipitation experiments have uncovered a secondary, non-canonical, complex formed after DISC formation (Varfolomeev et al, 2005). This secondary complex was found to contain FADD, RIP1 and TNF receptor associated factor 2 (TRAF2), NF-κB (nuclear factor kappa-light-chain-enhancer of activated B cells) essential modulator (NEMO)/IKKγ and is formed in a caspase-8 dependent manner. Whether or not the addition of TRAIL engages the canonical or non-canonical pathways and why is vague. There are reports suggesting the incorporation of death receptors into lipid rafts enables DISC formation and apoptosis while assemble outside of these hydrophobic microdomains correlates with non-canonical signalling (Song et al, 2007). Whether cells undergo apoptosis because of localization in lipid rafts or as a consequence of it remains unclear.

1.3.5.1 NF-κB

The mammalian NF-κB family consists of five proteins; NF-κB1 (p50), NF-κB2 (p52), RelA (p65), RelB and c-Rel. Homo/hetero-dimers of the aforementioned family members bind preferentially to particular sections of DNA which are 9-10 base pairs long called κB sites. In their inactive state dimers are retained in the cytoplasm by IκB proteins such as IκBα, IκBβ, IκBγ, IκBε, BCL3, p100, and p105. The IκB proteins can be phosphorylated by the IκB kinase complex (IKK). The IκB proteins are then polyubiquitinated and undergo proteasomal degradation. The NF-κB proteins translocate to the nucleus and alter gene expression (Plantivaux et al, 2009) (Fig. 1.5). Members of NF-κB family members are involved in inflammation and immune response. There has been an increased focus upon the role of NF-κB in cancer.

Activation of NF-κB by TRAIL was one of the first reported non-classical pathways. Since this discovery DR4, DR5 and DcR2 have been shown to induce NF-κB in a TRADD and RIP1 dependent manner (Chaudhary et al, 1997; Schneider et al, 1997b; Sheridan et al, 1997). The IKKγ subunit known as NEMO is reported to be in complex with FADD, RIP1 and TRAF2, c-IAP1, c-IAP2, HOIL and HOIP where it recruits IKKα/β causing phosphorylation and proteasomal degradation of the IκB proteins which allows the release and nuclear translocation of NF-κB (Varfolomeev et al, 2005). Thereafter the transcription of anti-apoptotic genes such as c-FLIP, Bcl-XL, cIAPs and Mcl-1 is initiated (Henson et al, 2003; Kreuz et al, 2001; Mitsiades et al, 2002; Ravi et al, 2001). In pre-clinical models of leukaemia, neuroblastoma, pancreatic cancer and non-small cell lung cancer (NSCLC) inhibition of NF-κB by pharmacological agents or by the overexpression of a dominant negative IκB protein could sensitize the cancer cells to TRAIL-induced apoptosis (Braeuer et al, 2006; Ehrhardt et al, 2003; Karacay et al, 2004; Voortman et al, 2007).

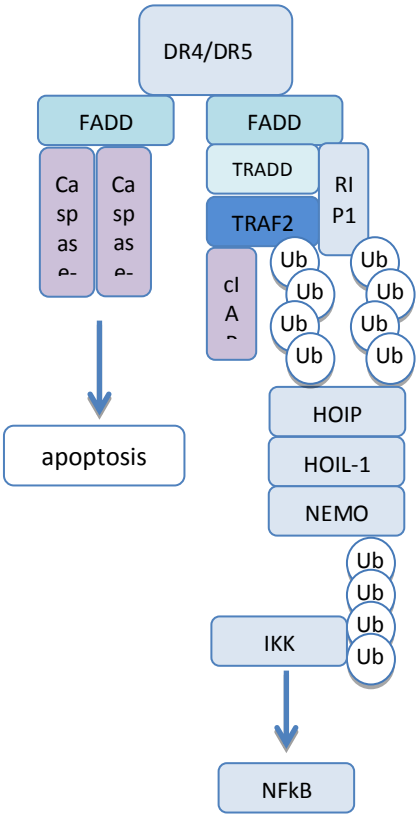

Figure 1.5: Schematic of TRAIL induced Nf-ƙB activation. The binding of TRAIL to DR4 or DR5 can induced apoptosis or activate Nf-ƙB. Upon activation the death receptors trimerize and recruit the death domain containing FADD and TRADD adapter proteins. TRAF2 is recruited stabilising the c-IAPs which ubiquitinate TRAF2 and RIP1. Thereafter HOIP and HOIL-1 polyubiquitinate NEMO resulting in the recruitment of IKK which phosphorylate Iƙb resulting in nuclear translocation of active Nf-ƙB.

1.3.5.2 MAPKs

Mitogen-activated protein kinases (MAPKs) control important processes such as gene transcription, motility, metabolism, cell division and cell death. Six distinct groups have been identified in mammals these are extra-cellular regulated kinase (ERK1/2), Jun NH2 terminal kinase (JNK1/2/3), p38 (α,β,γ and δ), ERK7/8, ERK3/4 and ERK5 (Chang & Karin, 2001).

The JNK, p38 and ERK1/2 can be activated by TRAIL in a number of cell lines with varying effects but they mostly contribute to proliferation and survival.

The exact mechanism of ERK1/2 activation by TRAIL is unknown. We do know that activation of ERK1/2 by other ligands is due to Ras/Raf signalling. ERK1/2 functions both up- and down-stream of cytochrome c release and may exhibit pro-apoptotic properties due to its inhibition of

AKT signalling. Phosphorylation of ERK1/2 has been observed in neuroblastoma cells treated with TRAIL and the inhibition of ERK1/2 in colon cancer cell lines resulted in enhanced TRAIL mediated cell death (Milani et al, 2003; Vaculova et al, 2006). Addition of TRAIL to small cell lung cancer (SCLC) which lack caspase-8 resulted in increased proliferation in a subset of cells which could be prevented by the knockdown or inhibition of ERK (Belyanskaya et al, 2008). Inhibiting ERK generally results in decreased expression of Bcl-2, Bcl-XL and Mcl-1 which may explain the increased sensitivity to TRAIL (Zhang et al, 2003).

In general the activation of JNK by TRAIL is considered a pro-apoptotic process. It would appear that activation via TRAIL is cell type specific either being caspase dependent or independent (Muhlenbeck et al, 1998). Interestingly the process does appear to be entirely independent of FADD. JNK activation in HEK293 cells was seen to involve TRAF-2, MEKK1 and MKK4. In fibrosarcoma cells a secondary complex containing RIP1 and TRAF 2 was shown to be required for JNK activation (Hu et al, 1999; Varfolomeev et al, 2005). Treating lymphoid cells with TRAIL has been seen to activate JNK which contributed to apoptosis. While the main target of JNK is the transcription factor c-Jun/AP1, the Bcl-2 family member BIM can also be phosphorylated causing stabilisation of the protein which can induce intrinsic apoptosis. This proposed mechanism has been shown in hepatocytes and cholangiocarcinoma cells (Corazza et al, 2006; Werneburg et al, 2007). In contrast the inhibition of JNK by siRNA increased TRAIL induced apoptosis in hepatocarcinoma (Mucha et al, 2009). It is known that JNK signalling is pro-apoptotic after prolonged activation due to TNF and protective after short transient periods of activation providing a potential explanation as to the dichotomous role for JNK in TRAIL mediated apoptosis (Ventura et al, 2006). Finally which isoform of JNK is present may be very relevant in determining outcome. Recent work has shown that the short isoforms of JNK (JNK1α1, JNK1β1) are anti-apoptotic but the long (JNK1α2, JNK1β2) are pro-apoptotic (Mahalingam et al, 2009).

While FADD is dispensable for the activation of JNK, it is required for p38 activation alongside TRAF2, RIP1 and caspase-8 (Varfolomeev et al, 2005).

Like JNK the role of p38 in TRAIL-mediated cell death is multifaceted. In prostate cancer cells TRAIL-induced p38 phosphorylation caused the up-regulation of Mcl-1 thereby protecting the cells against apoptosis. Furthermore chemical inhibition of p38 enhanced TRAIL-induced cell death in these cells (Son et al, 2010). A similar role for p38 has been reported in breast carcinoma suggesting activation of p38 by TRAIL can suppress apoptosis however p38 activation in HELA cells resulted in caspase activation and cell death (Lee et al, 2002; Weldon et al, 2004). Currently p38 is considered to be able to suppress or enhance TRAIL induced apoptosis depending on the cellular context.

1.3.5.3 AKT

AKT also known as protein kinase B (PKB) is active in a number of malignancies where is stimulates cell growth and survival. AKT signalling can be activated by receptor tyrosine kinases, cytokine receptors, B- and T-cell receptors, G-protein coupled receptors and integrins. AKT has been shown to influence cell cycle and proliferation through targeting the cyclin dependent kinase inhibitors (CDKI) p27 and p21 and indirectly regulating p53 and cyclin D expression. AKT signalling may also increase resistance to apoptotic stimuli by regulation of FoxO (Zhang et al, 2011).

The forkhead box (FOX) family of proteins represent divergent transcription factors. Several of these FOXA, FOXC, FOXM, FOXP and FOXO have been reported to have roles in the initiation and progression of cancer as well as resistance to chemotherapeutics (Lam et al, 2013). The best studied of these, FOXO, acts as a tumour suppressor confirmed by the formation of thymic lymphomas and systemic haemangiomas in mice with all four members of the FOXO subfamily deleted (Paik et al, 2007). The FOXO proteins can be regulated by a number of oncogenic pathways such as ERK, Nf-ƙB and AKT (Brunet et al, 1999; Hu et al, 2004; Yang et al, 2008). The phosphorylation of FOXO by AKT prompts binding with 14-3-3 proteins excluding the transcription factor from the nucleus and tags them for degradation by the proteasome (Matsuzaki et al, 2003). Inhibition of FOXO by AKT results in the decreased expression of BH3-only Bcl-2 family members Bim and Bad as well as TRAIL (Zhang et al, 2011).

The administration of TRAIL to Jurkat cells caused phosphorylation and activation of AKT in TRAIL resistant cell lines. Inhibition of AKT signalling by the inhibitor LY294002 could sensitize the cells to apoptosis (Zauli et al, 2005). Similar reports are available for TRAIL resistant ovarian, breast and NSCLC cell lines (Azijli et al, 2012; Xu et al, 2010).

1.3.6 Future prospects for TRAIL

Targeted delivery of anti-cancer agents to the site of action is an ongoing issue with drug development. TRAIL has been shown to possess an excellent safety profile but suffers from lack of efficacy. This issue could be resolved through the addition of a cancer specific delivery method leading to the increased accumulation of TRAIL in tumours. Of the various approaches described the most common is the development of TRAIL fusion proteins using antibody fragments specific for particular antigens which may be over expressed in certain tumours. A recent publication, for example, describes the production of Meso-TR3 a fusion of TRAIL and mesothelin. Mesothelin is known to interact with MUC16 a well characterized biomarker in a plethora of malignancies such as ovarian, breast and pancreatic cancers. Meso-TR3 was found to be a more potent inducer of apoptosis than TRAIL alone (Garg et al, 2014). Other successful methods for targeted delivery of TRAIL include conjugation to nano-particles and expression on the surface of mesenchymal stem cells and leukocytes (Gjorgieva et al, 2013; Mitchell et al, 2014; Perlstein et al, 2013). It is important to note that the conjugation of TRAIL to nanoparticles or incorporation into large fusion proteins can also increase bioavailability by making TRAIL large enough to avoid glomerular filtration in the nephron.

A number of labs including our own have developed receptor specific TRAIL variants. We have reported the generation of a DR5 selective TRAIL variant that was computationally designed. This variant has point mutations in aspartate at position 269 to a histidine residue and glutamate at position 195 to arginine which results in a 70-150 fold increase in preference of DR5 over DR4 than wild type TRAIL. Furthermore the DR5 variant was shown to be highly efficacious in tumour cell lines which respond to stimulation of DR5. No toxic side effects where observed for the DR5 variant in non-transformed cells. The increased potency of this variant may be ascribed either to increased affinity for DR5 or decreased binding to the decoy receptors (Reis et al, 2010). We have also generated a DR4 specific variant which exhibits increased specificity towards DR4 but

induces increased amounts of apoptosis in a number of cell lines tested (Szegezdi et al, 2011). The application of the receptor specific variants has allowed for the delineation of the specific contributions each death receptors makes during apoptosis and as such has proven to be a powerful research tool

Preclinical evidence exists endorsing the therapeutic potential of recombinant human TRAIL (rhTRAIL) as well as numerous monoclonal antibodies specific for DR4 (mapatumumab) or DR5 (lexatumumab, conatumumab, drozitumab, tigatuzumab and LBY135) which should evade decoy receptor mediated resistance to treatment. These antibodies also have the added advantage of having a significantly longer half-life than the rhTRAIL. In fact these agents have been moved into clinical trials.

There have been several single agent trials assessing the effects of conatumumab, rhTRAIL, lexatumumab and mapatumumab in which several of the aforementioned agents have been shown to have activity with isolated responses reported in follicular lymphoma, adenocarcinoma of the lung and synovial sarcomas (Camidge, 2008; Herbst et al, 2010a; Herbst et al, 2010b; LoRusso P, 2007; Wakelee et al, 2010). As expected there was minimal toxicity observed. Transaminitis was the most commonly reported side effect seen across a number of the tested agents (Camidge, 2008).

Combination therapy of TRAIL with various inducers of DNA damage such as etoposide or doxorubicin have proven fruitful *in vitro* greatly sensitizing to TRAIL induced cell death (Blay JY, 2008). Continuing on from this line of thought combination regimes of TRAIL and various monoclonal antibodies (conatumumab, lexatumumab and mapatumumab) with a bevy of first line treatments such as irinotecan (topoisomerase inhibitor) (Yee L, 2009), paclitaxel (disrupts microtubule formation) (Leong et al, 2009), vorinostat (histone deacetylase (HDAC)) inhibitor), bevacitzumab (targets vascular endothelial growth factor A) (Saltz., 2009) and cetuximab (targets epithelial growth factor receptor)(Yee L, 2009) have been tested. There was no observable increase in the toxicity associated with the various chemotherapeutics upon addition of rhTRAIL and the death receptor

specific monoclonal antibodies. Unfortunately none of these agents significantly improved response or patient disease-free survival. Considering the limited effects of monotherapy one should not be surprised at the apparently underwhelming effects observed in combination therapies. It must be noted that in phase II clinical trials involving NSCLC there was an increase of ~15 % in progression free survival implying these agents are functional and that lack of efficacy is likely due to patients who are resistant to treatment (Soria et al, 2011; Von Pawel J, 2010). As previously alluded to, the chemotherapeutics used in these trials tend to further sensitize cells which are responsive to TRAIL rather than remove resistance. This would explain the poor outcomes observed in these unselected clinical trials.

The development of a biomarker which could discern responders from non-responders might enable a more accurate assessment of TRAIL in clinical trials.

1.4 Machine learning techniques

During biological studies we may want to establish if an association between one or more variables exist. Correlation analyses aims to quantify the strength of association between these variables. One example of how this could be effective would be in the prediction of phenotypes using protein/gene expression values. If both variables in the correlation analysis are continuous then we can calculate the Pearson product moment correlation coefficient and if one of the variables is qualitative or non-parametric then we can utilize Spearman rank-order correlation. In either instance the strength of the relationship ranges from 0-1 with a value of 1 representing a perfect correlation. These values can be positive + or negative – which indicates the nature of the association. A correlation coefficient of +1 implies a perfect association between both variables. This means that as the value of one variable increases so does the other. Conversely a correlation coefficient of -1 indicates an inverse association between two variables where as one variable increases the other decreases. Importantly these approaches do not prove causation and are not well suited to large data sets due to being computationally expensive.

The biological sciences have begun transitioning towards high throughput systems biology approaches such as transcriptomics (DNA microarray), genome wide association studies (GWAS) and proteomics (mass spectrometry) in order to obtain quantitative features which can be used to identify novel drug targets or develop classifiers to predict patient prognosis and response to treatment. Subsequently there has been a drastic increase in the volume of biological data originating from the aforementioned approaches. These data pose two problems, the first being that they are difficult to store and manage. Secondly and more importantly the extraction of meaningful biological information from such complex and noisy data is difficult to achieve quickly and efficiently. A concern which current methods of analyses are ill suited to address.

The application of algorithms known as machine learning techniques to complex biological data sets began in 1958 when the perceptron algorithm was used for modelling neuronal behaviour and again years later when the

same algorithm would be used for defining translational initiation start sites in Escherichia Coli. These studies showed that through the utilization of past experiences (training data) these machine learning techniques could construct model systems which can be used for classification, prediction and pattern recognition. In this way the model identifies the useful information. Since then a working relationship between the field of machine learning and biological sciences has developed.

As a field, machine learning may be considered along two axes: supervised and unsupervised learning.

1.4.1 Supervised machine learning

Supervised machine learning aims to take a training dataset in which each sample has a known response or class label and features to build a predictive model. This predictive model can then be used to infer the response or class label in unseen or independent data sets. Machine learning techniques which may be considered supervised include artificial neural networks (ANN), support vector machines (SVM), K-nearest neighbours (KNN), classification and regression trees (CART) and random forest (RF).

Artificial neural networks: A machine learning technique inspired by the central nervous system (CNS). The first steps towards the establishment of supervised artificial neural networks (ANN) began as far back as 1958 when Frank Rosenblatt created the previously mentioned perceptron algorithm (Rosenblatt, 1958). Briefly the perceptron algorithm is composed of input, a threshold and an output. The output of the perceptron is Boolean such that it can only be one of two values (true or false, 1 or 0 and so on). Each input has an associated weight assigned to it. If the sum of these input values is greater than the threshold the perceptron is said to fire (have a value of 1, true and so on). The weights assigned to various inputs can be positive or negative and this directionality can infer agonistic or antagonistic properties to input values. Multilayer collections of perceptrons form artificial neural networks. The application of ANNs spiked in popularity in the 1980s when Rumelhart et al. developed the back propagation algorithm which allowed for the adjustment of the weight for each input until the desired output was

achieved (Rumelhart D. E., 1986). There are many different configurations for ANNs. The one most commonly applied to the biological sciences is the supervised feed forward ANN. These consist of 3 layers; input, hidden and output. The input is composed of a number of perceptrons or neurons equal to the number of features (Fig. 1.6 A) (Geman S., 1992). Neurons in each layer are connected via axons to the neurons in the immediate adjacent layer. Thus input neurons communicate directly with those neurons in the hidden layer which in turn can also communicate with the output layer (Fig. 1.6 A). The output layer typically consists of a singular neuron but may contain more than one should there exist more than one response variable (Geman S., 1992). In general however these ANNs tend to be able to detect all possible interactions between features, detect complex non-linear relationships and require minimal formal statistical training to construct. ANN methods tend to be inefficient and slow (SB., 2007). Due to back propagation these algorithms are prone to overfitting (Olden et al, 2008). Overfitting of a model implies that the model is too similar to the training data and as such will likely perform poorly on new data independent from the model.

Support vector machines: Samples of different classes may be separated in multi-dimensional space by using a decision boundary also known as the hyperplane (Larranaga et al, 2006; Tarca et al, 2007). Support vectors are the data points which lie closest to the hyperplane and as such are the most difficult to correctly identify. Support vector machines maximise the margin around the decision boundary thus optimizing the performance of the model as a classifier (Fig. 1.6 B). In this way SVMs approach classification from a relatively unique aspect concentrating specifically on the samples which are difficult to classify. The construction of SVM models is computationally cheap and tends to avoid overfitting (SB., 2007; Sommer & Gerlich, 2013). A major disadvantages of SVMs include a lack of transparency as the model does not directly provide a measure of performance rather these estimates are provided through the use of cross validation which is computationally expensive in large data sets. Cross validation being the random partitioning of the samples into n equally sized subsets. The majority of these subsets (n-

1) are used to train the model while the remaining subset is withheld to assess performance.

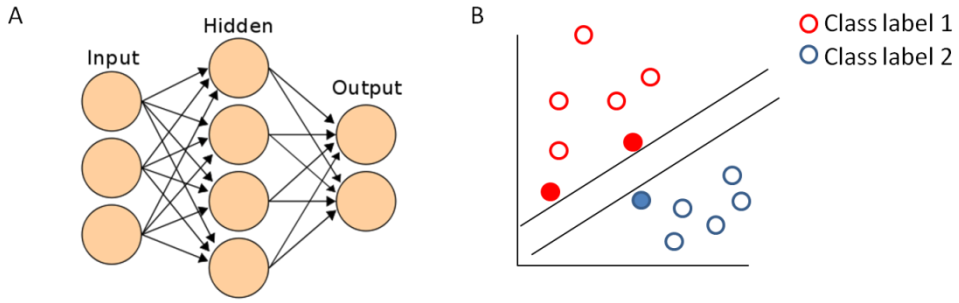

Figure 1.6: Example of artificial neural network and support vector machine learning algorithms. (A) Multilayer feed forward artificial neural network. The input is composed of a number of artificial neurons equal to the number of features. Neurons in each layer are connected via axons to the neurons in the immediate adjacent layer. The output layer typically consists of a singular neuron but may contain more than one should there exist more than one response variable. (B) Classification of training data using supervised support vector machines. Samples of different classes may be separated in multi-dimensional space by using a decision boundary also known as a hyperplane. Support vectors are the data points which lie closest to the hyperplane and as such are the most difficult to correctly identify. The support vectors are indicated here as the filled in circles. Support vector machines maximise the margin around the decision boundary thus optimizing the performance of the model as a classifier

K-nearest neighbours (KNN): The nearest neighbour algorithm aims to classify samples by assigning to the sample the majority class label possessed by K samples closest to it in multidimensional space (Fig. 1.7). This approach of course tends to be computationally expensive especially for large data sets because the algorithm has to search the entire dataset for each and every sample being classified (Larranaga et al, 2006). Similar to SVMs KNN requires cross validation to assess the performance of the model.

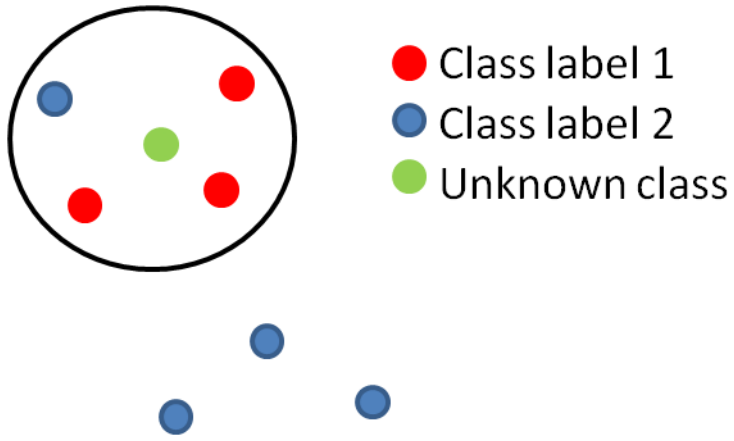

Figure 1.7: K-nearest neighbour model. In this example the training data has two classes coloured red and blue respectively. The class of an unknown sample is predicted as the class which is present with the highest frequency within the K-nearest neighbours or samples. In this case the unknown class when K=4 is class label 1. If K=7 then the sample with the unknown class would be assigned to class label 2

Classification and regression trees (CART): The first step in the construction of a CART involves partitioning the samples by their known class label into daughter nodes using the available features. If these daughter nodes contain samples with only one class then the model is complete. However in many instances this partitioning does not separate the samples into groups with only one class label. In these instances an additional feature is selected for each daughter node and is then used to partition the samples further (Fig. 3.1). This process known as recursive partitioning continues until nodes with only one class present are obtained. These nodes are known as pure or terminal nodes. There are many reasons why CART models might be particularly attractive for the analysis of large biological data set: (1) Insensitive to outliers; (2) able to detect and indicate interactions in the dataset; (3) can identify and rank features by their importance in model performance; (4) capable of dealing with missing variables; (5) typically quick to construct and easy to graphically interpret (Olden et al, 2008). These models however tend to suffer from overfitting, may be considered unstable (small changes in the data used to grow the tree can lead to changes in the features selected during splitting) and requires cross validation (Olden et al, 2008).

Random Forest (RF): At its core the random forest algorithm constructs a collection or ensemble of CARTs. It is therefore easy to accept that like CARTs the random forest models are insensitive to outliers, can detect interactions between features, can assign importance measures to each variable and can handle missing values in the data set (Diaz-Uriarte & Alvarez de Andres, 2006). Unlike singular CARTs, those grown in the RF model are not constructed from all the available samples. Instead each tree within the random forest is grown from a random subset of all samples. Those cell lines which are not used to grow the tree are subsequently classified by said tree to obtain a measure of the models performance as a classifier. This value is known as the out of bag error (OOB) (Breiman, 2001). There are two major advantages to this approach, it avoids overfitting and there is no need for cross validation. Construction of RF models is quick, computationally cheap and easy to interpret.

1.4.2 Unsupervised machine learning

During unsupervised machine learning there is no information available about the classes within the data set. Therefore unsupervised machine learning techniques typically group samples together based upon feature similarity. The clustering of samples by gene expression profiles using DNA microarray data for example can identify which genes are co-expressed across a large panel of samples. Widely used clustering methods include the following.

Hierarchical clustering: This clustering approach is directly related to the distance between the features. Initially each feature is defined as a singular cluster. Those clusters in close proximity to each other are then merged as per the specified linkage rule. This process is applied repeatedly yielding a object with a hierarchical structure known as a dendrogram. This approach is typically used to observe similarities between phenotypes (Gentleman et al, 2004; Sommer & Gerlich, 2013).

K-means clustering: Analysis by K-means clustering partitions the data into K clusters as specified by the user. To do this the central cluster points are selected at random and each feature is assigned to the nearest central cluster

point. The central cluster point is then iteratively recalculated based upon the mean value of the features assign to each point. This process continues until the central cluster points do not change beyond a user specified minimum significance threshold (Sommer & Gerlich, 2013).

Modern biology can and has benefited greatly from the application of machine learning techniques. Classification tree models have been used to identify the protein coding regions of DNA. Support vector machines and artificial neural networks have been used in conjunction to identify functional RNA genes. The K-nearest neighbour algorithm has been applied numerous times to predict the secondary structure of novel proteins. All of the previously mentioned supervised machine learning algorithms have been applied as classifiers in an attempt to predict clinically relevant phenotypes such as drug sensitivity using gene expression microarray data sets.

1.5 Aims and Objectives

TRAIL is a uniquely promising cancer therapy owing to its inherent ability to induce apoptosis in cancer cells only. Unfortunately approximately 50-60 % of tumour cell lines are resistant to TRAIL. Furthermore there is a body of literature to suggest that the addition of TRAIL to resistant cell lines may increase tumour aggression and propensity for metastasis.

Despite all we have learned of the regulation of the apoptotic pathway and mechanisms of resistance employed to evade TRAIL induced cell death there is currently a lack of a biomarker to predict whether or not tumours will respond positively to TRAIL.

Current methods employed to identify cancer specific drug able targets and/or identification markers from large datasets consider candidates in isolation comparing expression of one protein or gene to the corollary in another cell line or treatment condition. These approaches never consider the relationship between the variables themselves. We believe these interactions are pivotal in determining outcome to treatment.

Chapters 2 and 3 of this thesis aim to identify key gene/protein interactions, which can be used to predict a cell lines responsiveness to TRAIL with a high degree of sensitivity and specificity. Through the use of machine learning techniques a biomarker for TRAIL sensitivity will be generated and assessed for performance on both the protein and mRNA level.

In addition considering the mounting evidence pertaining to the importance of potassium channels in the regulation of apoptosis in chapter 1we address whether a correlation exists between the expression of the aforementioned channels and sensitivity to various apoptosis inducers.

1.6 Summary of Contents

During this study gene expression microarray data for 109 tumour cell lines from the Ashkenazi laboratory and an additional 40 tumour cell lines from the NIH was acquired and normalized (RMA algorithm) in the R statistical environment using the Bioconductor package known as Affy. Using the JetSet algorithm the microarray datasets were filtered to contain only one probeset for each gene in the transcriptome. On the protein level the expression values for a selection of potassium channels and the core components of the TRAIL apoptotic machinery (excluding the TRAIL receptors) were measured in 10 and 42 tumour cell lines respectively using Western blotting following by densitometry. Immunocytochemistry following by flow cytometry was used to measure the cell surface expression of the TRAIL receptors in 42 tumour cell lines.

In chapter 2 the sensitivity of a panel of 10 tumour cell lines to cisplatin, etoposide, ceramide, staurosporine and potassium channel blockers was measured by MTT viability assay. Correlation analysis between the expression of various potassium channels (on the gene and protein level) and sensitivity to the aforementioned agents was carried out using Pearson's correlation coefficient.

The identification of genes which may interact and thus predict/classify a phenotype was completed using the random forest machine learning algorithm in chapter 3. The gene expression data set acquired from the Ashkenazi lab was used by the algorithm to construct a model for predicting TRAIL sensitivity. Genes were ranked by their importance in the models ability to classify cell lines as resistant or sensitive. An iterative backward elimination of the lowest ranked genes was then employed to determine the core set of genes required for optimal performance of the model as a classifier of TRAIL sensitivity. The performance of these models was assessed on an independent test data set of 40 tumour cell lines acquired from the NIH.

In chapter 4 protein expression ratios (expression of one protein relative to another) for all possible pairings of the core components of the TRAIL apoptotic machinery were calculated. The range in expression of the core components of the TRAIL apoptotic machinery and the protein expression ratios between TRAIL resistant and sensitive cell lines was assessed by box-plot. Cell lines were classified as TRAIL resistant if they showed a less than 20% decrease in viability and sensitive if they showed more than a 50% decrease in viability using the MTT viability assay. 42 tumour cell lines were tested. A mechanistic model utilising a tetracycline inducible caspase-8 expression system and inhibition of Bcl-2 by the BH3-mimetic ABT-737 was established in order to confirm the role of the most predictive protein expression ratio, Caspase-8/Bcl-2, in TRAIL induced apoptosis. Cell death induced by TRAIL was assessed by crystal violet staining. A secondary mechanistic model overexpressing Bcl-2 with the dose dependent knockdown of caspase-8 by accell siRNA was optimised. Finally attempts were made to optimise the detection of the core components of TRAIL induced apoptosis by mass spectrometry (LC-QTOF). Unfortunately only 6 of the 9 proteins could be identified by mass spectrometry.

Chapter 2: Correlation between Potassium Channel Expression and Sensitivity to Drug-induced Cell Death in Tumour Cell Lines

Abstract

The potassium channels Kv1.1, Kv1.3, Kv1.5, Kv11.1 and IK have been reported as being able to influence cellular proliferation and contribute to apoptosis. For example Kv1.3, Kv1.5 and IK are located in both the plasma membrane and the mitochondria where they participate in apoptotic signalling. In the case of the Kv channels this is through direct interaction with the Bcl-2 family member Bax. The altered expression of these proteins has been reported in neoplastic tissues but as of yet the systemic quantification of the expression of the aforementioned channels in tumour cell lines of various origins has not been attempted. In this study we investigated whether expression of any of the measured potassium channels at the mRNA and protein level could be correlated with sensitivity to a selection of apoptotic inducers. The results show correlation between the protein expression of Kv1.1 and Kv1.3 and responsiveness to treatment with staurosporine, ceramide and cisplatin. In addition we investigated the correlation between the expression of the Kv1.3 potassium channel and sensitivity to three membrane-permeant Kv1.3 inhibitors which have recently been shown to induce apoptotic cell death and to reduce tumour volume in animal models. High levels of expression of Kv1.3 were found to correlate with a reduction in cell survival upon treatment with clofazimine (Kv1.3 inhibitor). These data suggest that expression of Kv1.1 and Kv1.3 increase sensitivity to various apoptotic stimuli. The potassium channel expression profiles reported here may be used to inform approaches aiming to reopen or abrogate the apoptotic process or proliferation respectively

2.1 Introduction

Deregulation cell growth and/or blocks in the apoptotic machinery can culminant in tumour formation. Bearing this in mind K^+ channels have been reported in the literature to play a pivotal role in both the proliferation and the executed death of cells (Lang et al, 2000; Pardo, 2004; Wang, 2004). Indeed increased expression of K^+ channels has been associated with actively proliferating lymphocytes and cancerous cells (Cahalan & Chandy, 2009; Stuhmer et al, 2006). To expand upon this studies have shown differential expression of several K^+ channel family members in various tumour cell lines compared to non-transformed cells (Arcangeli et al, 2009). Furthermore recent publications have reported significant decreases in tumour volume *in vivo* after intravenous or intratumoral injection of Margatoxin a well-established Kv1.3 channel blocker (Leanza et al, 2012a). Reports of a correlation between K^+ channel activity and proliferation (Cahalan & Chandy, 2009) have been made however no such connection has been made for cell death (Szabo et al, 2010).

During apoptosis the cell experiences volume change and loss of intracellular K^+ a process which is regulated by the K^+ channels present in the plasma membrane (Lang et al, 2000). This loss of K^+ results in a reduction of ionic strength which has been postulated to release the inhibition of the pro-apoptotic caspases. The validity of this belief has recently been contended (Borjesson et al, 2011). The step by step process of the execution of apoptosis is generally well understood and it is widely accepted that the mitochondria have a central role in this process by releasing cytochrome *c* thus facilitating the activation of the caspase cascade. There is now mounting evidence to suggest a crucial role in the regulation of apoptosis for K^+ channels localized in the mitochondria. The two-pore TWIK related acid sensitive TASK-1 and TASK-3, NMDA receptors, inward rectifying Kir channels and calcium dependent K^+ channels which are all found in the PM have been shown to contribute to apoptotic cell death. Various other Kv channel subunits such as Kv1.1,

Kv1.3, Kv1.5, Kv11.1 (HERG) and Kv2.1 have been implicated (Jehle et al, 2011; Szabo et al, 2010).

The voltage-gated potassium channels (Kv) are a large family of channels expressed both in excitable and non-excitable cells. In excitable cells they control resting membrane potential and the frequency of action potential. Conversely in non-excitable cells such as the pancreatic islets, immune system and epithelial cells they are a part of a feedback loop regulating PM potential thereby influencing diverse processes from secretion to the proliferation of cells (Cahalan & Chandy, 2009; Wulff et al, 2009). Each Kv gene encodes a protein subunit four of which may form homo- or hetero-tetramers (Kv1-Kv12). The ability to form hetero-tetramers has resulted in functional diversity as well as the association with various accessory proteins, post-translational modifications and alternative slicing

The Kv family member Kv1.3 was the first to be reportedly modulated during apoptosis and was subsequently shown to contribute to increased K^+ efflux an event detectable during lymphocyte apoptosis (Lang et al, 2007; Szabo et al, 1996). Following on from this, pharmacological targeting of the calcium dependent intermediate and big conductance IK(KCa3.1) and BK (KCA1.1) potassium channels revealed that staurosporine (STS) induced apoptotic volume decrease was dependent upon K^+ efflux through the IK channel whereas TRAIL induced apoptotic volume decrease was through the BK channel (McFerrin et al, 2012). Importantly the down-regulation of Kv1.3 by siRNA in human peripheral lymphocytes conferred resistance to apoptosis (Szabo et al, 2008). Furthermore the knockdown of Kv1.3 and Kv1.1 channels in rat retinal ganglion cells (RGC) significantly reduced the amount cell death observed while Kv1.2 knockdown exhibited a minor effect on RGC cell death (Koeberle et al, 2010). It has been shown that depletion of Kv1.3 results in decreased expression of the pro-apoptotic molecules caspase-3, -9 and Bad by an unknown mechanism and that Kv1.1 depletion increased the mRNA expression of the anti-apoptotic Bcl-XL (Hu et al, 2008a). The knockdown of Kv1.1 results in increased viability in cerebellar granular neurons however the overexpression of Kv1.1 has also

been reported to reduce glutamate induced hippocampal cell death which conflicts with the previously mentioned results (Shen et al, 2009).

In pulmonary arterial hypertension the down regulation of Kv1.5 has been linked to reduced apoptosis and the over expression of Kv1.5 in human pulmonary artery smooth muscle cells and COS-7 cells resulted in greater amounts of cell death (Brevnova et al, 2004; Krick et al, 2001; Yuan et al, 1998). In addition Kv1.5 has been reported to be activated by mitochondria-derived ROS, indeed a mitochondria-ROS-Kv1.5 axis has been described as an O^2 sensing mechanism (Caouette et al, 2003). Kv11.1 which is expressed in the nuclear membrane as well as the PM has been recently reported to mediate H_2O_2 induced apoptosis in a number of cancer cell lines (Chen et al, 2011; Wang et al, 2002). Interestingly cytochrome *c* has been shown to activate Kv channels while the anti-apoptotic Bcl-2 family members inhibit them (Remillard & Yuan, 2004). Bring this section to a close the overexpression of the K^+ channel TASK-2 attenuated apoptotic cell death in an immature B cell line (WEHI-231) resulting from BCR ligation (Nam et al, 2011).

Taken as a whole these findings suggest that the down regulation of Kv channels confers resistance to apoptotic stimuli in a number of, if not all, cellular contexts. Importantly these data strongly implicate potassium channels as promising oncological targets. The present work focused on the members of the Kv1 subfamily and IK mentioned above which have been reported to modulate sensitivity to a plethora of apoptotic stimuli. In the mitochondria these channels may regulate apoptotic signalling in fact mtKV1.3 has been described as a novel interactor with the pro-apoptotic Bcl-2 family member Bax (Szabo et al, 2008). There is evidence to suggest this interaction is physiologically relevant as the over expression of mutant BaxK128E which is unable to associate with Kv1.3 was not capable of mediating cell death in WT Bax double knock out MEFs challenged with numerous inducers of apoptosis (Szabo et al, 2011). It is important to note that this interaction with Bax is not limited solely to Kv1.3 and has been described for Kv1.1, mtKv1.5 and mtKCa1.1 (BK) (Cheng et al, 2011; Leanza et al, 2012b). Very recently three membrane permeant inhibitors of

Kv1.3 (Psora-4, PAP-1 and clofazimine) were reported for the first time to induce cell death by directly targeting the mitochondrial channel. Pivotally these Kv1.3 inhibitors were capable of inducing apoptotic cell death in MEF and Jurkat cells which completely lacked Bax and Bak. This effect was removed upon the knockdown of Kv1.3 highlighting the specificity of their action. *In vivo* the intraperitoneal injection of clofazimine was shown to reduce tumour size by approximately 90 % in an orthotopic melanoma mouse model and no adverse effects where noted in a number of healthy tissues (Leanza et al, 2012a).

Considering the important role of the Kv channels for the regulation of apoptotic cell death and the mounting evidence to suggest altered expression of Kv1.1, Kv1.3, Kv1.5, Kv11.1 and IK in cancers we have addressed whether a correlation exists between the expression of these channels and the sensitivity of several tumour cell lines towards apoptotic inducers and gold-standard chemotherapeutics. Bearing in mind the reported profound effect of mtKv1.3 inhibition we also measure apoptosis induced by Psora-4, PAP-1 and clofazmine.

2.2 Materials and Methods

2.2.1 Reagents

Membrane permeable Kv1.3 inhibitors, Psora-4, PAP-1 and clofazimine (CLZM) as well as etoposide (ETOP), cisplatin (CisPL), C2-ceramide (CRM) and staurosporine (STS) were from Sigma Aldrich. The concentrations used to induce cell death were the following: STS: 2µM; CRM: 10µM; CisPL: 10µM; ETOP: 10 µM; Psora-4 and PAP-1: 20 µM; CLZM: 10 µM if not otherwise indicated. MDRi CSH and Probenecid were used at 4 and 100 µM concentration, respectively.

2.2.2 Cell Culture

MCF-7 and MDA-MB-231 breast cancer, DLD-1 and Colo205 colon carcinoma and SHSY5Y neuroblastoma cells were maintained in DMEM (Life Technologies) supplemented with 10 % foetal bovine serum (FBS), 10 mM Hepes (Sigma Aldrich), 1% non-essential amino acids (Life Technologies), 100 U/ml Penicillin and 0.1 mg/ml Streptomycin. OCIAML-3, HL-60, K562, ML-1 and MOLM-13 acute myeloid leukaemia cells were cultured in RPMI medium (Life Technologies) with 10% FBS, 10 mM Hepes, 1% non-essential amino acids, 100 U/ml penicillin and 0.1 mg /ml streptomycin. All cell lines were maintained in incubators at 37°C with a 5% of CO2. K562 cells were a gift from Prof. Arianna Deana- Donella (University of Padova, Italy).

2.2.3 Enriched Membrane Fraction Isolation

6 x 107 cells were collected in a tube, washed with 5 ml of Phosphate Saline Buffer (PBS) and centrifuged at 400 g for 10 min at room temperature (RT). Cells were resuspended in 300 µL of TES buffer (100 mM TES + 1 M sucrose, 100 mM EGTA, 1X cocktail protease inhibitors and lysed by an electronic pestle (Kontes, Sigma Aldrich) for 5 min on ice. Unbroken cells were separated by centrifugation at 500 g for 10 min at 4°C. The supernatant was collected and the still intact cells were resuspended in 200 µl TES buffer and subjected for an additional 5 min to homogenization with the electronic pestle on ice. After a new centrifugation at 500 g for 10 min at 4°C, the supernatants were combined in an Eppendorf tube. The soluble

cytosolic fraction was separated from the membrane- enriched fraction by centrifugation at 19,000 g for 10 min at 4°C. Finally, the pelleted membranes were resuspended in TES buffer and stored at -80°C. Protein concentration was determined using the BCA method in a 96 well plate (200 µl total volume for each well) incubating at 37°C in the dark for 30 min. Absorbance at 540 nm was measured by a Packard Spectra Count 96 well plate reader.

2.2.4 Western Blotting

Membrane enriched fraction proteins from the different cell lines were separated by SDS-PAGE in a 10% polyacrylamide gel containing 6 M Urea. To enhance protein separation, samples were solubilized for 1 h at RT in Sample Buffer (30% Glycerol + 125 mM Tris/HCl pH 6.8 + 9% SDS + 0.1M DTT+ Bromophenol blue). After separation by electrophoresis, gels were blotted overnight at 4°C onto Polyvinylidene fluoride (PVDF) membranes. After blocking with a 10% solution of defatted milk, the membranes were incubated with the following primary antibodies overnight at 4°C: anti-Kv1.1 (mouse monoclonal, Abnova); anti-Kv1.3 (rabbit polyclonal, Alamone Labs APC-101); anti-Kv1.5 (rabbit polyclonal, Alamone Labs APC -004); anti-Kv11.1 (hHERG; rabbit polyclonal, Alamone Labs); anti-KCNN4 (IK, rabbit polyclonal, Abcam, ABC 65985); anti-SERCA (mouse monoclonal, Affinity Bioreagents MA3-910); anti-Na^+/K^+ ATPase (mouse monoclonal, Abcam ab7671); anti-Bcl-2 (mouse monoclonal, Santa Cruz SC-9746); Mcl-1 (rabbit monoclonal, Cell Signalling 4572); Bcl-XL (mouse monoclonal, Santa Cruz SC-8392); Bax (rabbit monoclonal, Cell Signalling 2772); After washing off the excess primary antibody, the membranes were developed using corresponding anti-mouse or anti-rabbit secondary antibodies (Calbiochem). Antibody signal was detected with enhanced chemiluminescence substrate (SuperSignal West Pico Chemiluminescent Substrate, Thermo Scientific). Densitometry was performed using the Quantity One 1-D software (Bio-Rad).

2.2.5 MTT Assay

Cells were seeded at 40,000 (AML) or 5,000 (solid tumour) cells per well in a 96 well plate the day before treatment. Cells were treated with the different compounds, as indicated in the figure legends, for 24 h at 37°C. Cell survival was determined based on the proportionate transformation of MTT into formazan following the instructions by the supplier (CellTiter 96 Aqueous One Solution, Promega). Formazan accumulation was quantified by measuring absorbance on a Packard Spectra Count 96 well plate reader at 490 nm. All measurements were performed in quadruplicate in each experiment.

2.2.6 Apoptosis by FACS Analysis

Cells were seeded at 80,000 per well in a 96 well plate and treated for 24 h at 37°C with different compounds as indicated in figure legends. Cells were then incubated with 2 µL of FITC conjugated Annexin-V (Roche) for 20 min at 37°C. After incubation cells were collected in FACS tubes and analysed by cytofluorimetry (FACSAnto II, BD biosciences).

2.2.7 Analysis of Microarray Data

Raw microarray data in .CEL file format produced by the Weinstein lab was acquired from the NIH cell-miner database (http://discover.nci.nih.gov). Background correction and normalization of the dataset has been performed using the Affy package of Bioconductor (RMA algorithm) in the statistical environment, R (version 2.15.1). The microarray probeset best representing the genes of interest has been selected using the JetSet method designed for scoring and ranking probe sets for specificity, splice isoform coverage and robustness against the degeneration of the transcript (Li et al, 2011). The selected representative mRNA probeset (Probe Set IDs: KCNA1 (230849_at), KCNA3 (207237_at), KCNA5 (206762_at), KCNN4 (204401_at) and KCNH2 (205262_at)) for each gene of interest was extracted from the normalised microarray data and graphed after sorting the cell lines by reducing expression level.

2.2.8 Correlation Studies: Acquisition of Cell Survival Data for Microarray Data

Cisplatin, etoposide and staurosporine-induced cytotoxicity in the NCI60 panel of cell lines has been obtained from the following public database. The drug concentration inducing 50% cell death (lethal concentration-50; LC50 value (Log10 (M)) has been determined for multiple treatments of etoposide (n=4), staurosporine (n=3) and cisplatin (n=4) dosages. Cell death was measured as follows. After 24 h, two plates of each cell line are fixed with TCA; this is a measurement of the cell population for each cell line at the time of drug application. Following drug addition, the plates are incubated for an additional 48 h at 37°C, 5 % CO2, 95 % air, and 100 % relative humidity. For adherent cells, the treatment is stopped by the addition of cold TCA. Cells are fixed by the gentle addition of 50 µl of cold 50 % (w/v) TCA (final concentration, 10 % TCA) and incubated for 60 minutes at 4°C. The supernatant is discarded, and the plates are washed five times with water and air dried. Sulforhodamine B (SRB) solution (100µl) at 0.4 % (w/v) in 1 % acetic acid is added to each well, and plates are incubated for 10 minutes at room temperature. After staining, unbound dye is removed by washing five times with 1 % acetic acid and the plates are air dried. Bound stain is subsequently solubilized with 10mM trizma base, and the absorbance is read at a wavelength of 515 nm. For suspension cells, the methodology is the same except that the assay is terminated by fixing settled cells at the bottom of the wells by gently adding 50 µl of 80 % TCA (final concentration, 16 % TCA). These values were largely comparable; therefore the mean LC50 value across the treatments has been calculated and used for correlation analyses.

2.2.9 Correlation Studies: Statistical Analysis

All analyses were done in R (version 2.15.1), and correlation graphics were produced using the R corrgram package (version 1.4). The mRNA and/or protein expression values for potassium channels (Kv1.1, Kv1.3, Kv1.5, Kv11.1 and IK) and a selection of apoptosis regulators (Bcl-2, BclxL, Mcl-1, Bax and XIAP) were treated as continuous variables. The association between gene expression and response to the studied treatments has been assessed using the *Pearson product moment correlation coefficient*. The correlation coefficient *r*, also called the *linear correlation coefficient* measures the strength and the direction of a linear relationship between two variables. The value of r is between -1 and +1. The closer the r value approaches -1 or +1, the stronger/closer the correlation is. A positive r value indicates that as one variable increases so does the other while a negative value describes an inverse relationship between the variables such that as one goes up the other goes down (e.g. as K^+ channel expression increases, viability in response to staurosporine treatment decreases). An r value of 0 indicates no correlation. Significance was determined using two-tailed paired t-test. Due to the limited availability of a relatively small sample number due to the technical limitations imposed

2.3 Results

2.3.1 Potassium Channel Expression in Different Tumour Cell Lines

Information on the expression of potassium channels in tumours and tumour cell lines is relatively limited. In order to assess this Affymetrix data was obtained for 59 cancer cell lines (Table 2.1). An analysis was performed to evaluate the expression of several potassium channels proteins on the mRNA level namely Kv1.1 (KCNA1), Kv1.3 (KCNA3), Kv1.5 (KCNA5), IKCa (KCNN4) and Kv11.1 (KCNH2). All of the potassium channels exhibited a narrow expression range with the exception of IK (KCNN4). This implies these genes are ubiquitously expressed at the mRNA level in the cell types tested. (Fig. 2.1 A)

Cancer type	Cell Lines	Cancer type	Cell Lines
Leukaemia	CCRF-CEM	NSCLC	A549
Leukaemia	HL-60	NSCLC	EKVX
Leukaemia	K-562	NSCLC	HOP-62
Leukaemia	MOLT-4	NSCLC	HOP-92
Leukaemia	RPMI-8226	NSCLC	H226
Leukaemia	SR	NSCLC	H23
Colon cancer	COLO 205	NSCLC	H322M
Colon cancer	HCC2998	NSCLC	H460
Colon cancer	HCT-116	NSCLC	H522
Colon cancer	HCT-15	CNS cancer	SF-268
Colon cancer	HT-29	CNS cancer	SF-295
Colon cancer	KM12	CNS cancer	SF-539
Colon cancer	SW-620	CNS cancer	SNB-19
Melanoma	LOXIMVI	CNS cancer	SNB-75
Melanoma	M14	CNS cancer	U251
Melanoma	MDA-MB-435	Ovarian cancer	IGROV1
Melanoma	SK-MEL-2	Ovarian cancer	OVCAR-3
Melanoma	SK-MEL-28	Ovarian cancer	OVCAR-4
Melanoma	SK-MEL-5	Ovarian cancer	OVCAR-5
Melanoma	UACC-257	Ovarian cancer	OVCAR-8
Melanoma	UACC-62	Ovarian cancer	NCI/ADR-RES
Renal cancer	786-O	Ovarian cancer	SK-OV-3
Renal cancer	A498	Prostate cancer	PC-3
Renal cancer	ACHN	Prostate cancer	DU-145
Renal cancer	CAKI-1	Breast cancer	MCF-7
Renal cancer	RXF393	Breast cancer	MDA-MB-231
Renal cancer	SN12C	Breast cancer	HS578T
Renal cancer	TK-10	Breast cancer	BT549
Renal cancer	UO-31	Breast cancer	T47D
		Breast cancer	MDA-MB-468

Table 2.1: Comprehensive listing of the 59 tumour cell lines for which affymetrix data was obtained from the NIH

We assessed whether the expression of potassium channels (Kv1.1, Kv1.3, Kv1.5, IK and KV11.1) on the mRNA level correlated with sensitivity to certain chemotherapeutics, namely cisplatin and etoposide, as well as the classical inducer of intrinsic apoptosis staurosporine. Firstly the mean LC50 (the concentration that caused 50% reduction in viability) of the cytotoxic drugs was determined as outlined in the materials and methods section. Next the Pearson's product moment correlation coefficient was determined as a measure of the strength of association between the mRNA expression level and drug sensitivity. No association was observed between any of the potassium channels and any cytotoxic drug (Fig. 2.1 B) which may be explained by the disparity between mRNA and protein expression levels which is well documented in the literature. Bearing this in mind we

measured the expression of the K^+ channel proteins in a panel of tumour cell lines of different origin including acute myeloid leukaemia cell lines (OCI-AML-3, HL-60, K-562, ML-1 and MOLM-13), breast adenocarcinoma (MCF-7 and MDA-MB-231), colon carcinomas (DLD-1 and COLO 205) and a neuroblastoma cell line (SHSY5Y) (Fig. 2.2 A).

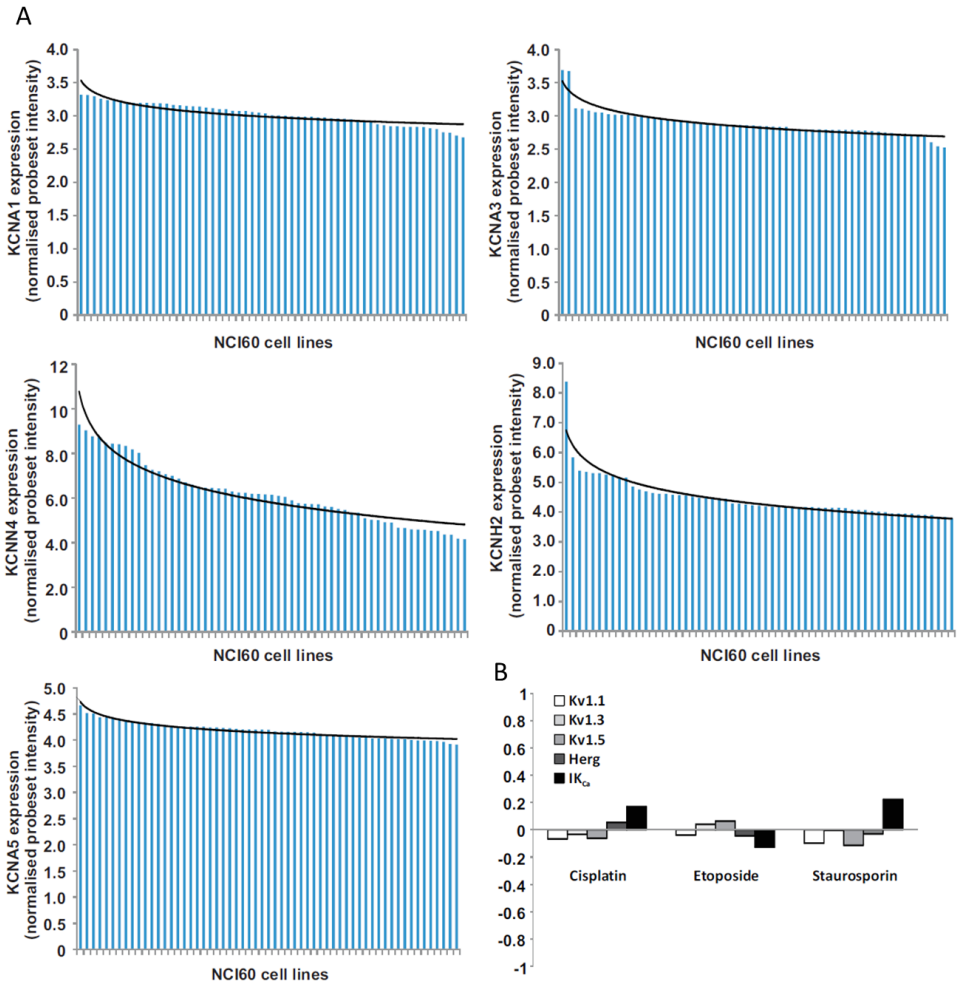

Figure 2.1: Lack of correlation between K^+ channel mRNA expression and susceptibility to cytotoxic drugs. mRNA expression values for (A) KCNA1 (Kv1.1), KCNA3 (Kv1.3), KCNA5 (Kv1.5), KCNN4 (IK or KCa3.1) and KCNH2 (Kv11.1 or HERG) were extracted for 59 tumour cell lines from a publicly available microarray data set. All of the above-mentioned channels appear to be expressed across the 59 lines (bars). (B) Correlation between K^+ channel mRNA expression and response (lethal concentration-50, LC50) to the cytotoxic agent cisplatin (cisPL), etoposide (ETOP) and staurosporine (STS). None of the correlation index values appeared to be significant using paired, two tailed t-test.

In order to determine K^+ channel protein expression by Western blot we used membrane-enriched subcellular fractions rather than whole cell lysates as the K^+ channels are relatively low abundance (Fig. 2.2 A). Antibodies against the endoplasmic reticulum calcium ATPase (SERCA) and the plasma membrane sodium-potassium ATPase (Na^+/K^+ -ATPase) were used as loading controls. Since the expression of Na^+/K^+ -ATPase at the mRNA level across the NCI-60 panel of cell lines was seen to be constant, K^+ channel protein expression was measured by densitometry and normalized to the Na^+/K^+ -ATPase signal. The expression of the studied K^+ channels at the protein level exhibited much more variation than at the mRNA level (Fig. 2.2 B)

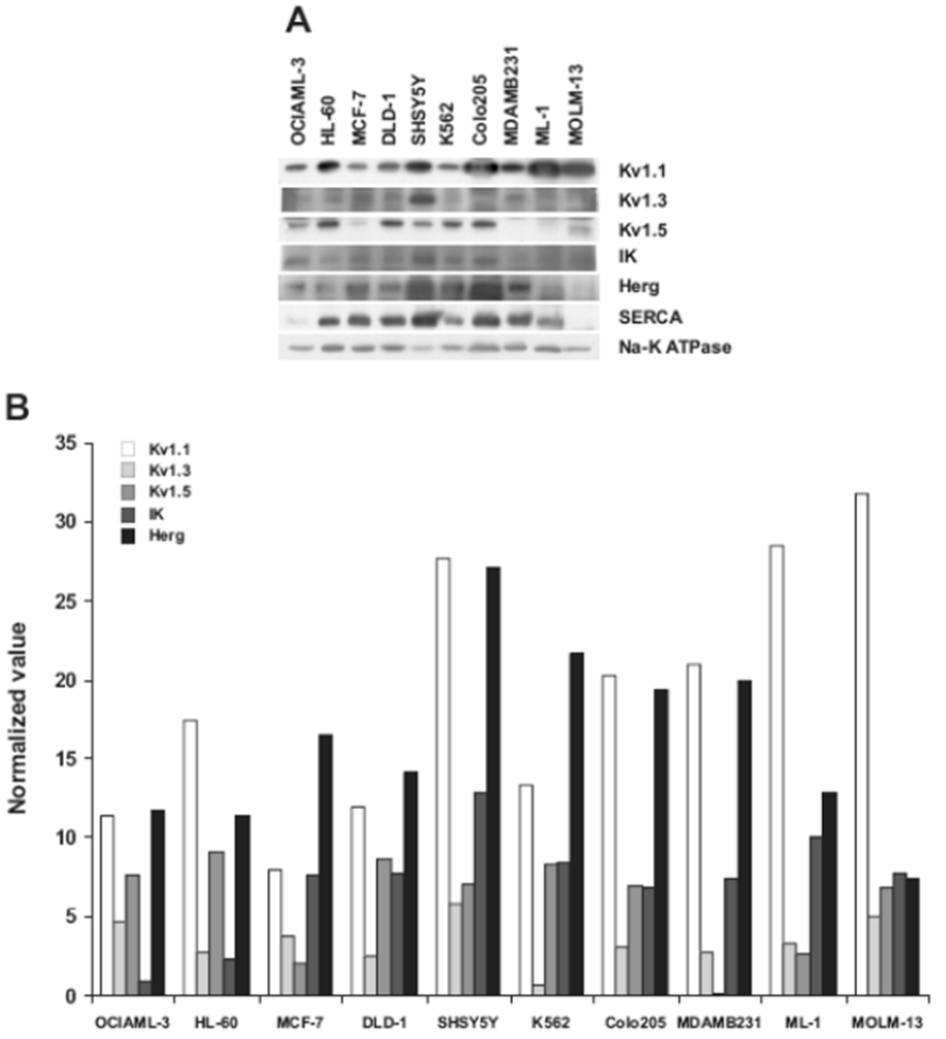

Figure 2.2: Expression of Kv1.1, Kv1.3, Kv1.5, IK and Kv11.1 proteins in nine different cancer cell lines. (A) Membrane-enriched fractions obtained from the indicated cell lines were loaded on SDS-PAGE (40 _g proteins/lane). Western blot was performed with specific antibodies against the indicated channel proteins. Na/K ATP-ase was used as loading control. Apparent molecular weights of the bands are the following: Kv1.3: 65 kDa; Kv1.1: 50 kDa; Kv1.5: 66 kDa; IKCa: 50 kDa; Herg: 135 kDa; PMCA: 140 kDa; SERCA: 104 kDa; Na^+/K^+ ATP-ase: 100 kDa. The blots shown derive from 2 gels processed together. Similar results were obtained in another experiment. (B) Quantification of K^+ channel expression based on densitometry. Values refer to those obtained following normalization as described in the text, from two WBs including the one shown in (A).

2.3.2 Tumour cell sensitivity to cytotoxic agents activate the mitochondrial apoptotic pathway

The literature reports compelling evidence in various systems which implicate low potassium channel expression as being able to decrease sensitivity to apoptotic stimuli while the opposite is observed upon over expression. Between the 9 cell lines we tested for K^+ channel expression at the protein level there was a marked differences in expression of the studied K^+ channels (Fig. 2.2A and Fig 2.2B). Thus we determined the sensitivity of the 9 cell lines to cytotoxic agents such as staurosporine (STS) and ceramide (CRM) and chemotherapeutics, namely etoposide (ETOP) and cisplatin (cisPL) using MTT viability assay (Fig. 2.3 A) and Annexin V staining (Fig. 2.3C). The response of each individual cell line to the apoptotic stimuli varied broadly but the drug's effects were closely correlated (Fig. 2.3B). Interestingly the two genotoxic agents etoposide and cisplatin had similar effects in approximately two thirds of the cell lines tested (OCI-AML-3, ML-1, SHSY5Y, COLO205, DLD-1 and MCF-7). Staurosporine and ceramide also displayed comparable effects in over half the cell lines tested (OCI-AML-3, ML-1, MOLM-13, SHSY5Y, DLD-1 and MDA-MB-231) which is indicative of these agent's closely associated mechanism of action (Fig. 2.3A, Fig. 2.3B). We observed a significant positive correlation between ceramide and both cisplatin and etoposide in that those cells which were sensitive to ceramide also appeared to be sensitive to etoposide and cisplatin (Fig. 2.3B). The normalized protein expression value of the K^+ channels (Fig. 2.2B) was then correlated with the MTT viability values as an indicator of sensitivity to the cytotoxic drugs (Fig. 2.3A). An inverse correlation was seen between Kv1.1 and sensitivity to staurosporine ($p=0.03$). Additionally the analysis revealed an inverse correlation between Kv1.3 and cisplatin sensitivity ($p=0.09$) as well as Kv1.3 and ceramide ($p=0.10$) (Fig. 2.3D).

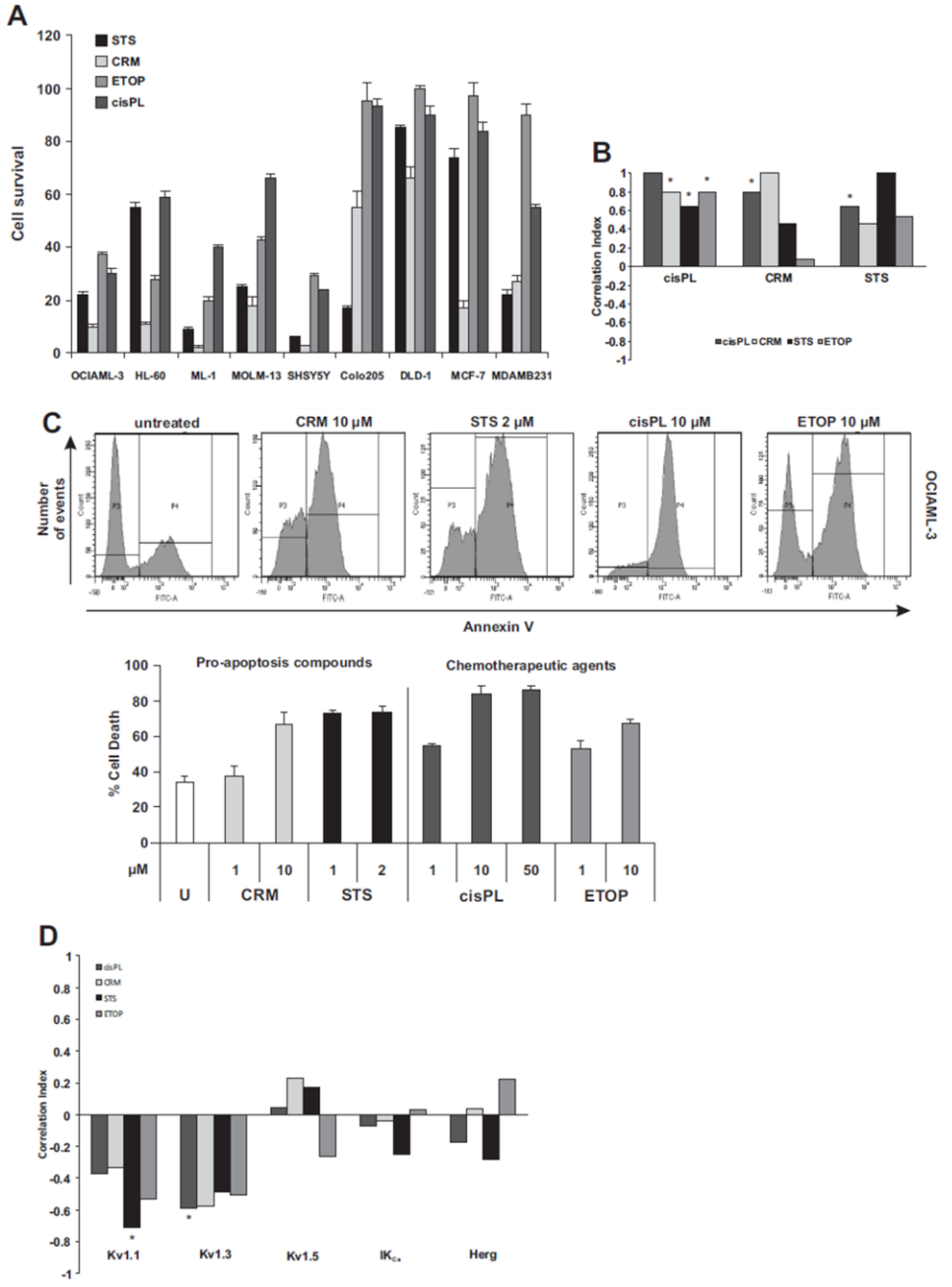

Figure 2.3: Sensitivity of cancer cell lines to cytotoxic drugs staurosporine, ceramide, etoposide and cisplatin as a function of K^+ channel expression. (A) The indicated cell lines were treated with the drugs for 24 hours and cell survival was determined by MTT assay (mean ±SD are shown). Measurements were performed in quadruplicate in 3 sets of separate experiments. (B) Correlation between all the cytotoxic drugs tested against each other. As can be observed from the graph each compound correlated 100% with itself (r=+/-1). This acted as a control for all correlation data analysis carried out. Significant correlations were observed for cisplatin/ceramide, cisplatin/Staurosporine, and cisplatin/etoposide. (C) Representative FACS analysis determining apoptosis (as assessed by Annexin binding) and percentage of apoptotic death following the indicated treatments (n=3) (mean ±SD are shown). (D) All treatments with cytotoxic compounds were shown to have a positive correlation with all K^+ channels examined in this study. Potassium channels that were shown to have a significantly strong positive correlation with cytotoxic treatments included Kv1.1 with STS (p=0.0302) and Kv1.3 with cisPL (p=0.09144).

The inverse nature of the correlation values, indicate that as the expression of the potassium channel goes down the resistance to the cytotoxic agents increases. There was significant inverse correlation between Kv1.1 and responsiveness to staurosporine which is in accordance with previous reports that cells which were otherwise resistant to treatment with staurosporine underwent apoptosis when expressing Kv1.1 (Fig. 2.3D). No significant correlation was observed for any of the other potassium channels (Kv1.5, IKCa and Kv11.1) with any of the cytotoxic agents (Fig. 2.3D).

2.3.3 Cancer cell sensitivity to membrane permeant Kv1.3 inhibitors acting upon the mitochondrial Kv1.3 potassium channel

It has previously been reported that permeant inhibitors of the Kv1.3 potassium channel can selectively kill cancer cells both *in vitro* and *in vivo.* Of the 9 cells lines which were assessed for expression of potassium channels on the protein level all expressed Kv1.3 except K-562 cells which were retained as a negative control (Fig. 2.2B). The tumour cell line panel was treated with the indicated doses of the permeant Kv1.3 inhibitors Psora-4, PAP-1 and clofazimine for 24 hours. Reduction in cell viability was assessed by MTT viability assay (Fig. 2.4A). Once again the decrease in viability was confirmed for the myeloid cell lines by Annexin V staining (Fig. 2.4C). The analysis described a significant inverse correlation between the expression of Kv1.3 and sensitivity to clofazimine treatment ($p=0.069$) confirming the specific action of the Kv1.3 inhibitor (Fig. 2.4D). The only other significant correlation observed was the positive correlation between HERG and Psora-4 implying HERG expression aids the cells in surviving Psora-4 treatment ($p=0.08$) (Fig. 2.4D)

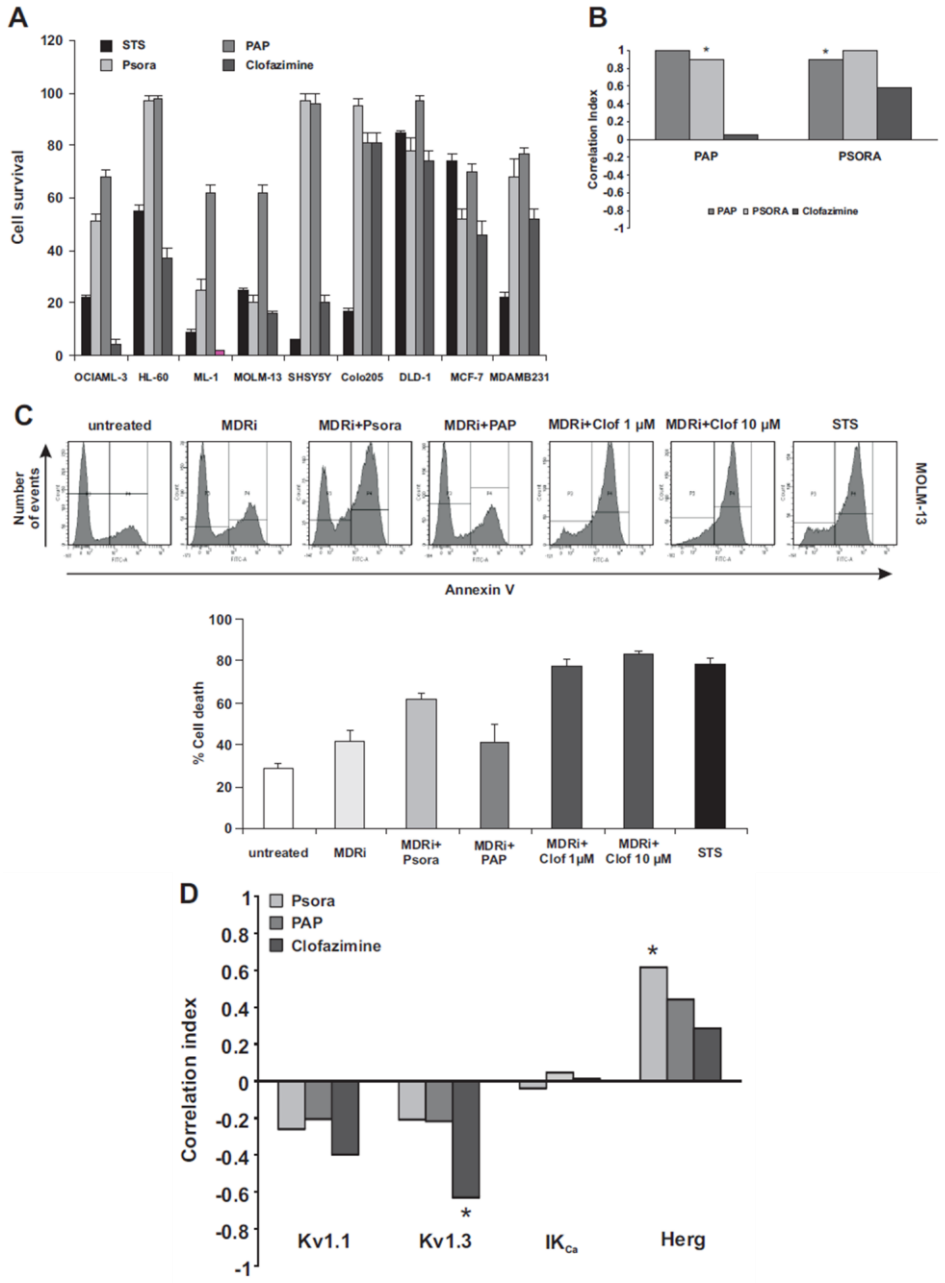

Figure 2.4: Sensitivity of cancer cell lines to membrane-permeant Kv1.3 inhibitors as a function of K^+ channel expression. (A) MTT assay and analysis as in (Fig. 2.3A). (B). The correlation between the Kv channels inhibitors were all in a positive direction. PAP-1 (PAP) correlated against Psora 4 showed the most significant correlation indicating the similarity of functionality in these compounds. As can be observed in the graph above each treatment correlates fully (r = +/-1) with itself. They therefore were included to act as experimental controls for data analysis in R (bioconductor). (C) A representative experiment in MOLM-13 cells, performed as in (Fig. 2.3C). (D) Association between K^+ channel protein expression and Kv1.3 channel inhibitor-induced cell death. The * denotes significant values determined by paired, two-tailed t-test.

We next questioned if there was an association between the expression of the Bcl-2 family members Bcl-2, Bcl-XL, Mcl-1 and Bax with the Kv1.3 inhibitors. Expression of the Bcl-2 family members was carried out using Western blotting followed by densitometry for the 9 tumour cell lines. Expression was normalized using the levels of the same protein in an internal reference cell line (HCT116, described in greater detail in chapter 4). The study uncovered no significant positive correlation between the expression of any of the Bcl-2 family members and reduction of cell viability after treatment with the permeant Kv1.3 inhibitors (Fig. 2.5). This indicates that induction of apoptosis by K^+ channel inhibition is independent of the Bcl-2 family (Fig. 2.5)

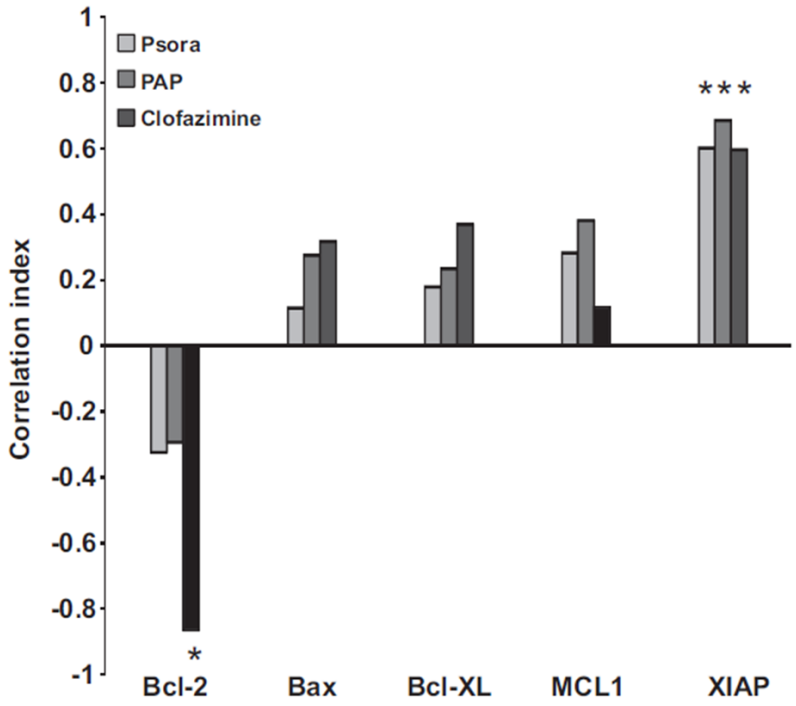

Figure 2.5: Relationship between the expression of Bcl-2 family members and reduction of cell survival induced by K^+ channel inhibitors. Correlation analysis was performed on the basis of Western blot and densitometry regarding expression of the indicated proteins (see chapter 4) and results of the MTT assay. Asterisks denote significant values determined by paired, two-tailed t-test.

On the other hand an inverse correlation does exist between Bcl-2 expression and sensitivity to clofazimine which suggests that cells with high expression of Bcl-2 tend to be more responsive to treatment with clofazimine (Fig. 2.5). Conversely expression of XIAP was closely linked to a reduction in sensitivity to all the Kv1.3 inhibitors which fits into the current model of action of how Kv channel inhibition induces cell death (Fig. 2.5).

2.4 Discussion

We assessed the expression of five potassium channels in 9 tumour cell lines which had previously been reported to play appreciable roles in the apoptotic programme (Fig. 2.2B). A correlation analysis was performed in order to understand whether or not potassium channels influence the responsiveness of cancer cell lines to treatment with a variety of cytotoxic agents. This approach identified a significant inverse correlation between the expression of Kv1.1 and Kv1.3 and sensitivity to staurosporine, cisplatin and ceramide (Fig. 2.3D). The channel Kv1.3 is of particular interest as its expression is known to be altered in several cell lines and the existence of specific inhibitors allows for targeted applications. To further elaborate the Kv1.3 is expressed in the early stages of prostate cancer progression, breast cancer specimens from patient show expression of Kv1.3 and the Kv1.3 gene is upregulated in B cell lymphoma as well as gliomas (Alizadeh et al, 2000; Preussat et al, 2003). Furthermore Jang and colleagues presented evidence that the expression of Kv1.3 is positively correlated with disease stage in breast cancer (Jang et al, 2009). The expression of both Kv1.3 and Kv1.5 is high in leiomyosarcoma (LMS) tumours compared to surrounding non-transformed tissues and a correlation was seen between potassium channel expression and tumour aggression (Bielanska et al, 2012). The membrane permeant inhibitor of Kv1.3 clofazimine caused a reduction in tumour volume (90%) in a melanoma model emphasizing the potential benefits of Kv1.3 inhibition in the treatment of cancers (Leanza et al, 2012a). This work provides detailed information about potassium channel expression in a number of cancer cell lines which were previously uncharacterised in this regard (Fig. 2.2B). While reports suggest acute myeloid leukaemia cell lines express high levels of Kv11.1 for example which correlates with an aggressive phenotype (Arcangeli et al, 2012) no such data exists for the OCI-AML-3 cell line which we noted in this study as expressing Kv11.1 as well as detectable levels of all other studied potassium channels (Fig. 2.2B). The ML-1 cell line expressed relatively high amounts of Kv1.1 in comparison to the other AML cell lines but no Kv1.5 while HL-60 expressed more Kv1.1 and less Kv1.3 than the OCI-

AML-3 cell line (Fig. 2.2B). The channels Kv11.1 and IK are not expressed to a significant extent in MOLM-13 cells while all other channels are (Fig. 2.2B). The remaining AML cell line K-562 was not seen to express Kv1.3 but did possess Kv11.1 which is in agreement with the literature (Fig. 2.2B). The breast cancer cell MCF-7 expressed all the studied potassium channels barring Kv1.5 and MDA-MB-231 cells which are derivatives of the MCF-7 cells with higher metastatic potential showed much higher levels of Kv1.1 and Kv11.1 and lower amounts of Kv1.5 than MCF-7 cells (Fig. 2.2B). In regard to colon cancer cell lines inhibition of potassium channels is known to block proliferation in DLD-1 cells while little to no information is available for Colo205 (Yao & Kwan, 1999). It is known that the Kv1.3, Kv1.5 and Kv11.1 genes are transcribed in primary colon cancer samples (Abdul & Hoosein, 2002; Ousingsawat et al, 2007) moreover Kv11.1 expression has also been associated with tumour stage in this disease (Lastraioli et al, 2004). The collated expression analysis within this study may be utilized in the near future in aiding research focused upon cellular proliferation and apoptosis. However further work is required in order to ascertain whether the protein expression is closely linked to functional channels.

Given the reported effect of mtKv1.3 and induction of apoptosis we expected to observe a close correlation between the expression of the aforementioned potassium channel and the amount of apoptosis induced by Kv1.3 inhibition by Psora-4, PAP-1 and clofazimine. As expected the potency of clofazimine was strongly inversely correlated with Kv1.3 expression across several cell lines (Fig. 2.4D). An effect which occurred despite very high expression of Bcl-2 which is known to occur in myeloid cell lines (Fig. 2.5). This data suggests that clofazimine, which is already in the clinic exhibiting an exemplary safety profile, may be applicable as a novel chemotherapeutic. As to why no correlation was seen between Kv1.3 expression and sensitivity to the other 2 membrane permeant inhibitors of Kv1.3 (Fig. 2.4D) it is known that clofazimine can also act as a multi-drug resistance (MDR) inhibitor. Therefore the concentration of clofazimine in cells may be much either than either Psora-4 or PAP-1. The induction of

apoptosis by clofazimine is unlikely to be independent of Kv1.3 as knockdown of said channel by siRNA has been reported to abrogate its ability to induce apoptosis. In addition the responsiveness of cells to Psora-4 was shown in this study to decrease upon expression of Kv11.1. The mechanism of which remains unknown (Fig. 2.4D).

The disparity between the sensitivity of myeloid and neuroblastoma compared to breast and colon cancer cell lines to the membrane permeant potassium channel inhibitors may be explained but clarification and validation is required. Potential explanations range from differential expression patterns of MDR pumps or the block of apoptosis downstream of the mitochondria by XIAP.

2.5 Future perspectives

Drug repositioning or the application of known drugs to new indications has become increasingly more popular as a fast and cost effective form of drug discovery. Examples of successful repositioning include Viagra and metformin. Currently clofazimine is marketed as lamprene an anti-leprosy agent in the treatment of lepromatous leprosy. In general lamprene is very well tolerated. The most consistent side effects seen were dose dependent and reversible upon cessation of treatment. These included a change in skin pigmentation to brownish black, abdominal pain, nausea, diarrhoea, burning or itchy eyes as well as the discoloration of urine or faeces. Our data suggest tumours expressing the Kv1.3 potassium channels are likely to undergo apoptotic cell death upon treatment with clofazimine (Fig. 2.4D). Being already available clinically with limited toxicity we believe clofazimine could very well represent a future drug repositioning success storey.

In closing this work presented here has identified a potential novel chemotherapeutic and provides experimental data which may be used in the near future for the study of the role potassium channels in various cellular contexts.

Chapter 3: Co-acting gene matrices predict TRAIL responsiveness of tumour cells with high accuracy

Abstract

TRAIL is a member of the TNF family of cytokines which can selectively induce apoptosis in cancerous cells. For this reason recombinant TRAIL is being considered for the treatment of cancer. During their development cancer cells disengage pivotal sections of the machinery required for apoptosis. This is also the case for the TRAIL pathway. Concurrently 50-60% of tumours are known to be resistant to TRAIL. Additionally reports found that TRAIL can initiate NF-κB -pro-survival pathways in resistant cell lines which may promote tumour aggression. Therefore a reliable biomarker that can identify responsive patients is needed. Biomarker discovery is often based on the identification of differentially expressed genes from transcriptome studies. In these analyses the threshold is a minimum arbitrary level (e.g. two fold induction.) in the majority of samples. This gene-by-gene approach cannot assess interaction between genes. Minimal forays have been made into identifying genes which potentially influence each other, i.e. their combined presence or ratio correlates stronger with a given phenotype. These co-acting genes, even if they are not robustly overexpressed or repressed, may better identify decisive interactions and predict response. Here we show that by utilising classification trees we could identify a panel of co-acting genes. As a model system we used the TRAIL pathway with transcriptomic data for 109 tumour cell lines with known TRAIL sensitivity. A singular probe-set for each gene was selected using the JetSet algorithm and these were used to build classification trees (CART). We ranked the co-acting genes by their Gini importance. From an initial top-predicting 1000 genes we identified the smallest grouping of co-acting genes that was most predictive. With this approach we achieved a very high prediction accuracy (AUC=0.85) with a set of 300 co-acting genes. We report that when the relationship between genes was considered the identified 300 co-acting genes performed better than other classifiers (0.72) which were developed on a gene-by-gene analysis in predicting TRAIL sensitivity

3.1 Introduction

Cancer therapy traditionally consists of surgery followed by sub-lethal administration of radiation or cytotoxic agents. Advances in the last 20 years have allowed for the development of therapeutics that target aberrant pro-oncogenic and or pro-survival proteins in tumours and thus induce cell death or sensitize the tumour cells to an additional drug such as genotoxic agents. One of the first of such targeted regimes is Trastuzumab a monoclonal antibody against the epithelial growth factor receptor (ErbB-2/Her-2). Her-2 is overexpressed in approximately 15-30% of breast cancer patients and in these cancers the tumour cells depend on Her-2-mediated pro-survival signalling (Brachmann et al, 2009; She et al, 2008; Slamon et al, 1987; Slamon et al, 1989). The inhibition of the Her-2 receptor improves response rate and survival in cohorts overexpressing the receptor (Montemurro et al, 2004).

While targeted therapies are very powerful the patient cohorts where the targeted aberrancy is present and thus would benefit from the treatment has to be identified. It is now well accepted that identification of powerful biomarkers that predict prognosis of treatment efficacy (theranostic markers) requires a systemic analysis usually through one (or more) of the omics technologies.

Owing to its high sensitivity and full coverage of the human genome transcriptomic studies are one of the most widely applied tools for biomarker search. Biomarkers are typically identified from transcriptome data by selecting genes that are differentially expressed in the majority of the samples or in a specific subgroup. This gene-by-gene approach only considers the altered expression of a gene between two sample groups (e.g. control and treated or responding versus non-responding) and does not compare the expression of one gene to another within the same sample. There are very few studies which address the question of how genes relate to each other although this may be crucial in determining biological outcome. Often the change in the expression of individual genes is minor

but it can be sufficient to significantly alter the relative expression or the expression ratios of interacting gene products. For example if the expression of Gene A increases 1.5 fold and expression of Gene B an inhibitor of Gene A reduces 1.5 fold the difference in the relative amount of the two genes changes 2.2 fold. Thus the relative expression of genes acting/participating in the same biological process may better describe the behaviour of a cell and better predict the response of a cell to a stimulus.

To test this hypothesis we chose a well-characterised signal transduction pathway. TRAIL is expressed by activated monocytes, natural killer and dendritic cells (Almasan & Ashkenazi, 2003; Bouralexis et al, 2005; Takeda et al, 2001a). TRAIL is involved in downregulating the immune response and probably most importantly TRAIL is a key effector in tumour immune surveillance (Griffith et al, 2007; Kayagaki et al, 1999; Takeda et al, 2001a). TRAIL has been found to selectively induce apoptotic cell death in cancerous cells through binding to its receptors DR4 and DR5. The activated receptors recruits FADD to which the proteases pro-caspase-8 and/or pro-caspase-10 bind. This protein complex known as the death-inducing signalling complex (DISC) serves as a platform for pro-caspase-8 and -10 autoactivation. Active caspase-8/10 then moves into the cytoplasm where they activate the effector caspases (caspase-3, -6 and -7) that execute the cell death programme. In addition to executioner caspases, caspase-8 can also cleave and thus activate the BH3-only Bcl-2 family member Bid (thus forming tBid); tBid engages the mitochondrial apoptotic pathway through the activation of Bax and Bak, resulting in MOMP. Once caspases-9 is active it amplifies the apoptotic signal by activating the executioner caspases (Mellier et al, 2010).

Due to the tumour-specific cytotoxicity of TRAIL its recombinant version is currently being tested in PhaseI/II clinical trials. Although the cells lose their resistance to TRAIL when they undergo malignant transformation tumours can re-acquire resistance at later stages of their progression. In the case of TRAIL there may be a selective pressure on the tumour cells to gain resistance in order to evade immune-mediated killing. While the TRAIL apoptotic machinery is well studied and a number of regulatory mechanisms

potentially functioning in tumour cells have been identified none of them have proven to be useful as a predictive marker.

Using the TRAIL apoptotic pathway as a model we tested whether the expression ratios of genes acting together in the pathway, i.e. their function being linked either directly or indirectly (co-acting genes) can predict the sensitivity of a given tumour cell line to TRAIL. As previously discussed (section 1.4) there are machine learning techniques such as SVM, K-nearest neighbours and random forest that can identify complex patterns in data allowing them to act as classifiers. The random forest algorithm was chosen for our analysis for a number of reasons. (1) First and foremost the random forest model partitions the samples using multiple variables sequentially. In this way the selection of the second variable is dependent on the performance of the first. Thus the model considers the expression of multiple genes relative to each other and can incorporate interactions between the predictor variables. (2) Returns measures of the importance of each gene in models construction and performance as a classifier. This facilitates the identification of the core non-redundant predictor variables. (3) Performs well as a classifier even when most variables are noise and can be used when there are many more variables than samples. This means that pre-filtering of the genes is not required. The technique can model the whole transcriptome.

In this study we report that when the relationship between expressed genes was considered with the help of random forest we could predict TRAIL responsiveness with high degree of sensitivity and specificity (AUC = 0.85). This is higher than the currently available best-performing gene signature consisting of 71 genes that can predict TRAIL sensitivity with AUC=0.72.

3.2 Materials and Methods

3.2.1 Analysis of microarray data

Raw microarray data in .CEL file format produced by the Ashkenazi lab was acquired from the Gene Expression Omnibus (GEO) accession number GSE8332 (Wagner et al, 2007), hereby referred to as the training data. Background correction and normalization of the dataset has been performed using the RMA algorithm in the Affy package of Bioconductor (Gautier et al, 2004) in the statistical environment, R (version 2.15.1). In order to reduce noise in the analysis caused by multiple probesets per gene, the probeset best representing each gene was selected using the JetSet algorithm designed for scoring and ranking probesets for specificity, splice isoform coverage and robustness against the degeneration of the transcript (Li et al, 2011). Microarray data for 40 tumour cell lines was acquired from NIH CellMiner (test data) which was normalized alongside the Ashkenazi data set.

Those genes differentially expressed in the training data were identified using Genespring GX v11. All .cel files were imported into Genespring using RMA summarization. Values were transformed (Log_2) and normalized to the 75^{th} percentile. Genes were filtered by expression retaining only those with an expression over the 20^{th} percentile in at least 75% of the cell lines with a greater than 2 fold change in expression between TRAIL sensitive and resistant cell lines. A one way ANOVA unequal variance (Welch) was used to test for significance. Multiple testing corrections were by Benjamini-Hochberg. Using a corrected p-value of <0.05, 312 genes were identified as differentially expressed.

3.2.2 Cancer cell line TRAIL sensitivity

The sensitivity of the cell lines included in the microarray was assessed and described by Wagner and colleagues (Wagner et al, 2007). Briefly, cell viability was assessed with MTT assay. A cell line was defined as being sensitive if the viability of the sample dropped below 50% after treatment

with recombinant human TRAIL at a concentration of 1ug/ml in a 72 h assay while in the presence of either high (10%) or low serum (5%) concentration. A cell line was deemed resistant to TRAIL if greater than 50% of the cells were viable after TRAIL treatment at a concentration of 1ug/ml for 72 h in the presence of either high or low serum concentration. Cell lines were considered moderately sensitive to TRAIL if they showed less than 50% viability in at least 1 but not all 3 biological repeats or at only one of the 2 serum concentrations. For the purpose of this study we used only those cell lines that were deemed TRAIL sensitive or resistant.

3.2.3 Gene relationship analysis

The selected representative mRNA probesets for each gene were extracted from the training microarray data and were then classified using random forest (RF) modelling (number of classification trees=10,000, mtry=default). The top 1000 probesets, ranked by mean decrease in Gini importance were used to identify the panel of co-acting genes which best predicts TRAIL sensitivity. Performance was measured by predicting TRAIL sensitivity of the test data set, calculating the area under the receiver operator curve (AUC) across 10 repeats. This was performed using the gplots package version 2.13 (Gregory R. Warnes et al, 2014). An AUC of 1 indicates a perfect prediction. In order to determine the core co-acting gene set, the ten lowest ranking variables (genes) were removed from the gene list and a new RF model was built with the remaining genes. This process was repeated until only the top 10 probesets remained.

Random forest modelling was carried out using randomForest package (Wiener, 2002) in the R environment (http://www.r-project.org/) version 2.15.1.

3.2.4 Statistical Analysis

Statistical significance was determined using two-tailed paired t-test in R (version 2.15.1)

3.3 Results

The aim of this study was to determine if the relationship between genes can describe decisive molecular interactions and thus predict/classify a biological response or behaviour. The focus of the analysis was to identify genes that potentially influence each other either by inhibition, potentiation or activation. We describe these as "co-acting genes".

As a model system for the analysis we used the TRAIL signalling pathway with transcriptomic data for 109 tumour cell lines classified as sensitive or resistant to TRAIL. First we identified a singular "best" representative probeset for each unique gene present on the microarray by using a newly developed algorithm, JetSet, that assesses each probeset for specificity, splice isoform-coverage and degradation rate (Li et al, 2011). The amalgamated information allows for an unambiguous mapping of the gene of interest to a singular "best" probeset. The 19,190 "best" probesets, hereafter simply referred to as genes, were fed into a classification analysis (random forest) which consisted of the following steps. First we built 10,000 classification trees with a series of sequential co-acting genes within each tree that classify the cell lines as TRAIL sensitive or resistant. An example of these classification trees is depicted in Figure 3.1.

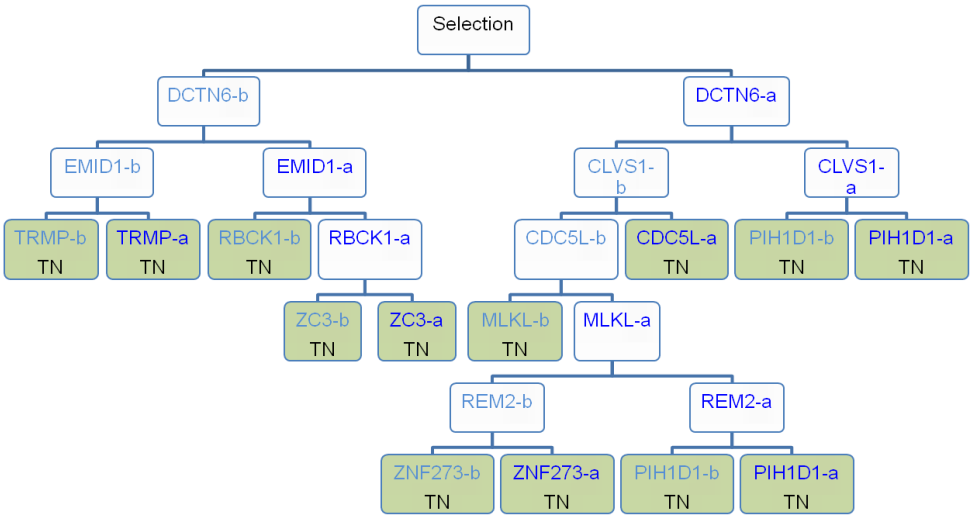

Figure 3.1: Depiction of a classification tree. A bootstrap or subset of all available cell lines and all available genes are taken at random. The gene from this random subset whose expression best divides the cell lines as cleanly as possible into sensitive and resistant is selected, in the example above this gene was DCTN6. The two groupings or daughter nodes are not pure, they have some resistant and some sensitive cell lines, so a new subset of genes is selected and the gene which best divides the cell lines is selected, in the example above these genes were EMID1 and CLVS1. This process is known as recursive partitioning and it is continues until terminal nodes are reached , these being groupings in which only sensitive or resistant cell lines are found. In this manner classification trees consider the expression of one gene in relation to another ("co-acting genes").

Next we determined the importance of each of the genes. To do this we permuted their expression value in all trees they appear then calculated the decrease in the ability of the model to partition the cell lines into sensitive and resistant groups. This measure is known as the mean decrease in Gini importance. The 19,190 genes were then ranked by their mean decrease in Gini importance. Genes present within the top 5th percentile (the highest ranking 1000 genes) were retained for further analysis (Fig. 3.2).

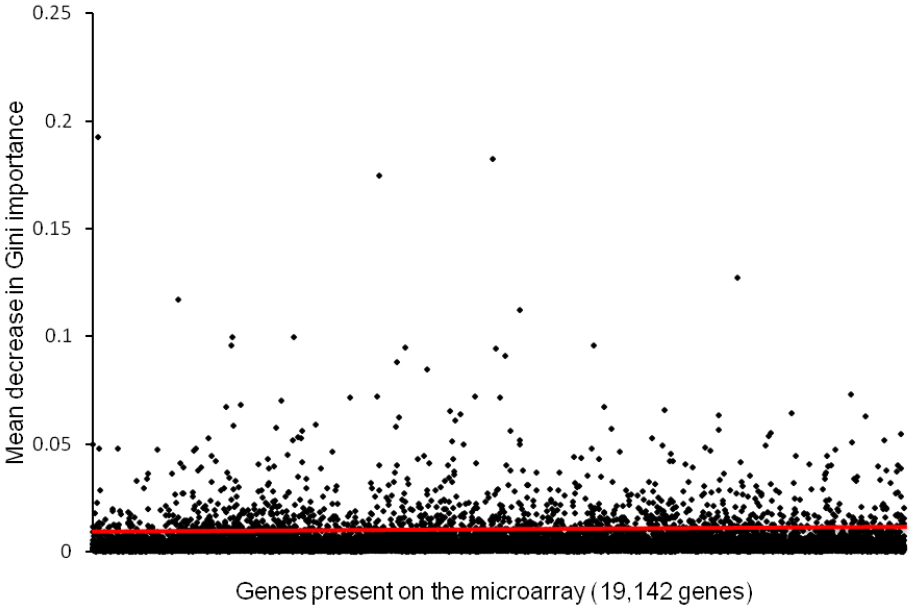

Figure 3.2: Genes ranked by their Gini importance. A singular "best" probeset for each unique gene in the transcriptome was used to grow 10,000 classification trees. The importance of each gene in classifying cell lines as sensitive or resistant to TRAIL was measured by mean decrease in Gini importance. The probesets above the red line represent the top 5th percentile (top 1000 genes) retained for further analysis.

We then assessed the performance of these 1000 genes in predicting the sensitivity of the tumour cell lines to TRAIL. Using the training set a new classification tree model was built with the top 1000 genes only. This model was then used to predict the sensitivity for the independent testing set. The true and false positive rates were plotted and the area under the receiver operator curve (AUC) was calculated. An AUC of 1 indicates perfect prediction. A total of ten repeats were carried out giving a mean AUC of 0.83 (Fig. 3.4A). During the construction of each individual classification tree a subset of cell lines are withheld (out of bag (OOB)) to assess internal classification error. The model grown using the 1000 co-acting genes exhibited OOB error of 1%. These data indicate that the panel of 1000 co-acting genes perform well in predicting TRAIL sensitivity. We then asked if we could identify the smallest grouping of co-acting genes with the best predictive power. Our workflow for this modelling process is illustrated in figure 3.3.

To do this we iteratively grew a classification tree model as previously described each time dropping the bottom 100 genes in the Gini importance rank list. As before the performance of each model was measured by calculating AUC (Fig. 3.3 and Fig. 3.4A). The highest AUC value achieved was 0.85 that utilised the top 350 co-acting genes from the Gini importance rank list.

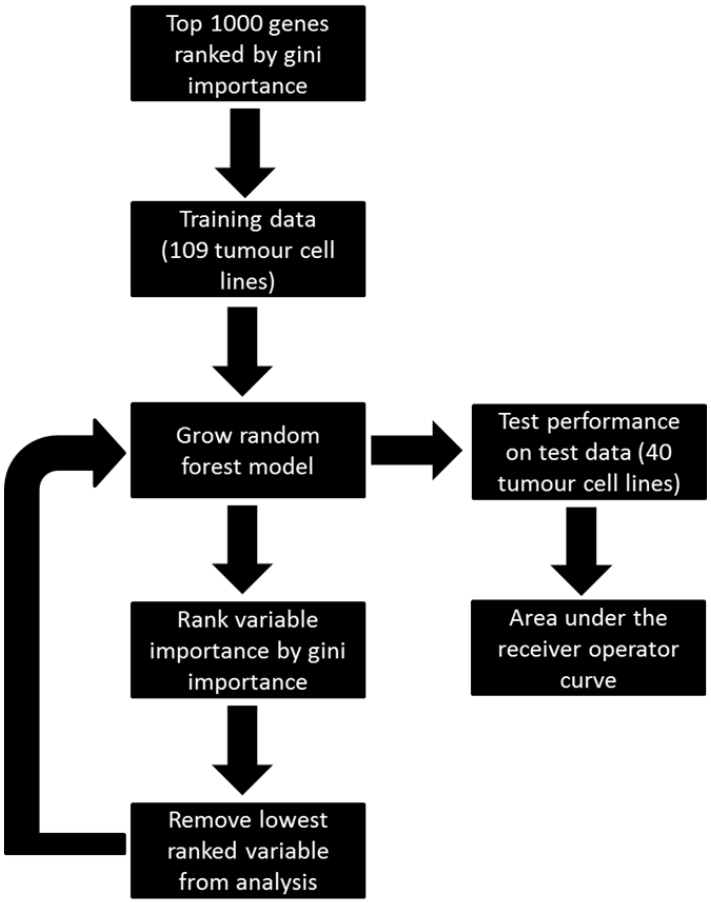

Figure 3.3: **Workflow for random forest (RF) modelling**. Gene expression data was imported for 109 tumour cell lines from the gene expression omnibus (GEO) and 40 tumour cell lines from CellMiner. Background correction and normalization was performed using the Affy package of Bioconductor (RMA algorithm) and single probesets for each gene were selected using the JetSet algorithm. The top 1000 genes ranked by their Gini importance we selected for the analysis. One data set was used to train the classification tree model. The performance of this RF model was then measured by predicting TRAIL sensitivity of the remaining independent data set, ROC curves were constructed and AUC calculated as an indicator of prediction accuracy. The RF model was then summarized by mean decrease in Gini importance .The top N-100 (10) genes were then used to build a new RF model. This process was repeated until the top 10 genes were identified.

Removal of genes up to the 700th gene from the bottom in the ranking list did not affect performance of the model (Fig. 3.4A). Exclusion of the next 100 genes worsened the performance of the model (Fig. 3.4A). Thereafter the removal of the next 100 genes improved performance (Fig. 3.4A).

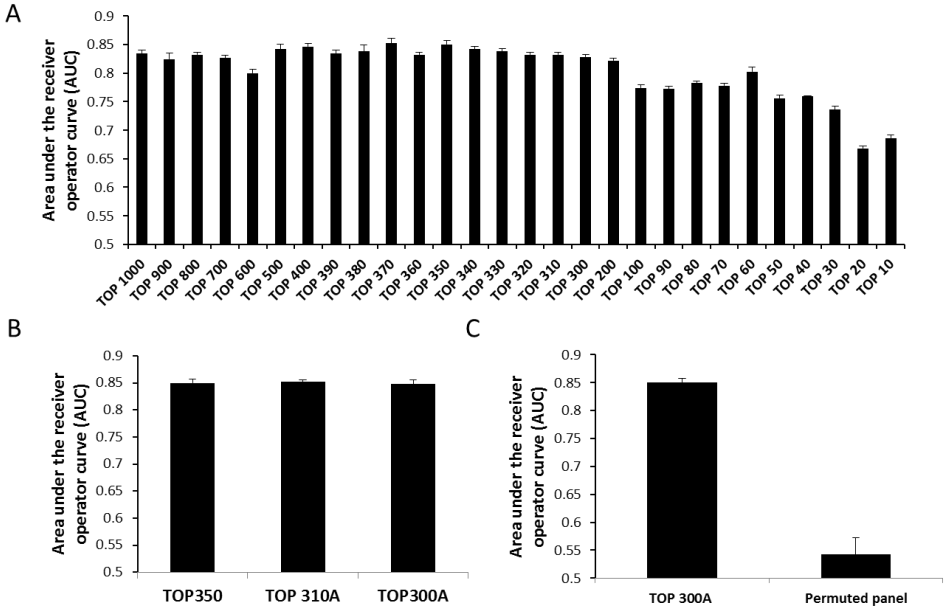

Figure 3.4: **Identification of the core-co-acting gene set**. (A) The top 1000 genes were used to construct a RF model. The performance of this model in predicting TRAIL sensitivity was assessed in an independent test set. An AUC of 1 indicates perfect prediction. The 100 (10) lowest ranked genes were stepwise removed and a new RF model constructed and accompanying AUC calculated. The performance of the model peaked with the top 350 co-acting genes (AUC=0.85). (B) Removal of any of these 350 genes causes a significant decrease in model performance ($p<0.05$) except for the genes ranked between 100th to 60th and 50th to 40th. When the 40 genes ranked between the 100th to the 60th were excluded from list of 350 co-acting genes the new 310 gene panel (TOP 310A) performed equally as well as the 350 co-acting genes. In addition when the 10 genes ranked between 50th and 40th were removed from the TOP 310A list the subsequent TOP 300A gene panel once again performed as well as the models previous best. (C) In order to determine if the model was describing a real connection between the co-acting genes and sensitivity we randomly changed the sensitivity of one half of the cell lines 10 times. The performance of this permuted panel is significantly diminished ($p<0.05$) compared to the 300co-acting genes.

The removal of genes between the 500th and 350th ranked had minimal effect on the performance of the model (Fig. 3.4A). Removal of genes beyond the 350th rank however resulted in the collapse of the model's ability to predict TRAIL sensitivity (Fig. 3.4A). Therefore the 700th to 600th genes were

reintroduced into the analysis alongside the 350 gene signature but did not appreciably improve model performance (data not shown). It was noted that removal of the 100th to 60th and the 50th to the 40th ranked genes had minimal effect on performance (Fig. 3.4A). These were removed from the panel of 350 co-acting genes resulting in panel of 300 genes with an AUC of 0.85 (OOB error of 1%) hereafter referred to as 300A (Fig. 3.4B). In order to determine if the identified panel of 300A co-acting genes was describing a real connection between TRAIL sensitivity and gene expression the sensitivity of one half of the cell lines was changed to the incorrect alternative 10 times. There was a significant difference ($p<0.05$) between the AUC value of the 300A co-acting genes and the permuted panel (Fig. 3.4C) implying that the AUC values generated for the 300A co-acting genes was highly unlikely to be achieved by chance.

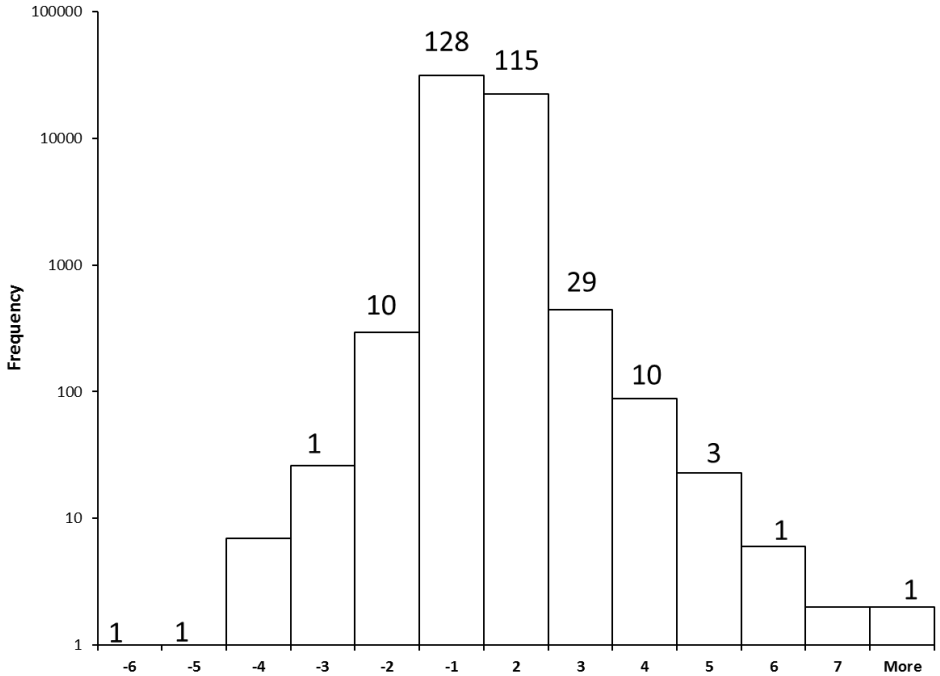

Figure 3.5: **Genes present in 300A panel of co-acting genes are not identified by differential expression analysis**. The mean fold change in expression between TRAIL sensitive and resistant cell lines was calculated for each gene present in the training microarray data set. The total number of genes within the given range of fold changes in expression is illustrated. The distribution of genes from the panel of 300A co-acting genes is indicated by the numbers above each column

We wanted to know how many if any of these co-acting genes would be highlighted by differential expression studies which typically only retain genes which are differentially expressed by a minimum of 2 fold. Using these criteria 312 genes differentially expressed between TRAIL sensitive and resistant cell lines were identified in Genspring GX v11. Of the 300A co-acting genes the majority (243 genes) exhibited a fold change below the typical two fold threshold (Fig. 3.5). In addition after significance tests only 41 were significantly differentially expressed and only 35 of these exceeded the minimum 2 fold change in expression and therefore would be included in differential expression studies.

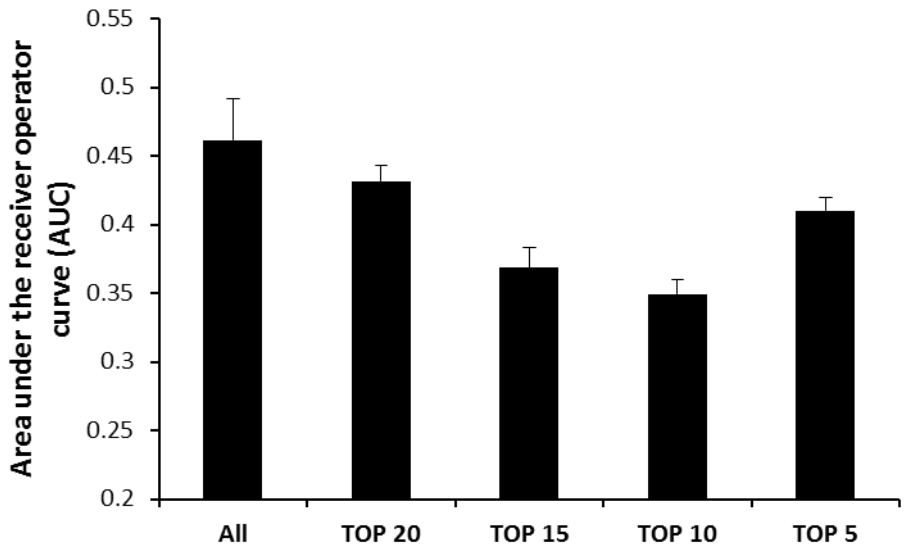

Figure 3.6: **Panel of co-acting genes composed of the core components of the TRAIL apoptotic machinery does not predict TRAIL sensitivity with a high degree of sensitivity and specificity.** The performance of the 26 TRAIL effectors as a classifier was assessed by plotting the true and false positive rates (receiver operating curve (ROC)) and calculating the AUC. The 5 lowest ranked genes were stepwise removed and a new RF model constructed and accompanying AUC calculated. The removal of any of the 26 core effectors caused a decrease in the models ability to predict sensitivity to TRAIL. The 26 core effectors predicted TRAIL sensitivity poorly (AUC=0.46)

As previously discussed cancers can become resistant to treatment by a variety of means. While a number of the mechanisms responsible for resistance to TRAIL treatment have been elucidated none appear promising as predictive markers. We applied the same methodology which uncovered the 300A co-acting genes to a group of known effectors in the TRAIL signalling pathway. To begin we identified what we believed to be the 26 core effectors for TRAIL signalling and then a random forest model was grown. The 26 core effectors of the TRAIL pathway could not predict response well (AUC=0.49) (Fig. 3.6). Backward elimination of the lowest ranked gene by mean decrease in Gini importance with the construction of a new classification tree model during each iteration revealed the removal of any of these 26 core effectors only worsened the prediction performance (Fig. 3.6)

3.4 Discussion

Biomarkers are pillars of diagnostic biology allowing for the detection and prognosis of a disease. Prominent examples of biomarkers include the BRCA gene tests for susceptibility to breast cancer (Werner & Bruchim, 2012) and the association of CA-125 levels with the development of ovarian cancer (Wilbaux et al, 2014). In the last number of years there has been a paradigm shift away from the identification of prognostic and diagnostic biomarkers to the search for biomarkers that can predict treatment efficacy. This refocusing has been facilitated by the advent of high-throughput technologies such as genome-wide association analysis, transcriptomics or metabolomics. For example biomarkers identified from transcriptomic and mutation analysis have been used to develop the Oncotype-DX biomarker panel for the identification of suitable treatments for breast cancer patients (Toole et al, 2014). Transcriptomic data has also been recently used to identify drugs that have the potential to reverse an unfavourable phenotype such as drug-resistance with the help of the so-called Connectivity mapping. In this approach the genes differentially expressed between drug-sensitive versus drug-resistant tumours are identified. This differential gene-expression pattern is compared to that induced by a large cohort of drugs. The drugs that induce a reciprocal expression pattern may have the potential to re-establish the drug-sensitive gene-expression profile and thus restore drug sensitivity.

The TRAIL apoptotic pathway has also been widely studied and some of the regulators of the pathways have been indicated as good prognostic biomarkers including c-FLIP, XIAP, DcR1 or DcR2 as individual markers or groups of differentially expressed genes (Chen et al, 2012). The performance of these biomarkers varies on a large scale. Currently the best classifier of TRAIL sensitivity is a 71-gene signature which is a group of genes differentially expressed between TRAIL-resistant and sensitive tumour cell lines (AUC=0.72) (Chen et al, 2012).

Biomarkers identified for other tumour types have displayed similar levels of performance. This prediction accuracy is considered to be good. However signal transduction pathways are not linear and thus a one-dimensional analysis e.g. compilation of differentially expressed genes does not have the power to precisely describe the pathway and thus accurately predict a biological response.

In this study we show that by identifying genes connected to each other in a biological system (co-acting genes) based on their relative expression to each other we can predict a biological response with high accuracy which is superior to that of the commonly available single-gene or differentially expressed group-biomarkers. In the model system we chose we could predict TRAIL responsiveness of tumour cells with excellent sensitivity and specificity (AUC=0.85) by identifying the best performing panel of co-acting genes (Fig. 3.4C).

The co-acting genes offer several advantages. For example signalling pathways may be better described by the relative amount of its components than by their individual absolute expression. For instance a 1.5 fold higher Bcl-2 expression in a TRAIL resistant cell line may not be considered as the main cause of the resistant phenotype. However if it is accompanied by a 1.5 fold reduction in pro-caspase-8 expression (resulting in a 2.2-fold change in the expression ratio of Bcl-2 to pro-caspase-8) it becomes a much stronger determining factor. Reduced pro-caspase-8 expression would indicate that the caspase activity emanating from the death receptor is weak and thus execution of apoptosis would require the mitochondrial amplification loop which may be impaired due to the increased expression of Bcl-2. Naturally additional factors such as Bid, Bax, Bak and XIAP expression may all contribute to the final outcome. The co-acting genes incorporate and simultaneously analyse a multitude of potential linkages and interactions between the co-acting genes.

It is also well established that not all cells utilize the same mechanism to block apoptosis. Therefore the description and analysis of such mechanisms has to incorporate this variability or redundancy. This highlights why single

genes or a group of genes cannot determine response with a high degree of accuracy. Random forest models can follow and identify branching gene interactions which provide a distinct advantage as they are able to simultaneously identify a number of potential routes of co-acting gene linkages that can dictate the cell's phenotype (Fig. 3.1). In other words the co-acting gene can overcome the low dimensionality of the traditional analyses and thus offer a tool for the precise analysis of non-linear signalling pathways.

There appears to be minimal overlap between those genes deemed most important by classification tree modelling and differential expression studies (Fig. 3.5). We observed that if we applied the typical criteria used during differential gene expression studies then only 12% of the top 300A co-acting genes would be retained as promising candidates. This implies differential expression studies exclude a large proportion of genes which may influence outcome/phenotype.

We also found that despite the fact that there is a tremendous amount of literature on the regulation of the TRAIL apoptotic pathway we still do not have full understanding of this pathway. Even when we constructed a random forest model using the well documented components of the TRAIL pathway the maximum performance of the model as a predictor was AUC=0.46 (Fig. 3.6). The 300A co-acting genes we identified from the whole transcriptome contain nine known components and regulators of the TRAIL signalling pathway. Six of those nine DR4, DR5, DcR2, Osteoprotegerin, Caspase-8 and heme-oxidized IRP2 ubiquitin ligase 1 (HOIL1) are well characterised. On the other hand many genes whose protein product is known to be a key regulator of TRAIL sensitivity in at least some tumour cells such as XIAP, Noxa or Mcl-1 are not in the top 100 predictor genes. This highlights that these gene products are either not the strongest determinants of TRAIL sensitivity or alternatively that the protein expression level does not correlate with the mRNA expression of these genes. This discrepancy between mRNA and protein expression levels has been reported to occur for approximately 50% of the transcriptome.

In addition to the 6 well-characterised TRAIL pathway regulators another 14 genes that have been linked to TRAIL sensitivity by at least one study are present in the panel of 300A co-acting genes. These genes are mixed lineage kinase domain-like (MLKL) (Remijsen et al, 2014), mucin-5AC (MUC5AC) (Hoshi et al, 2013), DNA-binding death effector domain-containing protein 2 (DEDD2) (Roth et al, 2002), galactocerebrosidase (Pannuzzo et al, 2010), eukaryotic translation initiation factor 4E type 2 (Bleumink et al, 2011), nuclear pore complex protein Nup98-Nup96 (Matte-Martone et al, 2011), interferon regulatory factor 3 (Kirshner et al, 2005), NADPH oxidase organizer 1 (Park et al, 2012), histone deacetylase 8, S100-A6 (Leong et al, 2007), serine-protein kinase ATM (Farooqi et al, 2011), polypeptide N-acetylgalactosaminyltransferase 14 (Stern et al, 2010), cyclin-dependent kinase 2 (Kim et al, 2004), histone deacetylase 2 (Schuler et al, 2010) and aryl hydrocarbon receptor (Stolpmann et al, 2012). The remaining 286 genes have never been reported or associated directly with TRAIL induced apoptosis. These genes may be co-regulated with other genes (bystanders) that regulate TRAIL sensitivity but have no effect on the pathway. It is also highly possible that many of these genes directly or indirectly regulate TRAIL sensitivity.

3.5 Future perspectives

In this work we have identified a panel of 300 co-acting genes that performs significantly better than previously reported biomarkers in predicting sensitivity to TRAIL in tumour cell lines.

This analysis can be applied to a number of chemotherapeutic agents such as cisplatin and etoposide for which microarray data and sensitivity to the aforementioned agents is available. The identification of biomarkers for these agents would corroborate the power of our analysis while being beneficial to patients as these agents are available in the clinic.

In summary these findings don't only explain why previous studies failed to find a reliable marker of TRAIL sensitivity but also pinpoint novel potential regulators of the pathway. The method described may be developed into a theranostic tool in the future by validation with chemotherapeutics for which clinical samples are available.

Chapter 4: Crosstalk between the death inducing signalling complex and mitochondria is the major determinant of TRAIL-mediated apoptosis

Abstract

TNF-related apoptosis-inducing ligand (TRAIL) has been shown to selectivity induce apoptosis in transformed cells via binding to the death receptors DR4 and DR5. However a high percentage of tumour cell lines have been shown to be resistant to TRAIL-induced apoptosis. A vast number of proteins inhibiting TRAIL-mediated apoptosis have been identified in different tumour cell lines but most of these proteins either only work in a small subset of cell lines or their effect is partial. Here we propose that rather than the absolute amount of the individual components of a signalling pathway it is the ratio of proteins, such as activators and inhibitors directly or indirectly interacting, which determine TRAIL sensitivity. To address this question 42 tumour cell lines have been assessed for TRAIL sensitivity, protein expression level of components of the TRAIL apoptotic machinery and cell surface expression of the TRAIL receptors by viability assay, Western blotting and immunocytochemistry respectively. The protein levels of the components were quantified and the expression ratio of every possible pairing of the proteins in each cell line was calculated. We found that the expression of caspase-8 relative to the expression of Bcl-2 tightly correlated with TRAIL sensitivity. This indicates that the crosstalk between receptor-level and mitochondrion-level signalling is a key determinant in TRAIL sensitivity. In order to confirm this we have established a mechanistic model that allows us to control the expression of Bcl-2 and caspase-8 independently. A tetracycline-inducible system was used to incrementally increase the expression of caspase-8 and the BH3-mimetic Abbott737 was applied to functionally inhibit Bcl-2. Increased caspases-8 expression and Bcl-2 inhibition had a synergistic effect on TRAIL sensitivity. On the contrary either increased Caspases-8 levels or diminished Bcl-2 function only marginally affected TRAIL sensitivity. These results highlight a novel so far underestimated crosstalk between the DISC and mitochondria and highlight the need to analyse the interaction between components of a signal transduction pathway rather than the proteins.

4.1 Introduction

In the past decade there have been considerable advancements in the characterization of human tumours primarily due to the collective maturation of genomics, proteomics and molecular imaging techniques. Armed with a better understanding of cancer at the molecular level a paradigm shift away from genotoxins and anti-metabolites towards the development of targeted therapies for cancer has ensued. Indeed there has been considerable success in targeting defined subsets of various tumour types. An example of which is the specific Bcr-Abl kinase inhibitor, imatinib mesylate, that has been shown to increase the five year survival rate from 50% to 89% in Philadelphia chromosome positive chronic myeloid leukaemia patients (Druker et al, 2006). Another example is Herceptin a monoclonal antibody targeting the human epithelial receptor 2 (HER-2) overexpressed in certain breast cancers. Herceptin has been shown to prolong overall survival in metastatic breast cancer patients from an average of 13 months to 41 (Berghoff et al, 2013). Unfortunately targeted therapies only exist for a small proportion of tumours in which one major factor drives tumour growth. A unique advantage of the death ligand TRAIL is that it has very low toxicity, just like targeted therapeutics, and is still able to target a broad range of tumours irrespective of the factor driving the malignancy.

Cancers often inactivate or disengage pivotal branches in the apoptotic machinery in order to survive. Moreover studies have shown that administration of TRAIL to resistant cell lines may result in increased aggression and propensity for metastasis. Therefore there is a need for a predictive biomarker capable of discerning responders and non-responders to TRAIL treatment. Proteomic analysis of the TRAIL apoptotic machinery in 21 tumour cell lines showed no significant correlation between the expression of the following proteins and TRAIL sensitivity: DR4, DR5, DcR1, DcR2, c-FLIP, Bcl-2, Mcl-1, Bcl-XL or XIAP (Wagner et al, 2007). In instances where correlations were seen they were observed in a small subpopulation of the studied samples. As previously discussed in the general introduction resistance to TRAIL is most often caused by the

overexpression of the anti-apoptotic Bcl-2 family proteins (Bcl-2, Bcl-XL, Mcl-1), c-FLIP, XIAP or the decoy receptors (DcR1 and DcR2). Resistance may also result from a reduction in the expression of pro-caspase-8 or its enhanced degradation. Overall the majority of reports in the literature attribute resistance to TRAIL to alterations in the expression of pro- and/or anti-apoptotic proteins. Thus on one hand resistance is associated with altered expression of components of the apoptotic machinery and on the other the individual expression of none of these proteins can be correlated with resistance across multiple tumour cell lines.

Based on the above the hypothesis that we examined in this project is that it is not the individual expression of a protein in a pathway that determines cellular response. Rather it is the relationship between the components of said pathway, their relative expression, which determines outcome. In this study we addressed this by assessing the stoichiometry of the TRAIL apoptotic machinery. The expression of each individual protein and all possible protein pairings were assessed for their ability to predict sensitivity to TRAIL-induced cell death. We show that the expression of caspase-8 relative to the expression of the Bcl-2 protein is higher in TRAIL sensitive cell lines (75% of resistant cell lines had a value less than the median in TRAIL sensitive cells) and may therefore be useful as a marker for sensitivity to TRAIL. In addition our mechanistic studies show that this relationship has a causative role in TRAIL sensitivity and may therefore represent a drug-able nodal point in the pathway.

4.2 Materials and Methods

4.2.1 Cell culture and treatments

Cells were maintained at 37°C in a humidified 5% CO_2 atmosphere. Cells were treated with Staurosporine (Sigma), ABT737 (Selleck Chemicals), rhTRAIL (non-tagged, fragment amino acids 114-281, Triskel Therapeutics, Groningen) or Doxycycline (Sigma). The Cell culture conditions of 53 tumour cell lines are indicated in Table 1.

Cell Line	Media	Supplements
A2780	RPMI 1640	2 mM glutamine, 10% FBS, 100 U/ml penicillin and 100 µg/ml streptomycin
Colo205	RPMI 1640	2 mM glutamine, 10% FBS, 100 U/ml penicillin, 1mM pyruvate and 100 µg/ml streptomycin
EM-2	RPMI 1640	2 mM glutamine, 10% FBS, 100 U/ml penicillin and 100 µg/ml streptomycin
HCT 15	RPMI 1640	2 mM glutamine, 10% FBS, 100 U/ml penicillin, 1mM pyruvate and 100 µg/ml streptomycin
HL-60	RPMI 1640	2 mM glutamine, 10% FBS, 100 U/ml penicillin, 1mM pyruvate and 100 µg/ml streptomycin
K562	RPMI 1640	2 mM glutamine, 10% FBS, 100 U/ml penicillin, 1mM pyruvate and 100 µg/ml streptomycin
KASUMI	RPMI 1640	2 mM glutamine, 10% FBS, 100 U/ml penicillin, 1mM pyruvate, 1% NEA and 100 µg/ml streptomycin
KG-1	RPMI 1640	2 mM glutamine, 10% FBS, 100 U/ml penicillin, 1mM pyruvate and 100 µg/ml streptomycin
ML-1	RPMI 1640	2 mM glutamine, 10% FBS, 100 U/ml penicillin, 1mM pyruvate and 100 µg/ml streptomycin
MOLM-13	RPMI 1640	2 mM glutamine, 10% FBS, 100 U/ml penicillin, 1mM pyruvate, 1% NEA and 100 µg/ml streptomycin
OCI-AML3	MEM	2 mM glutamine, 20% FBS, 100 U/ml penicillin, 1mM pyruvate, 1% NEA and 100 µg/ml streptomycin
T47D	RPMI 1640	2 mM glutamine, 10% FBS, 100 U/ml penicillin and 100 µg/ml streptomycin
DLD-1	RPMI-1640	2 mM glutamine, 10% FBS, 100 U/ml penicillin and 100 µg/ml streptomycin
HCA-7	DMEM	2 mM glutamine, 10% FBS, 100 U/ml penicillin and 100 µg/ml streptomycin
HCT116	McCoy's 5a	2 mM glutamine, 10% FBS, 100 U/ml penicillin and 100 µg/ml streptomycin
HCT116 Bax -/-	McCoy's 5a	2 mM glutamine, 10% FBS, 100 U/ml penicillin and 100 µg/ml streptomycin
HCT116 P53 -/-	McCoy's 5a	2 mM glutamine, 10% FBS, 100 U/ml penicillin and 100 µg/ml streptomycin
HeLa	DMEM	2 mM glutamine, 10% FBS, 100 U/ml penicillin, 1% NEA and 100 µg/ml streptomycin
HT-29	McCoy's 5a	2 mM glutamine, 10% FBS, 100 U/ml penicillin and 100 µg/ml streptomycin
MCF-7	EMEM	2 mM glutamine, 10% FBS, 100 U/ml penicillin, 1% NEA and 100 µg/ml streptomycin
PANC-1	DMEM	2 mM glutamine, 10% FBS, 100 U/ml penicillin and 100 µg/ml streptomycin
RKO	EMEM	2 mM glutamine, 10% FBS, 100 U/ml penicillin and 100 µg/ml streptomycin
SAOS-2	McCoy's 5a	2 mM glutamine, 10% FBS, 100 U/ml penicillin and 100 µg/ml streptomycin
ARP1	RPMI-1640	2 mM glutamine, 10% FBS, 100 U/ml penicillin and 100 µg/ml streptomycin
Ca Ski	RPMI-1640	2 mM glutamine, 10% FBS, 100 U/ml penicillin and 100 µg/ml streptomycin
Colo-320	RPMI-1640	2 mM glutamine, 10% FBS, 100 U/ml penicillin and 100 µg/ml streptomycin
H157	RPMI-1640	2 mM glutamine, 10% FBS, 100 U/ml penicillin and 100 µg/ml streptomycin
H460	RPMI-1640	2 mM glutamine, 10% FBS, 100 U/ml penicillin and 100 µg/ml streptomycin
H630	RPMI-1640	2 mM glutamine, 10% FBS, 100 U/ml penicillin and 100 µg/ml streptomycin
HeLa S3	MEM	2 mM glutamine, 10% FBS, 100 U/ml penicillin, 1% NEA and 100 µg/ml streptomycin
IM9	RPMI-1640	2 mM glutamine, 10% FBS, 100 U/ml penicillin and 100 µg/ml streptomycin
LoVo	RPMI-1640	2 mM glutamine, 10% FBS, 100 U/ml penicillin and 100 µg/ml streptomycin

Table 1: Summary of cell lines and cell culture conditions

Cell Line	Media	Supplements
ARH-77	RPMI-1640	2 mM glutamine, 10% FBS, 100 U/ml penicillin and 100 µg/ml streptomycin
HS-Sultan	RPMI-1640	2 mM glutamine, 10% FBS, 100 U/ml penicillin and 100 µg/ml streptomycin
KMS-18	RPMI-1640	2 mM glutamine, 10% FBS, 100 U/ml penicillin and 100 µg/ml streptomycin
SKBR3	McCoy's 5a	2 mM glutamine, 10% FBS, 100 U/ml penicillin and 100 µg/ml streptomycin
SF-539	RPMI-1640	2 mM glutamine, 10% FBS, 100 U/ml penicillin and 100 µg/ml streptomycin
U20S	McCoy's 5a	2 mM glutamine, 10% FBS, 100 U/ml penicillin and 100 µg/ml streptomycin
Punctu	RPMI-1640	2 mM glutamine, 10% FBS, 100 U/ml penicillin and 100 µg/ml streptomycin
Raji	RPMI-1640	2 mM glutamine, 10% FBS, 100 U/ml penicillin and 100 µg/ml streptomycin
UACC62	RPMI-1640	2 mM glutamine, 10% FBS, 100 U/ml penicillin and 100 µg/ml streptomycin
MM1R	RPMI-1640	2 mM glutamine, 10% FBS, 100 U/ml penicillin and 100 µg/ml streptomycin
M14	DMEM	2 mM glutamine, 10% FBS, 100 U/ml penicillin and 100 µg/ml streptomycin
SKMEL2	DMEM	2 mM glutamine, 10% FBS, 100 U/ml penicillin and 100 µg/ml streptomycin
OCI-AML-2	RPMI-1640	2 mM glutamine, 10% FBS, 100 U/ml penicillin and 100 µg/ml streptomycin
RPMI8226	RPMI-1640	2 mM glutamine, 10% FBS, 100 U/ml penicillin and 100 µg/ml streptomycin
H727	RPMI-1640	2 mM glutamine, 10% FBS, 100 U/ml penicillin and 100 µg/ml streptomycin
SiHa	RPMI-1640	2 mM glutamine, 10% FBS, 100 U/ml penicillin and 100 µg/ml streptomycin
A549	RPMI-1640	2 mM glutamine, 10% FBS, 100 U/ml penicillin and 100 µg/ml streptomycin
BT-20	EMEM	2 mM glutamine, 10% FBS, 100 U/ml penicillin and 100 µg/ml streptomycin
BT-474	DMEM	2 mM glutamine, 10% FBS, 100 U/ml penicillin and 100 µg/ml streptomycin
BxPC-3	RPMI-1640	2 mM glutamine, 10% FBS, 100 U/ml penicillin and 100 µg/ml streptomycin
Capan-1	DMEM	2 mM glutamine, 10% FBS, 100 U/ml penicillin and 100 µg/ml streptomycin
Colo-357	RPMI-1640	2 mM glutamine, 10% FBS, 100 U/ml penicillin and 100 µg/ml streptomycin
Hep-G2	DMEM	2 mM glutamine, 10% FBS, 100 U/ml penicillin and 100 µg/ml streptomycin
MDA-MB-231	RPMI-1640	2 mM glutamine, 10% FBS, 100 U/ml penicillin and 100 µg/ml streptomycin

Table 1 continued: Summary of cell lines and cell culture conditions

4.2.1.1 MTT viability assay

Cell viability was monitored by 2-(4, 5-dimethyltriazol-2-yl)-2, 5-diphenyl tetrazolium bromide (MTT) assay. Following treatment, MTT (0.5 mg/ml) was added to cells and incubated for 3 h at 37ºC. The reaction was stopped by addition of MTT stop solution (20% SDS in 50% dimethyl formamide). The precipitate generated was allowed to dissolve overnight on an orbital shaker. The colour intensity was measured at 550 nm on a Wallac Victor 1420 Multilabel counter (Perkin Elmer Life Sciences). Cell viability was expressed relative to the absorbance of untreated cells, which was taken as 100% viable.

4.2.1.2 Propidium iodide staining

Cells were seeded at the appropriate concentration in 24 well plates. After treatment the medium from wells was transferred into labelled Eppendorf tubes. Wells were then gently washed with 300 µl Hanks. The adhered cells were removed by the addition of 200 µl of 1x trypsin for 5 min at 37^{o}C. The trypsinized cells were combined with the medium in the Eppendorf tubes and incubated for 10 min at 37^{o}C with shaking a few times during incubation to allow recovery of minor damages of the membrane (caused by trypsin). The cells were collected by spinning at 5000 x g for 5 min using soft acceleration and brake. The supernatant was removed and the cells were resuspended in 300 µl of phosphate buffered saline (PBS) containing 4µl propidium iodide (PI) (50µg/ml). Samples were measured immediately on a FACSCantoII flow cytometer (BD Biosciences).

4.2.1.3 Crystal violet viability assay

Cells were seeded at the appropriate density in a 96 well plate. After treatment media is removed, wells washed with PBS and left to air dry. 100µl of crystal violet is added to the cells for 5 min and then removed. Cells are left to air dry. 100µl of 1% SDS was used to resuspend the cells. Absorbance was read at 595nm.

4.2.2 Classification of cell lines as TRAIL sensitive or resistant

Cell lines were categorized based upon reduction in viability as assessed by MTT assay. Reduction greater than 50% and the cells were classified as sensitive, less than 25% and they are resistant. Cell lines which had a reduction between 25-50% are deemed partially responsive to TRAIL

4.2.3 Preparation of protein lysates and Western blotting

Cells were seeded in T75 flash for 48 h before being harvested and lysed in 1% Triton X-100 lysis buffer containing 10% glycerol, 200mM NaCl, 100 mM Tris/HCl Ph 8.0, 5 mM EDTA, 1 µM phenylmethylsulphonyl fluoride (PMSF), 1.0 µg/ml Pepstatin, 10 µM Leupeptin, 2.5 µg/ml aprotinin, 10 µM leupeptin, 250 µM *N*-acetyl-leucyl-leucyl-norleucinal (ALLN), 10 mM NaF and 1 mM Na_3VO_4. Protein samples from 4 consecutive passages of the cells have been harvested and pooled together in order to reduce experimental error. These samples have been analysed in 3 independent Western blot runs to quantitate protein expression. The protein concentration was set to 3 µg/µl in all pooled lysates. For Western blotting 30 µg of protein was loaded onto 10% SDS polyacrylamide gel together with 10, 20, 30, 40 and 50 µg of the HCT116 internal control. Transfer was performed using the iBlot dry transfer (Invitrogen). After blocking for 1 h at room temperature in 5% milk and 0.05% Tween20 in PBS, blots were incubated with the following antibodies: mouse monoclonal antibodies against c-FLIP (1:500; Alexis), caspase-8 (1:1,000; Cell Signalling Technologies), Bcl-2 (1:200; Santa Cruz), Bcl-XL (1:200; Santa Cruz) and

XIAP (1:5,000, Enzo) and rabbit monoclonal antibodies against Mcl-1 (1:1,000; Cell Signalling Technologies) and Bax (1:1,000; Cell Signalling Technologies). Detection was by the appropriate horseradish peroxidase-conjugated goat secondary antibody. Protein bands were visualized with SuperSignal® West Pico Chemiluminescent Substrate (Pierce), Immobilon western HRP substrate (Millipore) or Western Lightning®–ECL, Enhanced Chemiluminescence Substrate (Perkin Elmer) on X-ray film (Agfa) at s number of exposure times to ensure the HRP reaction is captured in the linear range.

4.2.4 Quantification of intracellular protein expression values

Densitometry analysis was done on the Western blot results using the Genetools software. The optical density for each protein in all 42 tumour cell lines and the corresponding internal controls (HCT116 lysate) at multiple exposure times was measured by selecting the region around the protein band using the free hand tool. Standard curves were constructed using the optical density values for the internal standards for each exposure time in Microsoft Excel. Then expression of each protein was measured relative to the internal standards by interpolation off of the appropriate standard curve. The average expression value across the multiple exposure times was calculated. Measurements were repeated 3 times. The range in expression of these protein expression values were then assessed using Minitab 16

4.2.5 Calculation of protein expression ratios

An executable file called PaulPad was written to calculate the protein expression ratio (Protein A/ Protein B) for all possible pairings within each cell line. The protein expression values for each cell line were stored as text files labelled as CellLineName_Sensitivity.txt. A list file containing a complete directory of the cell lines to be assessed was loaded into PaulPad. The protein expression values were calculated and output as two text files. One for the TRAIL sensitive and one for the TRAIL resistant cell lines. The

range in expression of these protein expression ratios were then assessed using Minitab 16

4.2.6 TRAIL receptor immunocytochemistry

Cells were seeded at the appropriate density in a T25 flask and incubated for 48 h. At a density of 50-85% confluency the cells were collected by gentle trypsinization and the plasma membrane was allowed to recover at 37^{o}C for 10 min. The cells were centrifuged at 5,000 rpm for 5 min and washed twice by ice cold 1% BSA in PBS. Cells were then incubated with mouse monoclonal antibodies against the TRAIL death and decoy receptors (Alexis) for 45 min on ice. Afterwards the cells were washed twice by ice cold 1% BSA in PBS and incubated with anti-mouse IgG-FITC (Sigma) for 45 min on ice in the dark. As a negative control isotype control antibody was used. When the incubation was over the cells were washed twice by ice cold 1% BSA in PBS and then re-suspended in 1% formaldehyde in PBS to be measure within the next 24 h on a FACSCantoII flow cytometer (BD Biosciences). The range in expression of these cell surface expression values were then assessed using Minitab 16

4.2.7 Inducible expression of caspase-8

The caspase-8 gene obtained from Addgene was cloned into the pLenti CMVtight DEST vector (w769-1). The pLenti CMV rtTA3 vector encoding the tetracycline repressor A3 mutant and Lentivirus for caspase-8 and tetracycline repressor A3 mutant was generated by co-transfecting pLenti CMVtight Caspase-8 DEST or pLenti CMV rtTA3 vector with a 2nd generation lentivirus packaging system (Addgene, pMD2.G Cat#12259, psPAX2 Cat#12260, pRSV-Rev Cat#12253) into HEK-293T cells seeded at 1.5x10^{5}cells/ml using JET PEI transfection reagent (Polyplus Transfection, Cat#101-01N). Virus supernatant was harvested at 24 and 48h. The virus was stored in cryotubes at -80°C.

HCT15 cells were seeded at $1.5x10^5$cells/ml in a 6 well plate. Virus for rtTA3 was defrosted and incubated with 5 µg of polybrene per ml of virus at 37°C for 5 min. After 5 min the media was removed from the HCT15 cell line in the 6 well plate and replaced with 2ml of the virus/polybrene mixture. The 6-well plate was then centrifuged for 90min at 1,500rpm at 37°C. After centrifugation the cells were incubated at 37°C overnight. The next day the virus containing media was replaced with fresh media. Stable clones were generated through culture with blasticidin (10µg/ml) (Sigma) for 10 days. The stable clones were then transduced with virus for caspase-8 in the same manner as previously described. There was a subsequent additional round of selection by culture with hygromycin B (500µg/ml) for 10 days followed.

4.2.8 Cell free expression and purification of Pep-1-Bcl-2

Pep-1-Bcl-2 was generated in a Pet15b vector by Integrated DNA technologies (IDT Coralville, IOWA). Protein synthesis was performed using a cell free expression system (Invitrogen). Escherichia Coli (E-Coli) slyD extract (10µl) was mixed with 2.5x IVPS reaction buffer (10µl), 50mM amino acid (0.75µl), 75mM methionine (0.5µl), T7 enzyme mix (0.5µl), Brij 58 (0.05%) and 0.5µg of the DNA template. This reaction mix was brought to a total volume of 25µl with water (Sigma) and incubated, shaking, at 30^oC for 30 minutes. A feed buffer consisting of 2x IVPS (12.5µl), 50mM amino acids (0.75µl), 75mM methionine (0.5µl) and Brij 58 (0.05%) made up to 25µl with water (Sigma) was added to the reaction mix after the 30min incubation and then returned to shaking at 30^oC for 4 h. After the 4 h incubation the mix was spun down at 13,000 rpm for 5 minutes at room temperature, the supernatant was retained. Buffer exchange was performed using Zeba spin desalting columns 0.5ml (Thermo) the exchange buffer consisted of NaCl (125mM), Na_3PO_4 (25mM), DTT (2mM) and Brij 58 (0.05%) at pH7.4. Purification was done using HisPur Ni-NTA spin columns 0.2 ml (Thermo). Column was equilibrated using Na_3PO_4 (50mM), NaCl (300mM) and imidazole (10mM) at pH8.4. Protein was added to the column and incubated for 30min at 4^oC on an end-over-end mixer. Unbound protein was washed off with Na_3PO_4 (50mM), NaCl (300mM), imidazole

(25mM) and Brij 58 (0.05%) made up in PBS. The Pep-1-Bcl-2 protein was eluted using Na_3PO_4 (50mM), NaCl (300mM), Imidazole (500mM) and Brij 0.05% at pH8.0. The eluent underwent another buffer exchange as described above.

4.2.9 Transfection of siRNA's

Cells were pelleted and resuspended in NHDF Nucleofector solution (Amaxa) and PBS containing 50nM siRNA. Cells were transfected by nucleofection using program P-022. 24 h post-transfection fresh medium was added to the cells and cells were treated as specified in figure legends. The following Mcl-1 sequence was targeted: Mcl-1 5′-GAAUUGAUUACCCGCCGAA-3′

4.2.10 Accell siRNA

Cells were seeded in a 24 well plate for 24 h in RPMI 10% serum. The media was then replaced with Dharmacon media (0% serum). Cells were treated with range of accell siRNA concentrations (Thermo). After 24 h cells were retreated with the same concentration of siRNA. The next day the cells were split 1:2 into RPMI with 2.5% serum. Cells were left to adhere and were subsequently retreated with the siRNA. 24 h later the cells were harvested for Western blot.

4.2.11 Statistical Analysis

All analyses were done in R (version 2.15.1); Significance was determined using two-tailed paired t-test

4.2.12 Whole cell lysate tryptic digestion

HCT116 cells were seeded in a T175. After 48h the media was removed and the cells were gently wasted with 0.35M sucrose a total of three times. Lysis buffer was added to the cells (9.5M Urea, 2% Chaps and 20mM Tris). The lysed cells were then scraped and transferred into a 1.5ml tube. Lysate was placed on a vortex for 30 min at room temperature before centrifugation at 16,000g for 30 min. The supernatant was recovered. Protein concentration was determined by the Bradford method

Protein sample was precipitated by the addition of 4 times the sample volume of acetone cooled to -20°C. The tube was placed on a vortex and then incubated for 1h at -20°C. Afterwards the sample was centrifuged at 15,000g for 10min. The supernatant was removed. Sample was the reduced by the addition of 5µl of DTT. The sample was placed on the vortex and then incubated for 30 min at room temperature. The proteins were then alkylated by 20µl of iodoacetamide. The sample was placed on the vortex and then incubated for 30 min at room temperature. Finally added 20µl DTT and left the sample to stand at room temperature for 60 min. The urea concentration was diluted by the addition of 775µl MilliQ water. Trypsin was added in 1:50 ratio in relation to the total protein content. The digestion was left overnight at 37°C. Sample was spun down at 10,000rpm for 10 sec. The supernatant was transferred to a new tube and the volume was reduced in a speedy vac until dry (30-45°C). The peptides were resuspended in 12-20µl of 1% formic acid.

Samples were injected onto an Agilent RP chip (160nl) installed on a 1200 Series nanoflow high performance liquid chromatography (HPLC) connected to an Agilent 6520 quadrupole-ToF mass spectrometer. Acquired data was analysed by Spectrum Mill

4.2.13 In-gel tryptic digestion

Gel slices were cut using a clean scalpel washed with acetonitrile (ACN) and then placed into autoclaved tubes. The gel slices were covered in 5% acetic acid and stored at 4°C. The acetic acid was removed from the tubes. The gels were washed (70µl of 200mM NH_4HCO_3), shrunk (70µl of 200mM NH_4HCO_3/ACN in 2:3 ratio), rehydrated (70µl of 50mM NH_4HCO_3) and shrunk again (70µl of ACN). 50µl of 10mM DTT (in 100mM NH_4HCO_3) was then added to each tube and left to shake for 60 min at 56°C at 700rpm. The DTT was removed and 50 µl of iodoacetamide (in 100mM NH_4HCO_3) was added to each tube and shook for 15 min at room temperature in the dark. The samples were spun down (10,000rpm for 10 sec) and the solution removed. Gel slices were then washed (300µl

100Mm NH_4HCO_3) and shrunk by the addition of 300µl 20mM NH_4HCO_3/ACN in 1:1 ratio and then 100 µl ACN to each tube. At each step samples were shook for 10min at 37°C at 700rpm. Between each step samples were spun down at 10,000rpm for 10 sec and the solution removed unless otherwise stated. The sample was then spun down at 10,000 rpm for 10 sec and the supernatant discarded. Added 50 µl Trypsin (0.2 µg/µ/) to each sample and shook overnight at 37°C at 300-500rpm. The next day samples were spun down. The solution was transferred to a new 500 µl tube. To ensure all peptides were extracted 30 µl of 70% ACN / 4 % formic acid to each gel piece. Samples were spun down and the supernatant added to the liquid previously collected in the new tubes. The volumes of the samples were then reduced by speedy vac until they were dry (30-45°C). The dried peptides were then resuspended in 12-20 µl of 1 % formic acid.

At each step samples were shook for 10min at 37°C at 700rpm. Between each step samples were spun down at 10,000rpm for 10 sec and the solution removed unless otherwise stated. The sample was then spun down at 10,000 rpm for 10 sec and the supernatant discarded.

Samples were injected onto an Agilent RP chip (160nl) installed on a 1200 Series nanoflow high performance liquid chromatography (HPLC) connected to an Agilent 6520 quadrupole-ToF mass spectrometer. Acquired data was analysed by Spectrum Mill

4.2.14 Selection of crude peptides for mass spectrometry and spectral library construction

A total of six spectral libraries were loaded into the Skyline software. Transition lists were generated for caspase-8, c-FLIP, Bcl-2, Bcl-Xl, Mcl-1, Bax, Bak, XIAP and Bid using the following settings; tryptic digestion, canonical proteome, peptide length 8-25 amino acids, exclude 25 N-terminal amino acids, exclude ragged ends and methionine, modification carbamidomethyl cysteine, prediction monoisotopic, collision energy Agilent, precursor charge (2,3), ion charge (1,2), Y ions, always add N to proline and C to glutamate or aspartic acid, ion match tolerance of 0.8 Da, 10 ion products, min to max 50-1800, m/z tolerance 0.08 and precursor

exclusion window at 20. Theoretical and observed peptides that meet these criteria were selected. Crude peptides corresponding to these transition lists were ordered from Thermo Scientific.

Approximately 2µg of crude peptide was injected onto an Agilent RP chip (160nl) installed on a 1200 Series nanoflow high performance liquid chromatography (HPLC) connected to an Agilent 6520 quadrupole-ToF mass spectrometer. Acquired data was analysed by Spectrum Mill. Peptides deemed promising if they could be correctly mapped to their parent protein. The promising peptides were validated in the trans-protein pipeline (TPP). Those peptides correctly identified and validated were used to construct a spectral library in Skyline.

4.3 Results

4.3.1 Classification of tumour cell lines by sensitivity to TRAIL-induced apoptosis

In order to identify a biomarker capable of classifying cells as TRAIL sensitive or resistant we first categorized a panel of 56 cell lines based upon their responsiveness to TRAIL treatment. TRAIL was added to cells (10-500 ng/ml) for 24, 48 and 72h. The reduction in viability was assessed by MTT viability assay. Of the cell lines 18 where classified as sensitive to TRAIL, 8 as partially responsive and 30 as resistant to TRAIL (Fig. 4.1). The LC_{50} value for TRAIL (ng/ml) was calculated for the 72h time point for each cell line (GraphPad Prism 6). The LC50 value is the concentration of TRAIL which induces 50% reduction in cell viability.

Cell lines classified as resistant never exhibited a reduction in viability of more than 25%. This means they have arbitrarily large LC_{50} values. Thus while the sensitive and partially responsive cell lines can be ranked most to least sensitive no such distinction can be made within the resistant cell lines. Bearing this in mind all 53 cell lines have been categorized and ranked most to least sensitive where appropriate (Fig. 4.1). The identified partially responsive cell lines were excluded from further analysis.

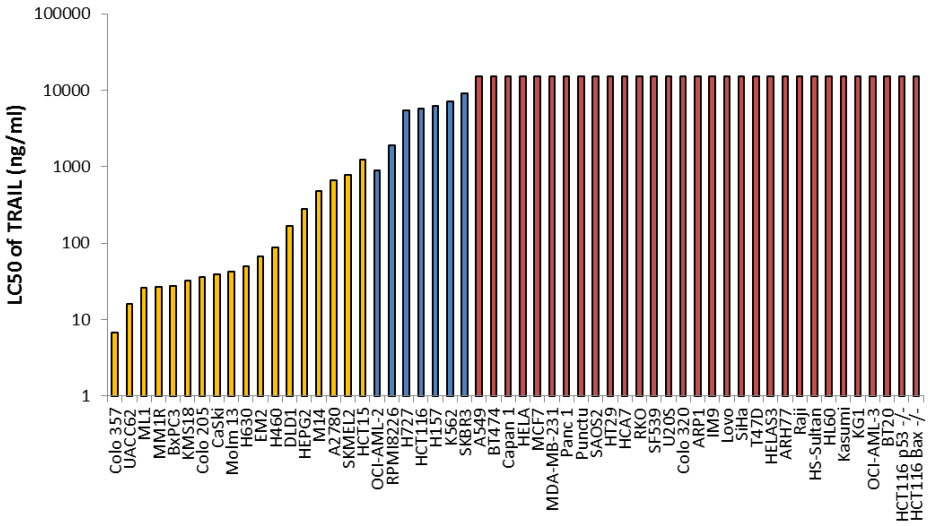

Figure 4.1: Categorization and ranking of cell lines by sensitivity to TRAIL. TRAIL sensitivity was assessed by MTT viability assay at 24, 48 and 72h after treatment. Cells which exhibited a reduction in viability of greater than 50% were deemed sensitive to TRAIL while those in which less than 25% reduction in viability was observed were classified as TRAIL resistant. Cell lines with a reduction in viability between 26-49% were identified as partially responsive to TRAIL. Using the 72h time point for each cell line the LC50 value of TRAIL was calculated for each cell line. All 56 cell lines were then ranked on the basis of their LC50 value.

4.3.2 Expression of the core effectors of TRAIL induced apoptosis in various cancer cell lines

The expressions of the components of the TRAIL apoptotic machinery were measured by Western blotting (caspase-8, c-FLIP, Bcl-2, Bcl-XL, Mcl-1, Bax and XIAP) or immunocytochemistry (DR4, DR5, DcR1 and DcR2).

The expression level of the intracellular proteins was measured in 42 tumour cell lines. To do this the optical density value for each of the proteins was measured at multiple exposures for all tumour cell line samples and an internal reference cell line HCT116. The optical density values for the internal reference cell line were used to construct standard curves at multiple exposure times (Fig. 4.2B). The expression of each protein was then measured relative to the HCT116 cell line by interpolation off of the corresponding standard curve. An example of such is provided for the XIAP protein (Fig. 4.2). A number of exposure times were tested for each protein to ensure that the exposures used for densitometry had luminescent signal that was still within the linear range of detection. For XIAP these were 30

sec, 1 min and 2 min (Fig. 4.2B). When we compared the relative expression value of XIAP from 2 separate repeats we see a linear fit along the 45° angle showing this method is reproducible (Fig. 4.2C). The quantification of the relative expression of the other intracellular proteins was optimised in the same manner.

XIAP (Fig. 4.3) was found to be expressed in 98% of the cell lines tested as is Mcl-1 (Fig. 4.5) while both Bcl-XL (Fig. 4.6) and Bcl-2 (Fig. 4.7) were expressed in 83% of the cell lines. Bax (Fig. 4.8) and caspase-8 (Fig. 4.4) were present in 91% of cell lines. c-FLIP (Fig. 4.9) could be detected in 79% of the cell lines.

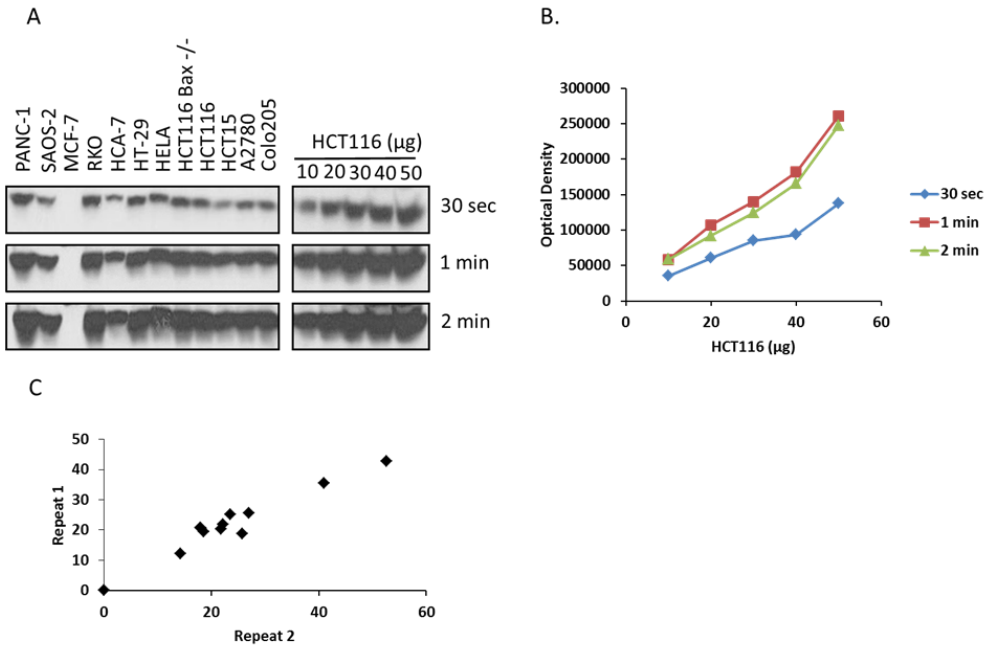

Figure 4.2: Optimisation of quantitation of Western blotting in tumour cell lines. As an example, the process of optimisation and quantitation is shown for XIAP. (A) Tumour cell line panels were probed for XIAP expression. One of 4 tested panels is shown here. Image was analysed by densitometry (B) Standard curve generated from densitometry values for HCT116 internal reference cell line. (C) The relative expression value of XIAP from two repeats plotted against each other ($R^2 = 0.95$).

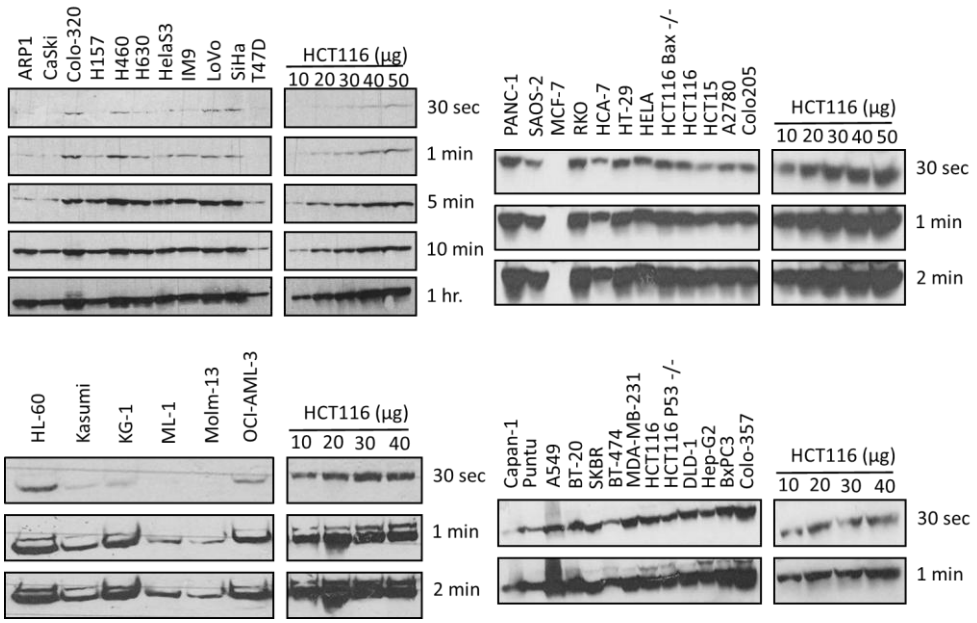

Figure 4.3: Quantification of XIAP expression in 42 tumour cell lines. Western blots for XIAP across 4 panels of tumour cell lines. The expression of XIAP was measured by densitometry. This figure shows a representative image of 3 independent experiments

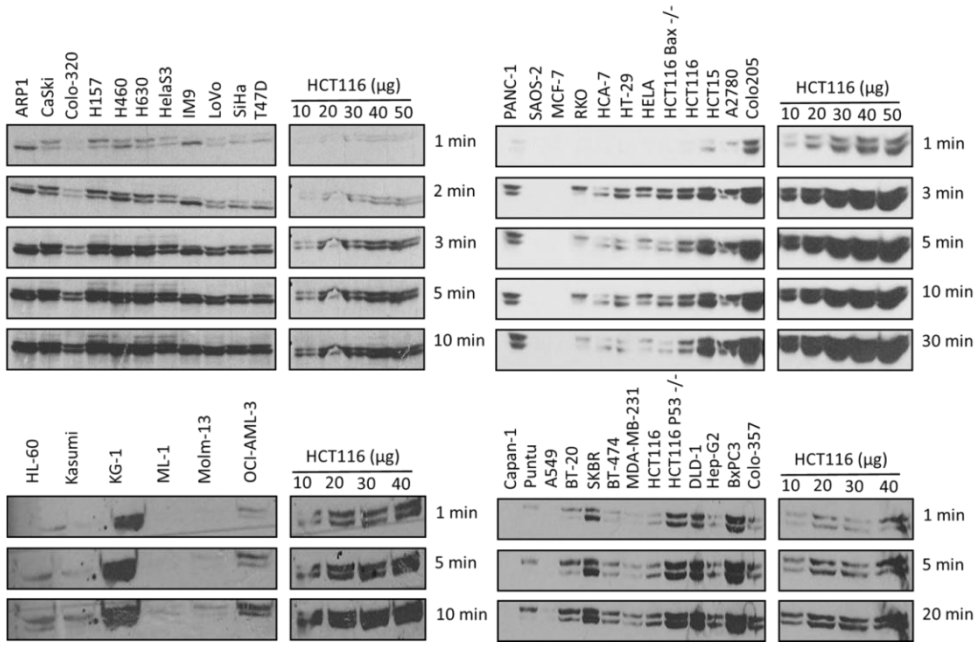

Figure 4.4: Quantification of Caspase-8 expression in 42 tumour cell lines Western blots for Caspase-8 across 4 panels of tumour cell lines. The expression of caspase-8 was measured by densitometry. This figure shows a representative image of 3 independent experiments

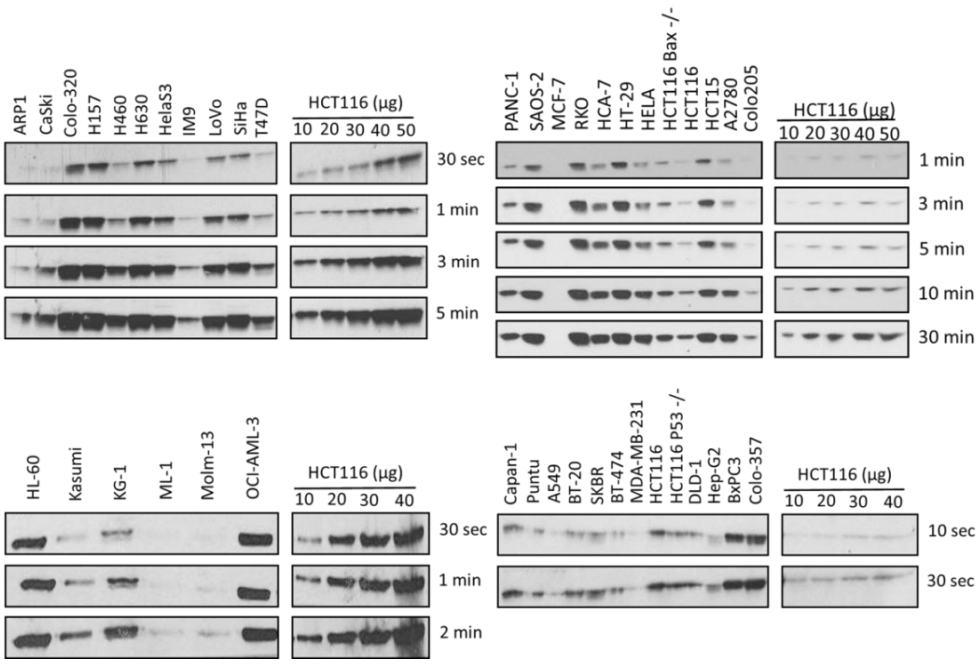

Figure 4.5: Quantification of Mcl-1 expression in 42 tumour cell lines. Western blots for Mcl-1 across 4 panels of tumour cell lines. The expression of Mcl-1 was measured by densitometry. This figure shows a representative image of 3 independent experiments

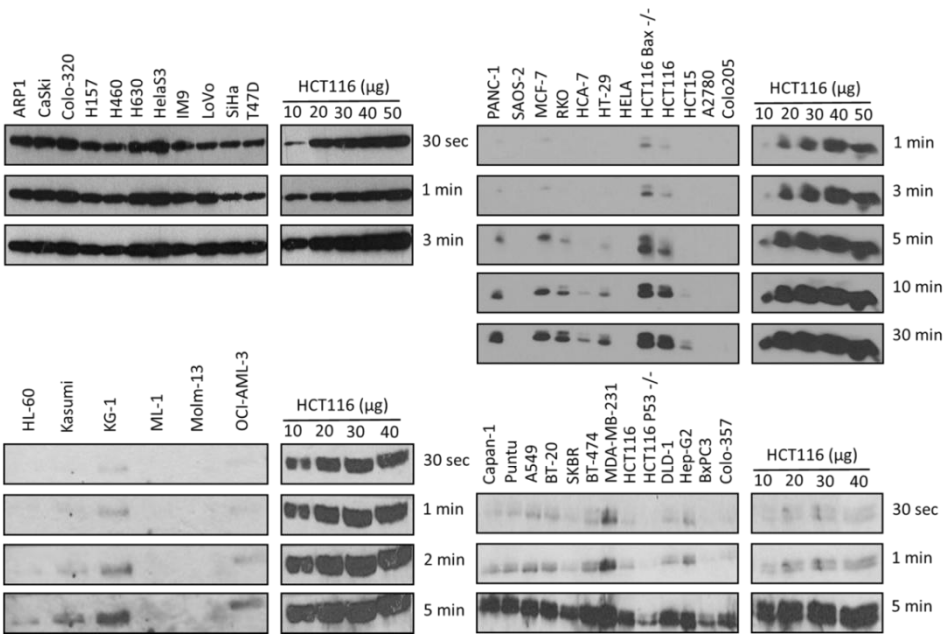

Figure 4.6: Quantification of Bcl-XL expression in 42 tumour cell lines. Western blots for Bcl-XL across 4 panels of tumour cell lines. The expression of Bcl-XL was measured by densitometry. This figure shows a representative image of 3 independent experiments

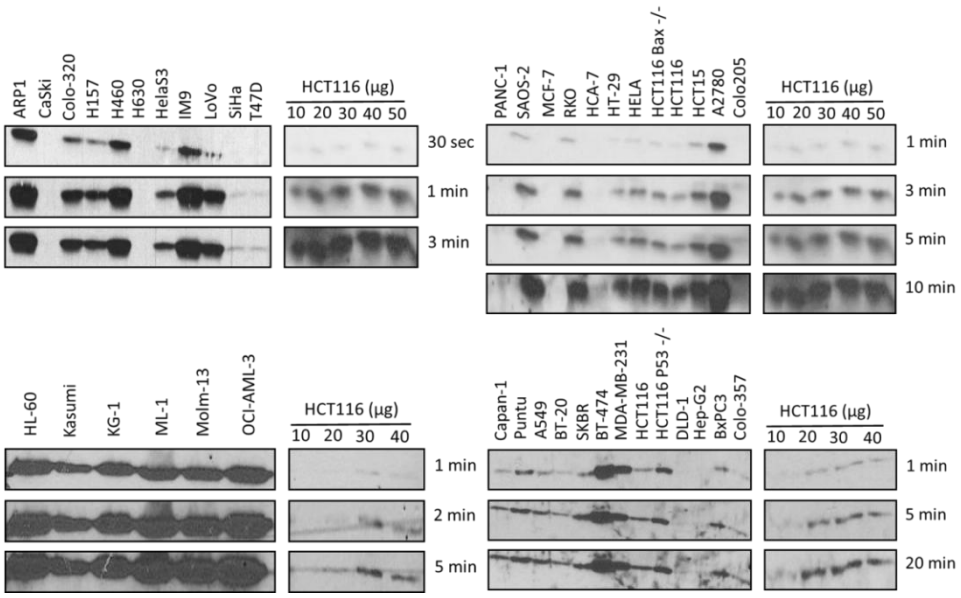

Figure 4.7: Quantification of Bcl-2 expression in 42 tumour cell lines. Western blots for Bcl-2 across 4 panels of tumour cell lines. The expression of Bcl-2 was measured by densitometry. This figure shows a representative image of 3 independent experiments

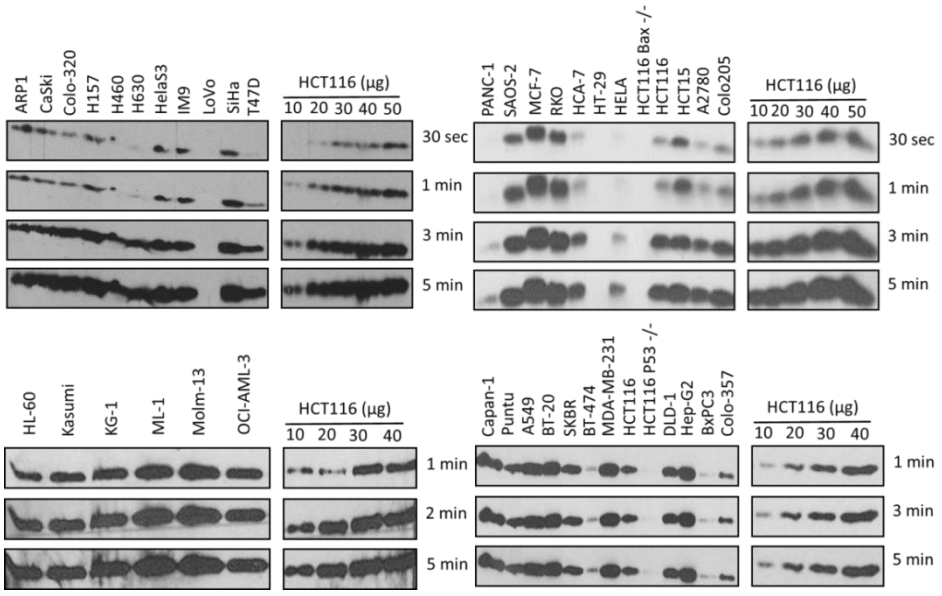

Figure 4.8: Quantification of Bax expression in 42 tumour cell lines. Western blots for Bax across 4 panels of tumour cell lines. The expression of Bax was measured by densitometry. This figure shows a representative image of 3 independent experiments

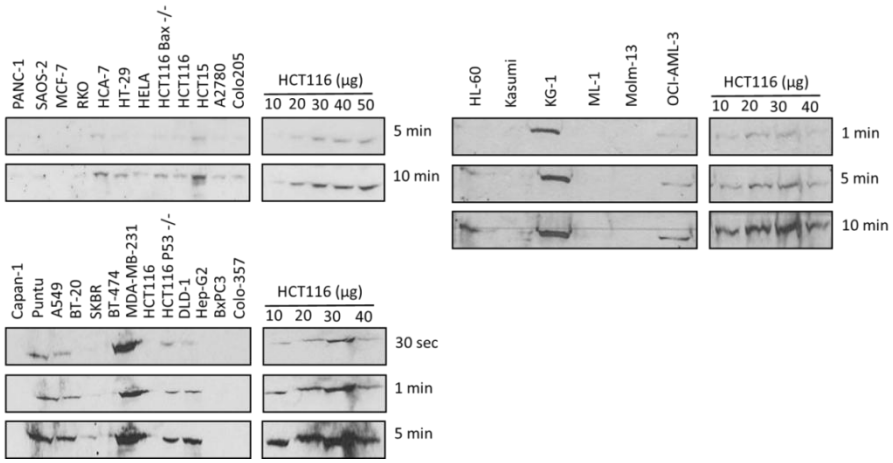

Figure 4.9: Quantification of c-FLIP expression in 42 tumour cell lines. Western blots for c-FLIP across 4 panels of tumour cell lines. The expression of c-FLIP was measured by densitometry. This figure shows a representative image of 3 independent experiments

Cell lines were ranked by the maximum observable reduction in viability seen after TRAIL treatment. No obvious trend was observed between increasing resistance to TRAIL induced apoptosis and the expression of any of the intracellular proteins (Fig. 4.10). We wanted to have a better idea of the overall shape and trend in the data therefore the expression values were grouped by TRAIL sensitivity into box plots. There was no clear distinction to be made between distribution in expression of XIAP, Bax, Bcl-XL or c-FLIP in TRAIL sensitive and resistant cell lines (Fig. 4.11F, Fig. 4.11A, Fig. 4.11G and Fig. 4.11D). In contrast Bcl-2 expression in TRAIL resistant cell lines was higher than in sensitive cell lines (Fig. 4.11B) and caspase-8 protein exhibited higher expression in TRAIL sensitive cell lines (Fig. 4.11C). Counter intuitively Mcl-1 expression appeared higher in TRAIL sensitive cell lines likely due to very high Mcl-1 expression in two of the most sensitive cell lines (Fig. 4.11E).

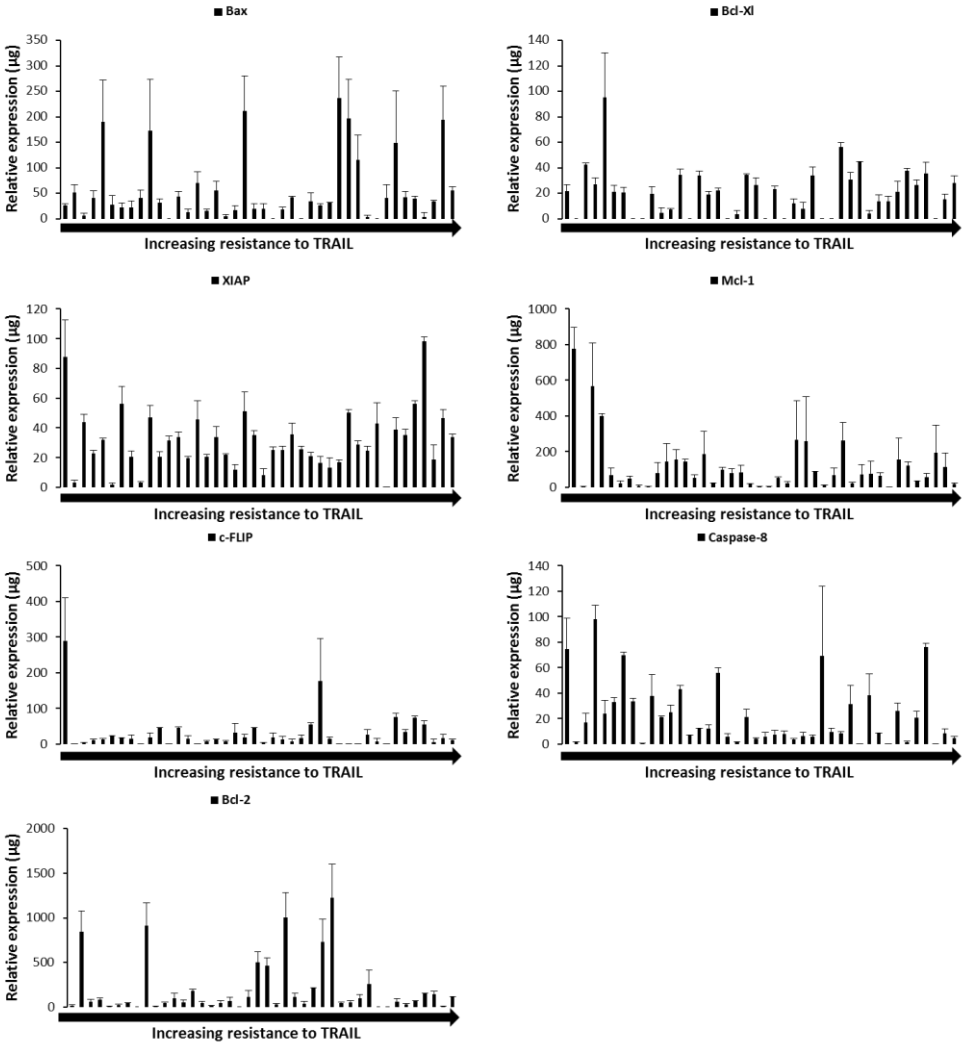

Figure 4.10: Expression of the intracellular components of the TRAIL apoptotic machinery. Relative expression value determined by Western blotting and densitometry in 42 tumour cell lines. Values shown are the mean of 3 repeats ± standard deviation. The maximal decrease in viability observed at the 72 h time point after treatment with TRAIL was used to rank the 42 tumour cell lines from least to most resistant to TRAIL.

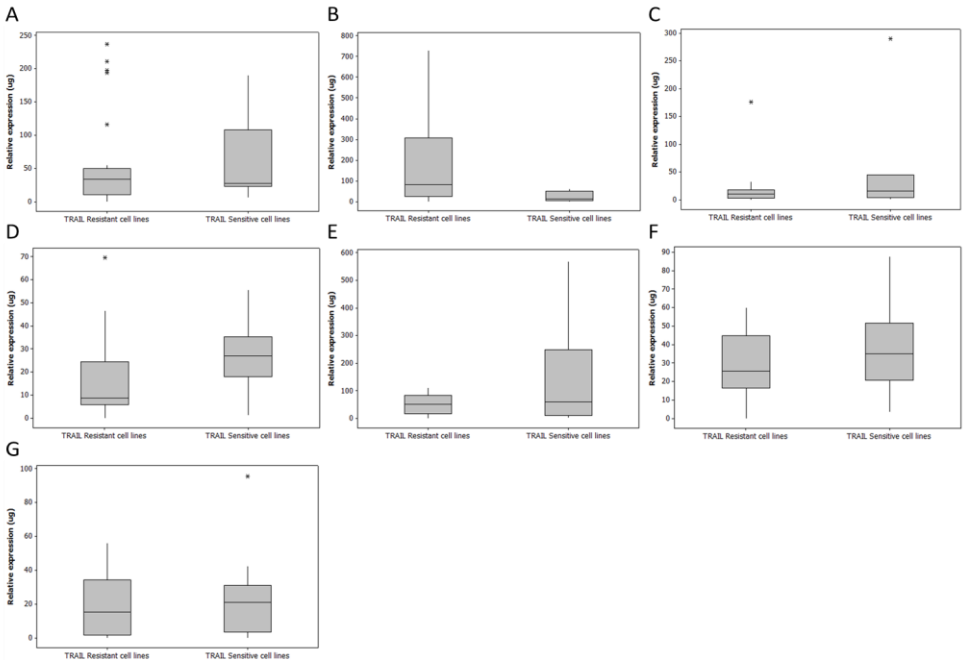

Figure 4.11: Boxplots displaying the expression range of the intracellular components of the TRAIL pathway in resistant and sensitive cell lines. Boxplots showing the spread in the range of expression values for the 7 proteins of interest across 42 tumour cell lines. (A) Bax (B) Bcl-2 (C) Caspase-8 (D) c-FLIP (E) Mcl-1 (F) XIAP and (G) Bcl-XL. The grey box area represents the inter quartile range. The top of this box the upper quartile indicates that 25% of the data points have a value equal to or greater than this. The lower quartile indicates 25% of the data points have a value equal to or less than this. The horizontal line is the median. The extended whiskers indicate the greatest and smallest value excluding outliers. Outliers are indicated by an asterisk

Next the cell surface expression of the death receptors (DR4 and DR5) and the decoy receptors (DcR1 and DcR2) was measured in the 42 tumour cell lines. This was done by immunocytochemistry. Cells were treated with one of the following primary antibodies; isotype control, DR4, DR5, DcR1 or DcR2. Thereafter the cells were treated with a FITC-conjugated secondary antibody. The geometric mean of FITC signal was measured by flow cytometry. The background signal, the isotype control, was subtracted from the values of the TRAIL receptors to give the mean FITC shift value. An example of which is provided below for DR4 and DR5 (Fig. 4.12A). As with quantification of the intracellular proteins we found these data where robust and reproducible (Fig. 4.12B)

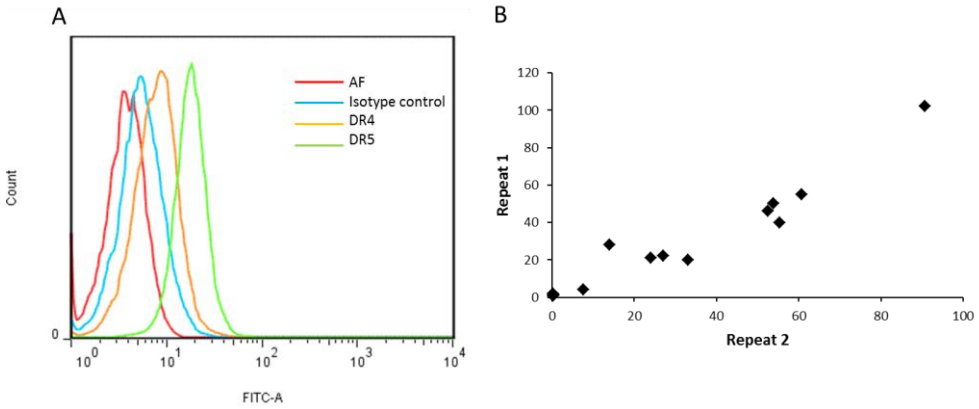

Figure 4.12: Optimisation of cell surface quantification of the TRAIL receptors. (A) Histogram overlay of the FITC intensity for the TRAIL death receptors. (B) The cell surface expression value of DR5 from two repeats was plotted ($R^2 = 0.91$).

When cell lines were ranked by their sensitivity to TRAIL there is no apparent trend in the expression of any of the TRAIL receptors and resistance to TRAIL treatment (Fig. 4.13).

When the spread of expression in TRAIL sensitive and resistant cell lines are compared by box-plot there is no distinction to be made between the two phenotypes by the cell surface expression of DR4, DR5, DcR1 or DcR2 (Fig. 4.14).

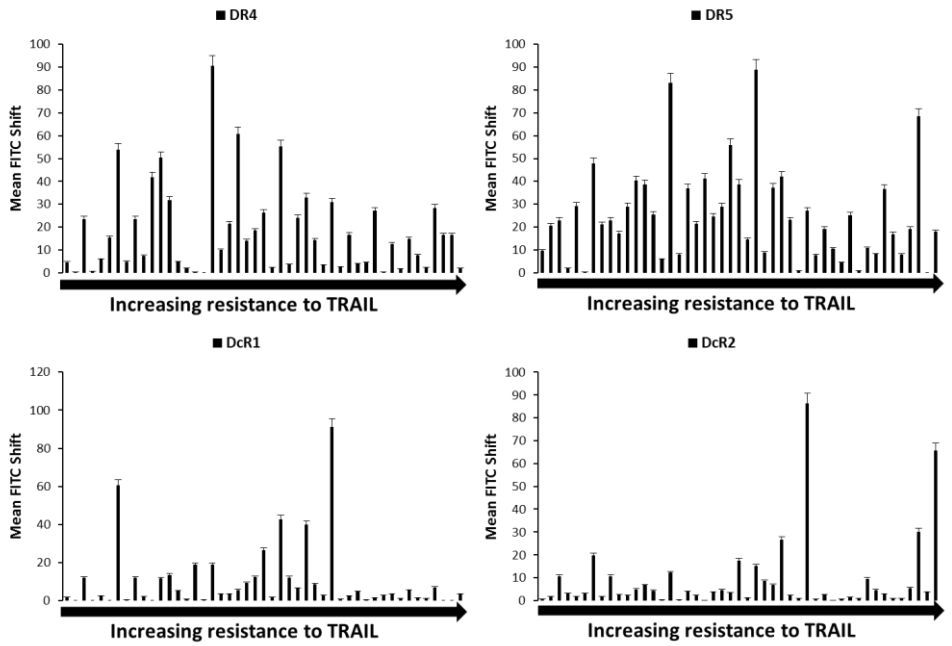

Figure 4.13: Cell surface expression of the TRAIL receptors. Cell surface receptor expression measured by immunocytochemistry followed by flow cytometry in 42 tumour cell lines. Values shown are for the mean of 3 repeats ± standard deviation. The maximal decrease in viability observed at the 72 h time point after treatment with TRAIL was used to rank 42 tumour cell lines from least to most resistant to TRAIL.

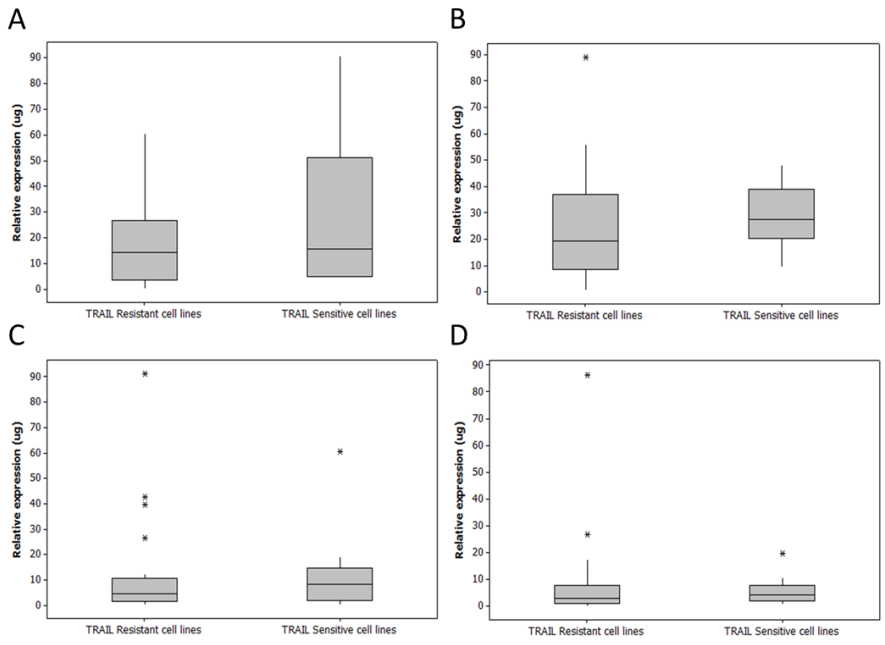

Figure 4.14: Boxplots displaying the cell surface expression range of the TRAIL receptors in resistant and sensitive cell lines. Boxplots showing the spread in the range of expression values for the 4 TRAIL receptors (A) DR4 (B) DR5 (C) DcR1 (D) DcR2. The grey box area represents the inter quartile range. The top of this box the upper quartile indicates that 25% of the data points have a value equal to or greater than this. The lower quartile indicates 25% of the data points have a value equal to or less than this. The horizontal line is the median. The extended whiskers indicate the greatest and smallest value excluding outliers. Outliers are indicated by an asterisk

4.3.3 Protein expression ratios predict TRAIL sensitivity with greater sensitivity

When we measured the expression of 11 components of TRAIL induced apoptosis only caspase-8 (Fig. 4.11C) and Bcl-2 (Fig. 4.11B) expression could separate resistant and sensitive cell lines well.

A computer script was written to calculate the expression ratio of all possible pairings of the 11 studied proteins generating 110 expression ratio values. We analysed the spread of the data between resistant and sensitive cell lines by box-plot (Fig. 4.15). The expression ratio which made the best distinction between the two phenotypes was Caspase-8/Bcl-2. In over 50 % of the sensitive cell lines the caspase-8/Bcl-2 ratio was much higher than all the resistant cell lines tested (Fig. 4.15A). Considering the high degree of redundancy in the function of the anti-apoptotic Bcl-2 family member's one might expect Caspase-8/Mcl-1 (Fig. 4.15B) or Caspase-8/Bcl-XL (Fig. 4.15C) to also appear predictive. This was not the case.

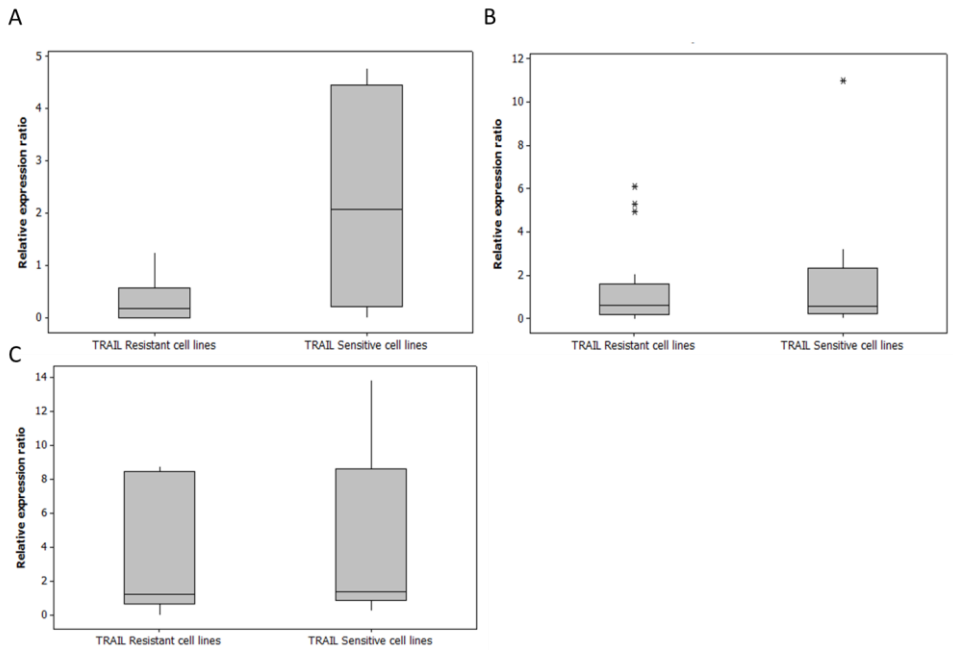

Figure 4.15: Caspase-8/Bcl-2 protein expression ratios predict TRAIL sensitivity better than protein expression values alone. Boxplots showing the spread in the range of expression values for the following expression ratios were generated (A) Caspase-8/Bcl-2 (B) Caspase-8/Mcl-1 and (C) Caspase-8/Bcl-XL. The grey box area represents the inter quartile range. The top of this box the upper quartile indicates that 25% of the data points have a value equal to or greater than this. The lower quartile indicates 25% of the data points have a value equal to or less than this. The horizontal line is the median. The extended whiskers indicate the greatest and smallest value excluding outliers. Outliers are indicated by an asterisk

4.3.4 Manipulation of Caspase-8/Bcl-2 ratio in vitro has a synergistic effect on TRAIL induced apoptosis

In order to mechanistically establish the importance of the caspase-8/Bcl-2 ratio in determining sensitivity to TRAIL we established a model system. This model utilized the following three cell lines; HL60 cells which are resistant to TRAIL and displayed very low caspase-8 to Bcl-2 ratio, Colo205 cells which are highly sensitive to TRAIL with very strong caspase-8 expression and undetectable Bcl-2 and HCT15 cells that express both caspase-8 and Bcl-2 at a medium level and are sensitive to TRAIL. The work has been completed for the HCT15 model and the results are shown here. Briefly we transduced HCT15 cells with a tetracycline inducible Tet-ON Caspase-8 lentiviral vector and then assessed the ability of various doses of doxycycline (Dox) (1-14 ng/ml) to induce caspase-8 expression

(Fig. 4.16A). Dox was shown to induce caspase-8 expression in a dose dependent manner. Furthermore a large induction of caspase-8 was observed as early as 2-4h post treatment (Fig. 4.16B) an effect which was sustained for up to 6h after washout of Dox from the cells (Fig. 4.16C). The effect of Dox (7.5, 10 and 12.5 ng/ml) on TRAIL sensitivity was measured by crystal violet assay (Fig. 4.16D). At all doses doxycycline was slightly toxic by itself likely due to autoactivation of overexpressed caspase-8. This was confirmed by the analysis of caspase-8 induction by doxycycline where autoprocessing of a portion of the overexpressed caspase-8 was detectable (Fig. 4.16B). To test the effect of increasing capase-8 expression the cells were treated with a dosage of TRAIL for 24 h after which TRAIL-induced cell death was determined with Crystal violet staining. This increased expression of caspase-8 lead to a minimal increase in sensitivity to TRAIL (Fig. 4.16D).

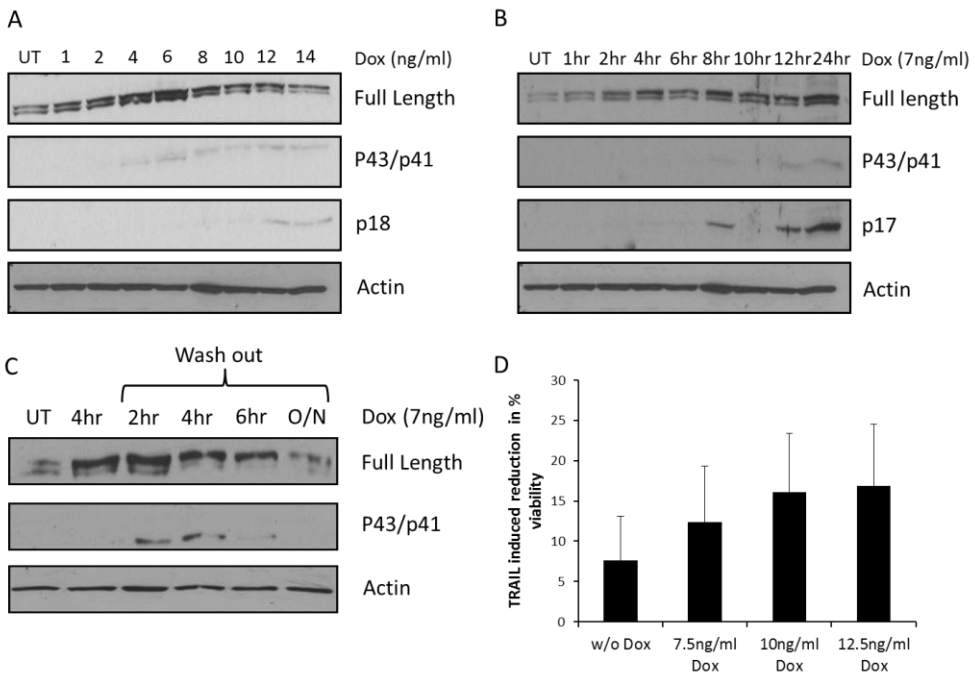

Figure 4.16: Over-expression of caspase-8 increases sensitivity to TRAIL induced apoptosis. (A) Tet-ON caspase-8 HCT15 cells treated with a dose range of doxycycline (Dox) for 24h. Lysates were analysed for caspase-8 expression. (B) Tet-ON caspase-8 HCT15 cells treated with Dox (7ng/ml) over a time course. Lysates analysed for caspase-8 expression. (C) Tet-ON caspase-8 HCT15 cells treated with 7ng/ml Dox. After 4h Dox was washed out of the cells. Samples were collected 2, 4 and 6h after washout as was an overnight sample. Lysates were analysed for caspase-8. (D) Tet-ON caspase-8 HCT15 cells were pretreated with in the indicated concentrations of Dox for 3h. Cells were then treated TRAIL (50ng/ml) for 24h. Effects on viability were measured by crystal violet assay. The TRAIL induced reduction in % viability = (% Viability of TRAIL +Dox treatments)-(%Viability of Dox treatments). Values shown are averages of 3 repeats ± SEM. All images shown are representative of 3 independent experiments

If the ratio of caspase-8 and Bcl-2 is a stronger determinant of TRAIL sensitivity than either protein alone then we would expect the simultaneous induction of caspase-8 and inhibition of Bcl-2 would sensitize to TRAIL in a synergistic manner. If not then their combined effect should be merely additive. To test this we measured the effect of reducing Bcl-2 expression and increasing caspase-8 simultaneously. In order to be able to tightly control the level of functional Bcl-2 in the cells we used the ABT737 compound a BH3-mimetic that blocks the function of Bcl-2 and Bcl-XL in a dose dependent manner. HCT15 cells express minimal levels of Bcl-XL and high amounts of Mcl-1. In order to be able to assess the role of the ratio of caspase-8 to Bcl-2 without the influence of Mcl-1 we knocked Mcl-1 down (Fig. 4.17).

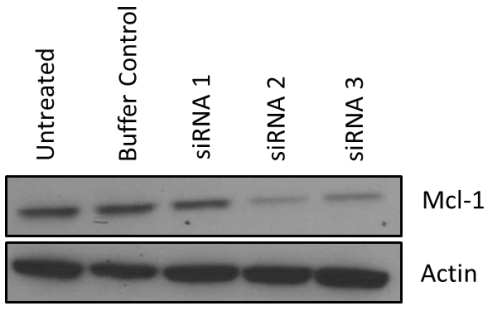

Figure 4.17: Knockdown of anti-apoptotic Mcl-1 Protein. Lysates from Tet-ON caspase-8 HCT15 cells transfected with siRNA targeting Mcl-1 were analysed for Mcl-1 expression. This figure shows a representative image of 3 independent experiments.

To gradually reduce Bcl-2 function and thus alter caspase-8/Bcl-2 ratio the cells were treated with a range of concentrations of ABT737. The induction of caspase-8 was able to modestly increase sensitivity to TRAIL at 25 (Fig. 4.18A) and 50ng/ml of TRAIL (Fig. 4.19A). The effect is best seen at the 50ng/ml treatment of TRAIL (Fig. 4.19A). The addition of ABT737 had no effect on TRAIL sensitivity at the lower dose of TRAIL (Fig. 4.18A). Neither did it have an effect at said dose when Mcl-1 was knocked down (Fig. 4.18B). At the higher dose of TRAIL a small increase in cell death was detectable upon the addition of ABT737 (Fig. 4.19A). This effect was potentiated by the knockdown of Mcl-1 (Fig. 4.19B).

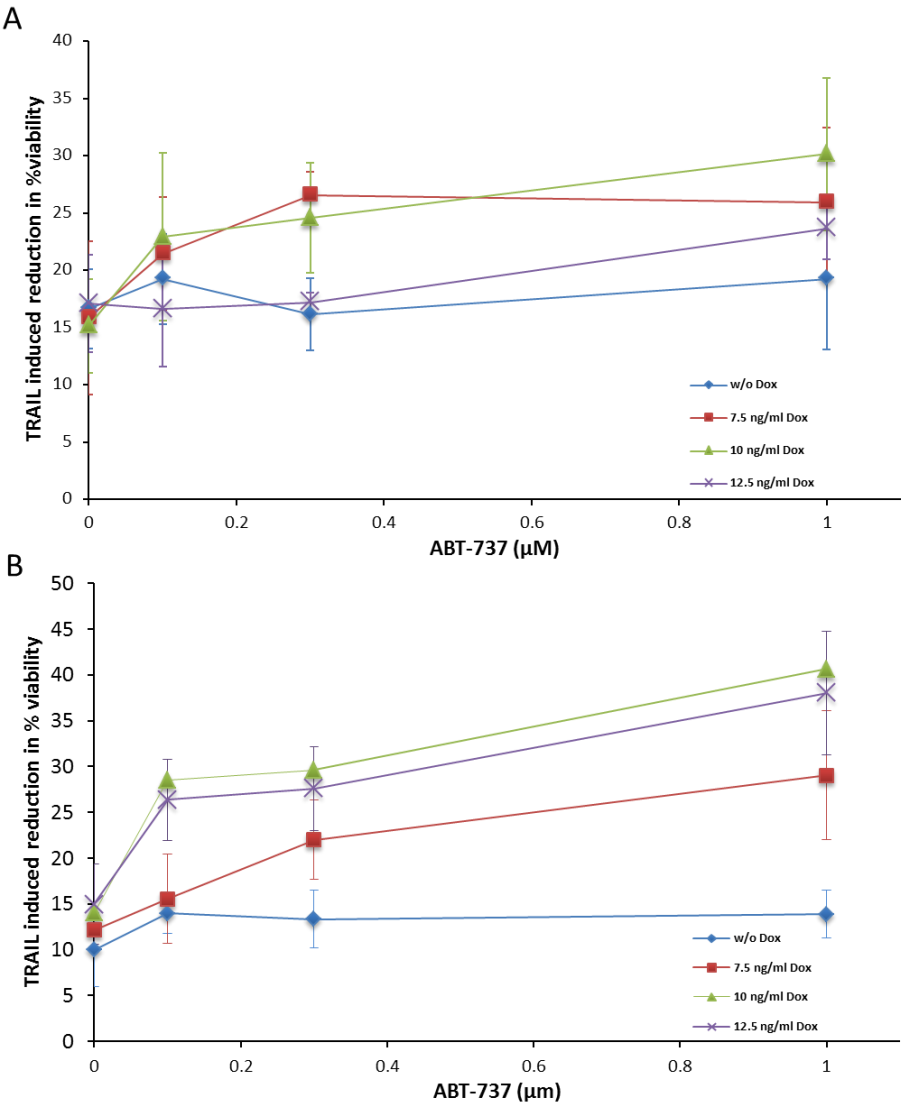

Figure 4.18: Induction of caspase-8 and functional knockdown of Bcl-2 in combination did not sensitize to low dose of TRAIL (25ng/ml) in the absence of Mcl-1 (A) Tet-ON caspase-8 HCT15 cells were transfected with control siRNA against GFP. Cells were pretreated with a range of Dox concentrations for 3h after which they treated with a range of ABT737 concentrations. One hour later the cells received TRAIL (25ng/ml). (B) Tet-ON caspase-8 HCT15 cells were transfected with siRNA against Mcl-1. Cells were pretreated with a range of Dox concentrations for 3h after which they treated with a range of ABT737 concentrations. One hour later the cells received TRAIL (25ng/ml).Viability was measured by crystal violet assay. The TRAIL induced reduction in % viability = (% Viability of TRAIL +Dox treatments)-(%Viability of Dox treatments). Values shown are averages of 3 repeats ± SEM

Concurrent inhibition of Bcl-2 and induction of caspase-8 expression resulted in a more than additive effect (CI=<1). The combination index (CI) was calculated in the compuSyn software. A CI value of less than 1 indicates synergism while greater than one means the effect is additive. The synergistic effect was measured in the absence of Mcl-1 where it is seen at the lowest dose of ABT737.

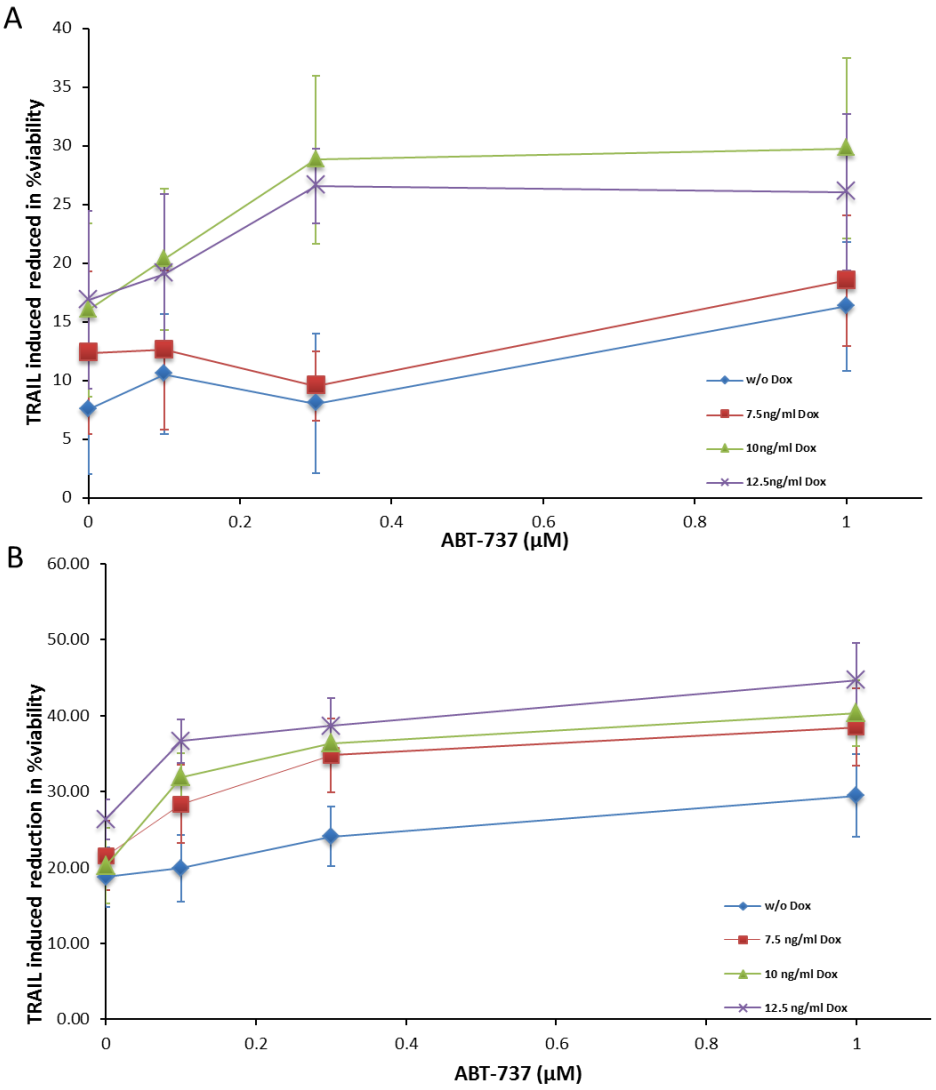

Figure 4.19: Induction of caspase-8 and functional knockdown of Bcl-2 in combination sensitizes to high dose of TRAIL (50ng/ml) in the presence and absence of Mcl-1. (A) Tet-ON caspase-8 HCT15 cells were transfected with control siRNA against GFP. Cells were pretreated with a range of Dox concentrations for 3h after which they treated with a range of ABT737 concentrations. One hour later the cells received TRAIL (50ng/ml). (B) Tet-ON caspase-8 HCT15 cells were transfected with siRNA against Mcl-1. Cells were pretreated with a range of Dox concentrations for 3h after which they treated with a range of ABT737 concentrations. One hour later the cells received TRAIL (50ng/ml).Viability was measured by crystal violet assay. The TRAIL induced reduction in % viability = (% Viability of TRAIL +Dox treatments)-(%Viability of Dox treatments). Values shown are averages of 3 repeats ± SEM

A secondary mechanistic model is in the process of being established in the Colo205 cell line. Here the anti-apoptotic Bcl-2 protein expression can be increased and the expression of caspase-8 can be decreased at the same time. Initially we intended to increase the abundance of Bcl-2 in a controlled manner by directly titrating recombinant Bcl-2 fused with a cell penetrating peptide (Pep-1-Bcl-2) into cells. The Bcl-2 protein however possesses a highly hydrophobic c-terminus and thus overexpression in a cellular context results in issues with protein solubility, the formation of protein aggregates and toxicity. Studies have circumvented this issue by structurally modifying Bcl-2 (Pedersen et al, 2011). We utilized the Invitrogen cell free expression system to produce Pep-1-Bcl-2 with an intact hydrophobic c-terminus. This was possible because the approach allowed for the addition of detergents to the reaction mixture to keep the protein soluble. The protein was purified on His-trap column and underwent buffer exchange (Fig. 4.20A). The Pep-1-Bcl-2 protein was shown to enter Colo205 (Fig. 4.20B) and HCT15 cells (Fig. 4.20C) successfully 3h post treatment in a dose dependent manner. The Colo205 cell line expresses small amounts of the Bcl-2 protein so the multiple myeloma cell line IM9 known to express Bcl-2 was included as a positive control (Fig. 4.20B and 4.20C). Colo205 cells were pre-treated with Pep-1-Bcl-2 or buffer alone (containing the detergent used to keep Pep-1-Bcl-2 soluble (Brij58)) 3h prior to the addition of staurosporine (STS). STS induced significant levels of cell death as assessed by propidium iodide (PI) staining (Fig. 4.20D). The Pep-1-Bcl-2 protein appeared to provide minor protection against STS induced cell death. This protection however was also seen in samples which received the buffer alone (Fig. 4.19D). Similar results were seen upon TRAIL treatment. We concluded that the Pep-1-Bcl-2 protein was not biologically active.

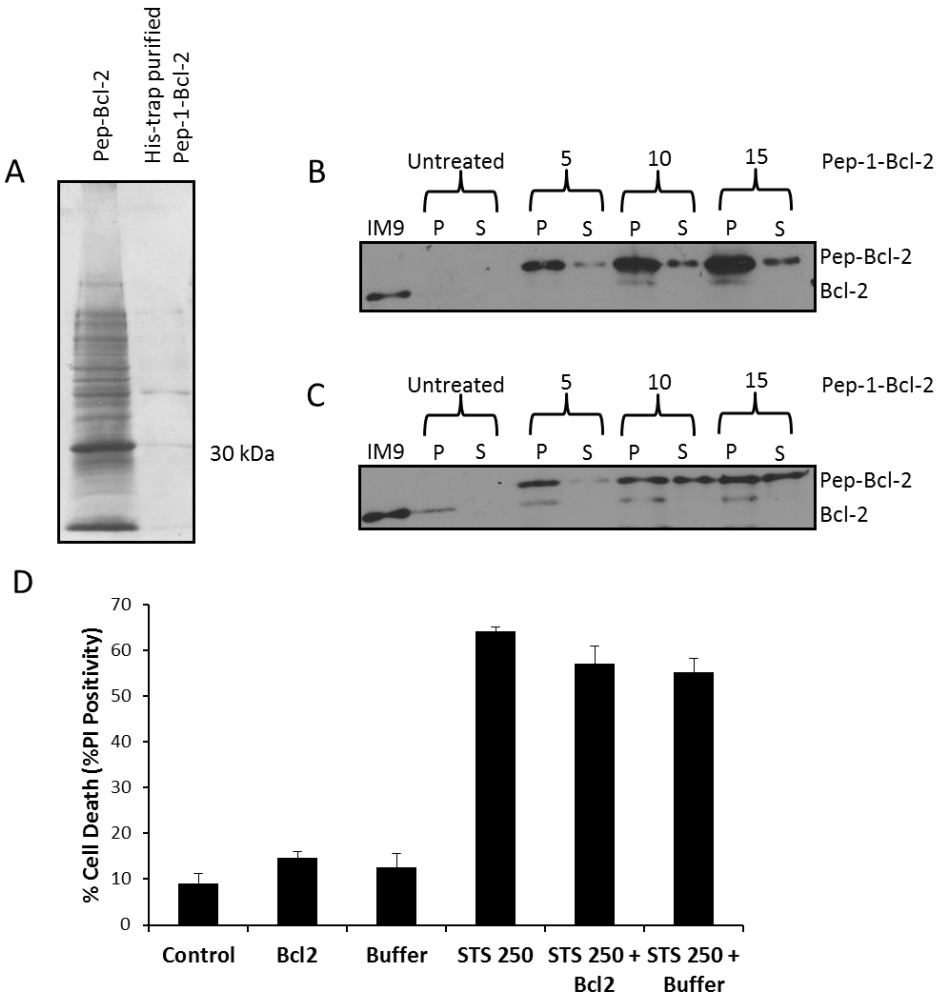

Figure 4.20: Pep-1-Bcl-2 recombinant protein could not protect against apoptotic cell death. (A) Pep-1-Bcl-2 recombinant protein was purified on a His-trap column. Purity was assessed by gel electrophoresis and coomassie staining. (B) Colo205 cells were treated with a range of Pep-1-Bcl-2 recombinant protein. Western blots show Pep-2-Bcl-2 protein enters Colo205 and HCT15 cells 3h after treatment in a dose dependent manner. While some Pep-1-Bcl-2 remained in the supernatant (S) the majority entered the cells (P). The multiple myeloma cell line IM9 was included as a positive control for the detection of Bcl-2. (D) Colo205 cells were pretreated for 3h with Pep-1-Bcl-2 (10µl) or its storage buffer containing the detergent Brij 58 required to keep Pep-1-Bcl-2 soluble (10µl). Cells were then treated with staurosporine (STS) for 15h. Cell death was assessed by propodium iodide staining and flow cytometry. Values shown are averages of 3 repeats ± standard deviation.

Instead we utilized a Colo205 cell line stably overexpressing Bcl-2 previously generated in house (Fig. 4.21A). We wanted to know if Bcl-2 overexpression could protect these cells against TRAIL induced cell death. Wild type Colo205 cells transduced with RFP control (Colo205-pCDH-RFP) and Colo205-Bcl-2 were treated with TRAIL (50, 125 and 250 ng/ml) for 15h. The effect of TRAIL on viability was assessed by MTT (Fig. 4.21B). TRAIL induced cell death at the 125 and 250 ng/ml concentrations in wild type and pCDH-RFP only. The over expression of Bcl-2 protected the Colo205 cells against TRAIL induced cell death at the 250ng/ml dose of TRAIL ($p<0.05$) (Fig. 4.21B).

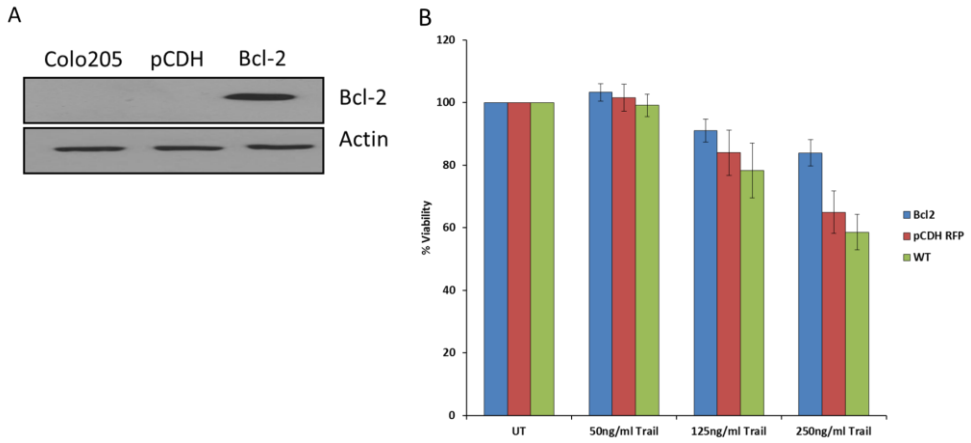

Figure 4.21: Stable overexpression of Bcl-2 in Colo205 cells protects against TRAIL induced apoptosis. (A) Western blot showing the overexpression of Bcl-2 in the Colo205 cell line. Cells treated transduced with control pCDH-RFP showed no increased expression of Bcl-2 compared to wild type. (B) Wild type, pCDH-RFP and Bcl-2 over expressing cells were treated with a range of TRAIL concentrations. Effects of TRAIL induced cell death were assessed by MTT assay.

The knockdown of caspase-8 expression by accell siRNA technology, which enters cells without the need for transfection reagents or viruses, has been optimised. Colo205 cells were treated with 0.75, 1.5, 3 and 6 µM of accell siRNA targeting caspase-8. A dose dependent decrease in caspase-8 expression was observed 72 h after treatment (Fig. 4.22).

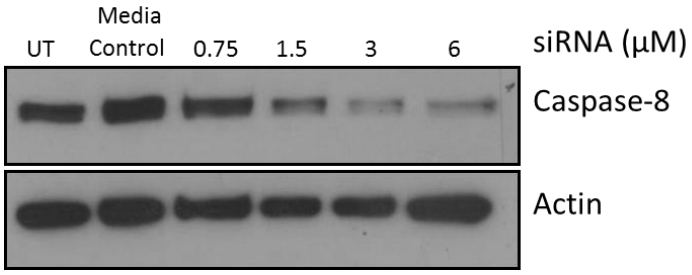

Figure 22: Dose dependent knockdown of caspase-8. Colo205 cells were treated with a range of accell siRNA for 72 h resulting in a dose dependent knock down of caspase-8

4.3.5 Optimization of mass spectrometer for protein quantification

Despite all efforts to optimise Western blotting for quantification of relative protein abundance there is still considerable error associated with this detection method owing most likely to the non-linearity of the horseradish peroxidase enzyme reaction. The measurement of protein abundance by mass spectrometry, however, has the potential for reproducible and accurate protein quantification.

Quantification by mass spectrometry first requires the identification of peptides which the mass spectrometer can detect and that can be mapped back to the correct parent protein with a high degree of surety. The list of which ionized peptides and ion fragments are best for protein identification and should be observed is known as a transition list. These lists are typically constructed from the observations of previous mass spectrometry runs known as spectral libraries in the Skyline software. Our goal was to optimise the detection of the following proteins (Bcl-2, caspase-8, c-FLIP, Bcl-XL, Mcl-1, XIAP, Bax, Bak and Bid) by mass spectrometry. Once this was complete we could develop protocols for the quantification of the

previously mentioned proteins at a later date. Using the Skyline software we constructed transition lists using peptides from spectral libraries and theoretical peptides which such be produced upon digestion with trypsin. We were unable to detect any of the proteins of interest in tryptically digested HCT116 whole cell lysates by quadruple time of flight mass spectrometry (QTOF) (data not shown). In the context of the whole proteome apoptotic proteins are of relatively low abundance. Therefore we postulated that the mass spectrometer failed to detect these proteins because of a lack of sensitivity.

Separation of samples by gel electrophoresis has become a cornerstone in proteomic analysis. These gels are stained, cut into pieces, destained, reduced, alkylated and finally undergo tryptic digestion. This is known as in-gel tryptic digestion. By spreading the proteome across a number of gel slices the relative expression of all proteins is increased and concurrently the number of unique peptides that can be detected also increases. Bearing this in mind we loaded 30µg of HCT116 lysate onto a 10% polyacrylamide gel. After electrophoresis the gel was stained with coomassie-brilliant blue. Gel slice regions containing the proteins of interest were excised before being destained, reduced, alkylated and tryptically digested (Fig. 4.23). We could detect peptides for Bcl-2, Mcl-1, Bcl-XL, caspase-8 and XIAP by QTOF using spectrum mill for protein identification (Table 4.1). Unfortunately we could not observe peptides for Bax, Bak, c-FLIP or Bid. The spectral libraries available to us were from whole cell lysates or plasma in which apoptotic proteins are again in low abundance. Indeed there was no previously recorded identification of Bax, Bak, c-FLIP or Bid in said libraries. Using the skyline software we had identified the best theoretical peptides which should be produced upon tryptic digestion for these proteins.

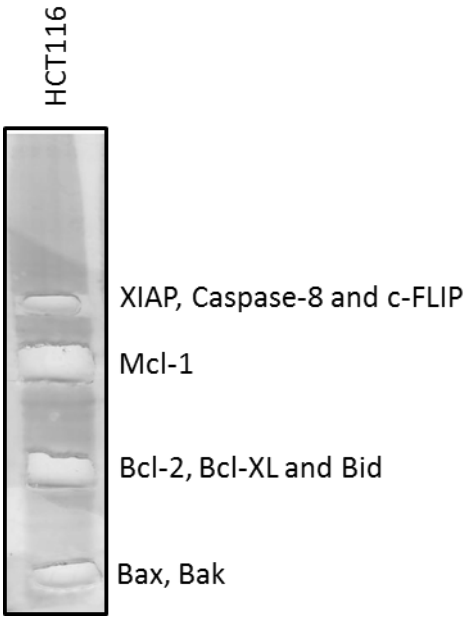

Figure 4.23: In gel tryptic digestion. HCT116 lysate (30µg) was loaded onto 10% polyacrylamide gel. Gel was stained with coomassie brilliant blue. Using the protein ladder gel regions were excised which should contain the indicated proteins. These gel slices were then destained, reduced, alkylated and tryptically digested. The peptides were then extracted from the gel and run on a QTOF mass spectrometer. This is a representative image of 3 independent experiments.

Protein	Sequence	Protein	Sequence
Bcl-2	FATVVEELFR	XIAP	GQEYINNIHLTHSLEECLVR
Bcl-2	TSPLQTPAAPGAAAGPALSPVPPVVHLTLR	XIAP	TFANFPSGSPVSASTLAR
Bcl-XL	EAGDEFELR	Mcl-1	IVTLISFGAFVAK
Caspase-8	VMLYQISEEVSR	Mcl-1	LLFFAPTR
Caspase-8	VFFIQACQGDNYQK	Mcl-1	QSLEIIR
Caspase-8	EQDSESQTLDK		

Table 4.1: Peptide identified after in-gel tryptic digestion by QTOF mass spectrometry. Whole cell lysate for the HCT116 cell line was run on QTOF mass spectrometer. The peptides listed here were identified with a high degree of confidence.

To circumvent this issue we decided to construct our own spectral library. To do this we first generated a list of peptides previously observed in the spectral libraries and peptides which should be theoretically generated upon tryptic digestion for the proteins of interest (Table 4.2). This peptide screening was done using the Skyline software. These peptides were purchased from thermo scientific as crude peptides.

Each peptide (2µg) was then run on a QTOF mass spectrometer. We could correctly identify 34 out of the 48 peptides these represent 7 of the 9 proteins of interest (Table 4.3). We compiled this data into a spectral library using the trans-peptide-pipeline (TPP) and skyline. The TPP carries out protein identification and validation in a more stringent manner than spectrum mill. On the basis of this stringency 22 of the 34 peptides detectable by QTOF were included in the spectral library representing 6 of the 9 parent proteins (Table 4.4). Those not included are Mcl-1, Bcl-2 and Bax. No peptides for Mcl-1 or Bcl-2 were correctly associated to their parent protein in spectrum mill whereas 4 peptides for Bax were correctly identified in spectrum mill but none met the minimum criteria for inclusion in TPP.

Protein	Sequence	RI	Protein	Sequence	RI
Caspase-8	NLYDIGEQLDSEDLASLK	41.9	c-FLIP	DVAIDVVPPNVR	28.6
Caspase-8	VMLYQISEEVSR	30.03	c-FLIP	DLLDILR	33.31
Caspase-8	FLLQEEISK	28.34	c-FLIP	LSVGDLAELLYR	40.62
Caspase-8	IINDYEEFSK	22.03	c-FLIP	NPHLVSDYR	16.42
Caspase-8	EQDSESQTLDK	7.31	c-FLIP	QSVQGAGTSYR	4.95
Caspase-8	VFFIQACQGDNYQK	27	c-FLIP	NVLQAAIQK	19.6
Caspase-8	GIPVETDSEEQPYLEMDLSSPQTR	34.87	c-FLIP	DPSNNFR	9.75
Caspase-8	NPAEGTWYIQSLCQSLR	38.91	c-FLIP	DTFTSLGYEVQK	29.43
BID	IEADSESQEDIIR	19.31	c-FLIP	DYDSFVCVLVSR	37.97
BID	HLAQVGDSMDR	14.63	Bcl-XL	ELVVDFLSYK	40.23
BID	SIPPGLVNGLALQLR	44.68	Bcl-XL	GYSWSQFSDVEENR	24.99
BID	DLATALEQLLQAYPR	41.87	Bcl-XL	EAGDEFELR	20.49
BID	DVFHTTVNFINQNLR	42.49	Bcl-XL	AFSDLTSQLHITPGTAYQSFEQVVNELFR	56.36
Bcl-2	TSPLQTPAAPGAAAGPALSPVPPVVHLTLR	45.89	Mcl-1	EIGGGEAGAVIGGSAGASPPSTLTPDSR	23.2
Bcl-2	QAGDDFSR	6.38	Mcl-1	LLFFAPTR	32.34
Bcl-2	FATVVEELFR	37.48	Mcl-1	QSLEIISR	22.39
XIAP	TFANFPSGSPVSASTLAR	33.09	Mcl-1	IVTLISFGAFVAK	47.44
XIAP	TGQVVDISDTIYPR	30.15	Bax	TGALLLQGFIQDR	44.04
XIAP	NPSMADYEAR	11.03	Bax	MIAAVDTDSPR	14.16
XIAP	SLEVLVADLVNAQK	39.8	Bax	VAADMFSDGNFNWGR	34.39
XIAP	SFQNWPDYAHLTPR	31.31	Bax	VVALFYFASK	39.33
XIAP	AGFLYTGEGDTVR	26.32	Bax	TIMGWTLDFLR	48.55
Bak	QLAIIGDDINR	28.67	Bak	VVALLGFGYR	37.81
Bak	IATSLFESGINWGR	39.23	Bak	LALHVYQHGLTGFLGQVTR	47.48

Table 4.2: An overview of crude peptides used in the construction of spectral library

Protein	Peptide Sequence	Protein	Peptide Sequence
Caspase-8	NLYDIGEQLDSEDLASLK	c-FLIP	DPSNNFR
Caspase-8	VMLYQISEEVSR	c-FLIP	LSVGDLAELLYR
Caspase-8	FLLQEEISK	c-FLIP	NPHLVSDYR
Caspase-8	IINDYEEFSK	c-FLIP	DTFTSLGYEVQK
Caspase-8	VFFIQACQGDNYQK	c-FLIP	DYDSFVCVLVSR
Caspase-8	GIPVETDSEEQPYLEMDLSSPQTR	c-FLIP	DLLDILR
Bak	VVALLGFGYR	c-FLIP	QSVQGAGTSYR
Bak	IATSLFESGINWGR	c-FLIP	NVLQAAIQK
Bak	LALHVYQHGLTGFLGQVTR	c-FLIP	DVAIDVVPPNVR
XIAP	SLEVLVADLVNAQK	BID	SIPPGLVNGLALQLR
XIAP	SFQNWPDYAHLTPR	BID	DVFHTTVNFINQNLR
XIAP	TFANFPSGSPVSASTLAR	BID	IEADSESQEDIIR
XIAP	TGQVVDISDTIYPR	BID	HLAQVGDSMDR
XIAP	NPSMADYEAR	BID	DLATALEQLLQAYPR
XIAP	AGFLYTGEGDTVR	Bcl-XL	AFSDLTSQLHITPGTAYQSFEQVVNELFR
Bax	MIAAVDTDSPR	Bax	VAADMFSDGNFNWGR
Bax	TIMGWTLDFLR	Bax	TGALLLQGFIQDR

Table 4.3: Crude peptides correctly mapped to their parent protein. Peptides were run on QTOF mass spectrometer. Those peptides, 34 of the 48, which were observed and had their parent protein correctly identified are listed here

Protein	Peptide Sequence	Protein	Peptide Sequence
Caspase-8	IINDYEEFSK	c-FLIP	LSVGDLAELLYR
Caspase-8	FLLQEEISK	c-FLIP	NPHLVSDYR
XIAP	SLEVLVADLVNAQK	c-FLIP	DTFTSLGYEVQK
XIAP	SFQNWPDYAHLTPR	c-FLIP	DYDSFVCVLVSR
XIAP	TFANFPSGSPVSASTLAR	c-FLIP	QSVQGAGTSYR
XIAP	TGQVVDISDTIYPR	c-FLIP	NVLQAAIQK
XIAP	AGFLYTGEGDTVR	c-FLIP	DVAIDVVPPNVR
Bcl-XL	AFSDLTSQLHITPGTAYQSFEQVVNELFR	BID	SIPPGLVNGLALQLR
Bak	IATSLFESGINWGR	BID	DVFHTTVNFINQNLR
Bak	VVALLGFGYR	BID	IEADSESQEDIIR
Bak	LALHVYQHGLTGFLGQVTR	BID	DLATALEQLLQAYPR

Table 4.4: Peptides present in spectral library. The 34 peptides correctly identified were used to construct a spectral library using the trans-peptide-pipeline (TPP) and Skyline. 22 of the 34 peptides passed stringency criteria and were included in the library.

Two of the three crude peptides for Bcl-2 were indicated to have retention index values of <10 and >40 (Table 1) meaning they are hydrophilic and hydrophobic respectively and as such may require further optimised conditions for detection. In addition one of the four Mcl-1 peptides was hydrophobic also (Table 4.1). We must not forget that these are crude peptides and that potentially they were not correctly mapped to their parent protein because of poor signal intensity in the mass spectrometer due to impurity in the sample.

4.4 Discussion

Targeting death receptors using TRAIL, as with traditional chemotherapeutics, has encountered issues with inherent resistance to treatment. The study of TRAIL resistance by top down approaches has identified a multitude of mechanisms contributing to this resistance such as the up-regulation of Bcl-2 family members, XIAP, survivin or c-FLIP or the reduction in expression of pro-apoptotic proteins namely caspase-8. Proteomic analysis of the TRAIL apoptotic machinery failed to reveal a strong correlation between the expression of any of these proteins and resistance to TRAIL (Wagner et al, 2007).

The ability to identify particular tumour sub-types that are susceptible to TRAIL would be beneficial to its future clinical applications. Therefore we assessed the role of protein-protein interactions in predicting TRAIL sensitivity. In order to do this we measured the expression of 11 core components of the TRAIL apoptotic machinery by immunocytochemistry and Western blotting followed by densitometry where appropriate in 42 tumour cell lines from several different tissue types. Our results were in accordance with the literature for the most part with only Bcl-2 (Fig. 4.11B) and caspase-8 (Fig. 4.11C) expression predicting TRAIL sensitivity. When we assessed the predictive power of protein pairs, the expression of one protein relative to another, we uncovered a powerful predictor of sensitivity in the caspase-8/Bcl-2 pairing (Fig. 4.15A). Furthermore we have experimental evidence to suggest that this ratio is not only associated with sensitivity but is a causative element in this phenotype as artificially increasing or decreasing the ratio by induced expression or functional knockdown caused increased sensitivity to TRAIL (Fig. 4.19B). Inflating the expression ratio by concurrently inducing caspase-8 and inhibiting Bcl-2 had a synergistic effect (Fig. 4.19B). We interpret this as an indication that these two proteins are operating along the same pathway rather than in parallel and therefore their performance as a predictor of TRAIL sensitivity is dependent on their relationship to each other. There is indirect evidence in

the literature to support this. For example the expression of caspase-8 and Bcl-2 was correlated with TRAIL sensitivity in neuroendocrine tumour cells which could be sensitized to TRAIL via the down-regulation of Bcl-2 by Raf265 which is a novel inhibitor of Raf (Zitzmann et al, 2011). It must be noted that approximately 50% of resistant cell lines exhibited Caspase-8/Bcl-2 protein expression ratios within the same range as some sensitive cell lines (Fig. 4.15A). Therefore for these resistant and sensitive cell lines the Caspase-8/Bcl-2 ratio does not predict TRAIL sensitivity. In the future it would be interesting to subset these cell lines. The rationale being that in the absence of those cell lines for which the Caspase-8/Bcl-2 ratio is predictive we may be able to identify protein expression ratios other than Caspase-8/Bcl-2 capable of predicting TRAIL sensitivity. Should this prove successful we may identify numerous predictive protein expression ratios useful for the classification of subsets of cell lines. In combination these classifiers could predict TRAIL sensitivity to a much higher degree of accuracy than any alone.

While this approach seems simple in concept only a few examples of this type of analysis can be found in the literature. The best known example is the ratio of HOXB13 and interleukin 17 receptor B (IL17BR) which is a prognostic marker of early stage breast cancer predicting recurrence risk in ER-positive, lymph node-negative breast cancer patients. Furthermore there are studies showing this ratio not only predicts clinical outcome but is also associated with tumour aggression and sensitivity to Tamoxifen treatment (Jansen et al, 2007). In the last year Rehm and colleagues reported that they could predict TRAIL sensitivity with 91% accuracy in small panel of multiple myeloma cell lines. They did this through the construction of a mathematical model integrating protein interactions or relationships and position in the pathway alongside expression data (Passante et al, 2013). This approach like our own considered proteins not in isolation but in relation to each other and thus likely better encapsulates the complex biology involved.

Quantification of protein expression using chemiluminescent Western blotting has issues with systemic error due to the saturable enzyme kinetics

of the detection method. Despite our best efforts we were unable to eliminate these issues entirely. This means that we may be under estimating the expression level of proteins whose signal appears to approach saturation. Examples of which can be seen in figure 4.3 and 4.7. Alongside concerns of the accuracy of these protein expression values this issue also limits the sensitivity of the protein expression ratio analysis. Therefore it is conceivable that protein expression ratios capable of predicting TRAIL sensitivity are being overlooked. It is also plausible that the difference in Caspase-8/Bcl-2 protein expression ratio between TRAIL sensitive and resistant cell lines might have been over- or underestimated. However our mechanistic analysis confirmed that altering the Caspase-8/Bcl-2 ratio had a direct effect on TRAIL induced apoptosis (Fig. 4.19). This suggests that the identification of Caspase-8/Bcl-2 ratio is unlikely to be an experimental artefact. Extensive efforts have been made to improve the quantitative ability of our protein expression profiling namely the construction of a custom spectral library for detection of components of the TRAIL apoptotic machinery using mass spectrometry and the optimization of Western blot detection by near infra-red fluorophores developed by LI-COR biosciences. We have been unable to correctly identify peptides for Bcl-2, Mcl-1 or Bax for incorporation into the spectral library and as such cannot as of yet detect all the proteins of interest by mass spectrometry (Table 4.4). The near infra-red detection system on the other hand has recently been optimised in-house. For this reason future expansion of the protein expression profiling will be done using the LI-COR system.

The use of individual protein expression values as predictive biomarkers have had mixed success. We believe that predictors or biomarkers utilizing multiple values while considering their relationship to each other will prove more robust as biomarkers as they better describe complicated biochemical pathways. Here we have reported the elucidation of the caspase-8/Bcl-2 expression ratio as a powerful predictor of TRAIL sensitivity. This relationship describes a crucial role for death receptor-mitochondrial interplay in determining TRAIL sensitivity.

4.5 Future perspectives

Ex vivo experiments have shown that administration of TRAIL to resistant cell lines results in the exacerbation of the malignant disease state likely through the activation of pro-survival signalling pathways such as Nf-ƙB, MAPK or AKT. Moreover the majority of combination therapies with TRAIL in clinical trials lead to increased sensitivity but were unable to reverse a resistant phenotype. In this study we have identified a protein pairings whose relative expression can predict sensitivity to TRAIL. The predictive performance of the ratio will be validated in chronic lymphoblastic leukaemia (CLL) patient samples.

The advent of omic-technologies and the curation of the accompanying online databases represent a vast source of expression data. The human protein atlas for example contains millions of high resolution images showing protein distribution and expression intensity in 44 normal tissue types, 20 cancer types and 46 cancer cell lines. The majority of these samples have protein array expression data which may be applied in an analysis similar to own for other chemotherapeutics which are already available in the clinic such as cisplatin or etoposide.

Chapter 5: General Discussion

Deeper understanding of the molecular characteristics of cancer has enabled the recognition of the genes or proteins responsible for driving tumour progression. This has lead to the development of novel therapies which target the aforementioned driver gene or protein. Therefore driver genes or proteins may be considered a predictive biomarker indicating the probable patient response.

Using predictive biomarkers as a guide to determining patient treatment regimes has resulted in patient benefits such as improved outcome and reduced treatment related side-effects. So far predictive biomarkers have been incorporated into the clinic for the treatment of a range of cancers; breast, lung and gastric cancer. Unfortunately tumour driving factors have only been identified in a small number of tumours. This means that there is a limited scope of application for targeted therapeutics. On the other hand the traditional cytotoxic chemotherapeutics such as cisplatin and etoposide have broad applications but no predictive marker to indicate patient responsiveness.

In order to address these concerns in chapter 2 we measured the expression of a number of potassium channels in 9 tumour cell lines which have been reported in the literature to play a role in apoptosis. With this in mind we postulated that the expression of one or more of these potassium channels would associate with sensitivity to a range of cytotoxic drugs and apoptotic inducers. This approach identified a statistically significant inverse correlation between viability after staurosporine, ceramide or cisplatin treatment and the expression of the potassium channels Kv1.1 and Kv1.3. Therefore the expression of these channels could be used as a predictive biomarker for sensitivity to the tested cytotoxic agents. Many malignancies especially the acute myeloid leukaemia's (AMLs) over express Bcl-2 family members in order to evade death via apoptosis. Evidence from the literature suggests that the aforementioned potassium channels function downstream of the Bcl-2 family members Bax/Bak and therefore directly targeting these might circumvent Bcl-2 family related resistance mechanisms. Indeed our

collaborators have shown that the administration of a membrane permeant Kv1.3 inhibitor could cause a large reduction in tumour volume in a mouse melanoma model. We have shown here that there is a close inverse correlation between the expression of the Kv1.3 potassium channel and cell viability after treatment with the Kv1.3 inhibitor clofazimine. Therefore high levels of Kv1.3 indicate sensitivity to clofazimine and might therefore be used as a predictive biomarker. Whereas previous targeted therapies possessed a limited range of application, the inhibition of the widely expressed Kv1.3 potassium channel should have wide spread application as an anti-cancer therapeutic. Furthermore since this approach circumvents Bcl-2 family mediated resistance to apoptosis it might represent an ideal option for difficult to treat malignancies.

One of the major advantages of targeted therapeutics aside from their efficacy is their relatively benign side effects. The death ligand TRAIL shares a similarly low toxicity but unlike targeted therapeutics is able to affect a variety of tumours. As was previously mentioned a large proportion of tumour cell lines are resistant to TRAIL induced apoptosis. Furthermore co-treatments with TRAIL and other chemotherapeutic agents served to further sensitized tumours already responsive to TRAIL rather than reversing a TRAIL resistant phenotype. Attempts to identify a predictive biomarker for TRAIL sensitivity have for the most part proven unsuccessful. In chapter 4 we show that the expression of the core components of TRAIL induced apoptosis was not indicative of sensitivity to TRAIL. We proposed that it is not the absolute expression of an individual component in a pathway which determines response rather it is the relative expression of said components which determines biological outcome. Our results show this with the Caspase-8/Bcl-2 expression ratio correctly predicting TRAIL sensitivity > 50% of the time. Further analysis could be carried out upon those cell lines for which the Caspase-8/Bcl-2 expression ratio was not predictive. It is likely that this subset of cell lines could be classified by an expression ratio pair which was previously obscured. Protein expression ratios which appear as promising predictive biomarker will require validation in patient samples.

While the TRAIL apoptotic pathway is clearly outlined allowing us to define a set of core components the same is not true for all chemotherapeutics. Moreover by using expression values for proteins already known to play a role in cell death we preclude the opportunity to uncover novel components of the pathway which may be integral in the development of a predictive biomarker. Therefore in chapter 3 we applied the machine learning technique random forest to gene expression data from 109 tumour cell lines with known TRAIL sensitivity. The random forest model provides measures of the importance of each gene in classifying cell lines as TRAIL sensitive or resistant. Through the backward elimination of the lowest ranked genes we identified a panel of 300 co-acting genes which could predict TRAIL sensitivity in an independent data set with a much higher degree of sensitivity and specificity (AUC=0.85) than the previously published best (AUC=0.72). Importantly this transcriptomic approach does not require the identification of candidates and/or the optimization of the detection method (antibodies for example). This would allow for the development of a predictive biomarker for agents whose mechanism of action is less well established than TRAIL induced apoptosis. There are a number of such agents which are clinically available for which drug sensitivity and gene expression data are freely available. Examples of which would include cisplatin and etoposide.

Interestingly less than 5 % of the predictive co-acting gene panel have been reported in the literature as known components of the TRAIL induced apoptotic pathway. The possible reasons for this were discussed in chapter 3. To add to this we have preliminary pathway analysis data (not shown) which suggests that the predictive co-acting genes tend to function upstream of pro-survival signalling pathways such as AKT or NF-κB and as such are not likely to be immediately associated with TRAIL induced apoptosis in the literature.

Throughout the course of this work we acquired gene and protein expression values for a large panel of tumour cell lines which were used in our analyses. Gene expression values were obtained from Affymetrix microarrays freely available from public databases. Affymetrix is the industrial leader in the field of oligonucleotide microarrays which allow for the detection of splice variants and removal of background signal via mismatch controls. While the use of multiple probes for improved coverage of the mRNA transcript and the identification of splice variants is a clear advantage they can also provide conflicting measures of gene expression. The typical way to address this, calculating the mean across the probes, is far from ideal. We employed a newly developed algorithm known as JetSet which indicates which probe should be used to represent the gene of interest. This not only addressed the aforementioned concern but also greatly reduced the dimensionality of the data set making it easier to manage and reduced computing times.

The expression of intracellular proteins was determined using Western blotting followed by densitometry. This approach was chosen as we had optimized protocols for the detection of all of the potassium channels and core components of the TRAIL apoptotic pathway and had access to the required equipment, facilities and software. As previously discussed in chapter 4 this technique suffers from a narrow linear range of detection owning to the saturable enzyme kinetics of the horse-radish peroxidase and the limited sensitivity of the film. This may result in inaccurate measures of protein expression. In stark contrast the quantification of protein expression by mass spectrometry should have no such concerns. However we found that in the context of detecting proteins important in apoptotic signalling that samples need to be fractionated. This is likely because apoptotic proteins are relatively low abundance compared to histone and cytoskeleton proteins for example. By separating the proteome by SDS-PAGE we could increase the relative abundance of some of the apoptosis related proteins to detectable levels. The identification of proteins by mass spectrometry is through the detection of peptide fragments originating from parent proteins. These peptides are typically selected based on their appearance in previous

experiments known as spectral libraries. Unfortunately the majority of spectral libraries available to us during the course of this study were generated from whole cell lysates or plasma where yet again apoptotic proteins are in low abundance. Thus we were not able to detect all of our proteins of interest. Attempts to construct our own spectral library from crude peptides rather than fractionated lysates allowed us to detect most if not all of our target proteins. Going forward it is likely that higher dimensional separation than carried out here may be required for the adequate detection of apoptotic proteins. One way in which this could be done would be to separate the sample by SDS-PAGE and then by isoelectric point.

Quantification of the TRAIL receptors by Western blotting would not be able to discern between those receptors present in the plasma membrane and those not. Therefore we would not accurately represent the proportion of functional TRAIL receptors. Bearing this in mind we measured the cell surface expression of the TRAIL receptors by immunocytochemistry. It must be noted that this technique provides a relative abundance for each receptor compared to the isotype control. As such the cell surface expression value of one receptor cannot be directly compared to another. For example a 2 times higher value for DR5 than DR4 does not imply that there is 2 times more of the DR5 receptor or even that DR5 is more abundant than DR4. While we do directly compare the expression of the death and decoy receptors to each other in our analysis we made no conclusions based on this value alone. Instead we looked at the distribution of this value across two phenotypes. Should we have seen a difference in the protein expression ratio between TRAIL sensitive and resistant cell lines we could only conclude that the amount of DR5 relative to DR4 was different across the two phenotypes.

In closing we have shown the expression of the Kv1.1 and Kv1.3 potassium channels can function as a predictive biomarker for the efficacy of a range of cytotoxic agents in particular the clinically available cisplatin. In addition to this we identify the expression of the Kv1.3 channel as a predictive biomarker for clofazimine treatment. Carrying on from this we illustrated

using the TRAIL apoptotic pathway as a model system that the relative abundance of genes or proteins performs better as predictors of phenotype than the expression of genes or proteins alone. Thus while the expression of Kv1.1 and Kv1.3 correlates strongly with outcome upon treatment with various cytotoxic agents the application of the random forest algorithm or protein expression ratio analysis might identify even more powerful predictive biomarkers for these and other compounds.

Bibliography

Abdul M, Hoosein N (2002) Voltage-gated potassium ion channels in colon cancer. *Oncology reports* **9:** 961-964

Aktas O, Smorodchenko A, Brocke S, Infante-Duarte C, Schulze Topphoff U, Vogt J, Prozorovski T, Meier S, Osmanova V, Pohl E, Bechmann I, Nitsch R, Zipp F (2005) Neuronal damage in autoimmune neuroinflammation mediated by the death ligand TRAIL. *Neuron* **46:** 421-432

Alizadeh AA, Eisen MB, Davis RE, Ma C, Lossos IS, Rosenwald A, Boldrick JC, Sabet H, Tran T, Yu X, Powell JI, Yang L, Marti GE, Moore T, Hudson J, Jr., Lu L, Lewis DB, Tibshirani R, Sherlock G, Chan WC, Greiner TC, Weisenburger DD, Armitage JO, Warnke R, Levy R, Wilson W, Grever MR, Byrd JC, Botstein D, Brown PO, Staudt LM (2000) Distinct types of diffuse large B-cell lymphoma identified by gene expression profiling. *Nature* **403:** 503-511

Almasan A, Ashkenazi A (2003) Apo2L/TRAIL: apoptosis signaling, biology, and potential for cancer therapy. *Cytokine & growth factor reviews* **14:** 337-348

Arcangeli A, Crociani O, Lastraioli E, Masi A, Pillozzi S, Becchetti A (2009) Targeting ion channels in cancer: a novel frontier in antineoplastic therapy. *Current medicinal chemistry* **16:** 66-93

Arcangeli A, Pillozzi S, Becchetti A (2012) Targeting ion channels in leukemias: a new challenge for treatment. *Current medicinal chemistry* **19:** 683-696

Ashkenazi A, Dixit VM (1998) Death receptors: signaling and modulation. *Science* **281:** 1305-1308

Ashkenazi A, Dixit VM (1999) Apoptosis control by death and decoy receptors. *Current opinion in cell biology* **11:** 255-260

Ashkenazi A, Pai RC, Fong S, Leung S, Lawrence DA, Marsters SA, Blackie C, Chang L, McMurtrey AE, Hebert A, DeForge L, Koumenis IL, Lewis D, Harris L, Bussiere J, Koeppen H, Shahrokh Z, Schwall RH (1999) Safety and antitumor activity of recombinant soluble Apo2 ligand. *The Journal of clinical investigation* **104:** 155-162

Aydin C, Sanlioglu AD, Karacay B, Ozbilim G, Dertsiz L, Ozbudak O, Akdis CA, Sanlioglu S (2007) Decoy receptor-2 small interfering RNA (siRNA) strategy employing three different siRNA constructs in combination defeats adenovirus-transferred tumor necrosis factor-related apoptosis-inducing ligand resistance in lung cancer cells. *Human gene therapy* **18:** 39-50

Azab NA, Rady HM, Marzouk SA (2012) Elevated serum TRAIL levels in scleroderma patients and its possible association with pulmonary involvement. *Clinical rheumatology* **31:** 1359-1364

Azijli K, Yuvaraj S, Peppelenbosch MP, Wurdinger T, Dekker H, Joore J, van Dijk E, Quax WJ, Peters GJ, de Jong S, Kruyt FA (2012) Kinome profiling of non-canonical TRAIL signaling reveals RIP1-Src-STAT3-dependent invasion in resistant non-small cell lung cancer cells. *Journal of cell science* **125:** 4651-4661

Baines CP, Kaiser RA, Sheiko T, Craigen WJ, Molkentin JD (2007) Voltage-dependent anion channels are dispensable for mitochondrial-dependent cell death. *Nature cell biology* **9:** 550-555

Belyanskaya LL, Ziogas A, Hopkins-Donaldson S, Kurtz S, Simon HU, Stahel R, Zangemeister-Wittke U (2008) TRAIL-induced survival and proliferation of SCLC cells is mediated by ERK and dependent on TRAIL-R2/DR5 expression in the absence of caspase-8. *Lung cancer* **60:** 355-365

Berghoff AS, Bago-Horvath Z, Dubsky P, Rudas M, Pluschnig U, Wiltschke C, Gnant M, Steger GG, Zielinski CC, Bartsch R (2013) Impact of HER-2-targeted therapy on overall survival in patients with HER-2 positive metastatic breast cancer. *The breast journal* **19:** 149-155

Bergsbaken T, Fink SL, Cookson BT (2009) Pyroptosis: host cell death and inflammation. *Nature reviews Microbiology* **7:** 99-109

Bielanska J, Hernandez-Losa J, Moline T, Somoza R, Cajal SR, Condom E, Ferreres JC, Felipe A (2012) Increased voltage-dependent K(+) channel Kv1.3 and Kv1.5 expression correlates with leiomyosarcoma aggressiveness. *Oncology letters* **4:** 227-230

Blay JY CS, Demetri GD. (2008) A Phase 1b Open-label Study of AMG 655 in Combination with Doxorubicin for the First-line Treatment of Patients with Locally Advanced or Metastatic, Unresectable Soft Tissue Sarcoma; CTOS 2008. 20060324 study.

Bleumink M, Kohler R, Giaisi M, Proksch P, Krammer PH, Li-Weber M (2011) Rocaglamide breaks TRAIL resistance in HTLV-1-associated adult T-cell leukemia/lymphoma by translational suppression of c-FLIP expression. *Cell death and differentiation* **18:** 362-370

Boatright KM, Renatus M, Scott FL, Sperandio S, Shin H, Pedersen IM, Ricci JE, Edris WA, Sutherlin DP, Green DR, Salvesen GS (2003) A unified model for apical caspase activation. *Molecular cell* **11:** 529-541

Bock J, Szabo I, Jekle A, Gulbins E (2002) Actinomycin D-induced apoptosis involves the potassium channel Kv1.3. *Biochemical and biophysical research communications* **295:** 526-531

Borjesson SI, Englund UH, Asif MH, Willander M, Elinder F (2011) Intracellular K+ concentration decrease is not obligatory for apoptosis. *The Journal of biological chemistry* **286:** 39823-39828

Bosque A, Pardo J, Martinez-Lorenzo MJ, Iturralde M, Marzo I, Pineiro A, Alava MA, Naval J, Anel A (2005) Down-regulation of normal human T cell blast activation: roles of APO2L/TRAIL, FasL, and c- FLIP, Bim, or Bcl-x isoform expression. *Journal of leukocyte biology* **77:** 568-578

Bouralexis S, Findlay DM, Evdokiou A (2005) Death to the bad guys: targeting cancer via Apo2L/TRAIL. *Apoptosis : an international journal on programmed cell death* **10:** 35-51

Brachmann SM, Hofmann I, Schnell C, Fritsch C, Wee S, Lane H, Wang S, Garcia-Echeverria C, Maira SM (2009) Specific apoptosis induction by the dual PI3K/mTor inhibitor NVP-BEZ235 in HER2 amplified and PIK3CA mutant breast cancer cells. *Proceedings of the National Academy of Sciences of the United States of America* **106:** 22299-22304

Braeuer SJ, Buneker C, Mohr A, Zwacka RM (2006) Constitutively activated nuclear factor-kappaB, but not induced NF-kappaB, leads to TRAIL resistance by up-regulation of X-linked inhibitor of apoptosis protein in human cancer cells. *Molecular cancer research : MCR* **4:** 715-728

Breiman L (2001) Random Forests. *Machine Learning* **45:** 5-32

Brennan MA, Cookson BT (2000) Salmonella induces macrophage death by caspase-1-dependent necrosis. *Molecular microbiology* **38:** 31-40

Brevnova EE, Platoshyn O, Zhang S, Yuan JX (2004) Overexpression of human KCNA5 increases IK V and enhances apoptosis. *American journal of physiology Cell physiology* **287:** C715-722

Brunet A, Bonni A, Zigmond MJ, Lin MZ, Juo P, Hu LS, Anderson MJ, Arden KC, Blenis J, Greenberg ME (1999) Akt promotes cell survival by phosphorylating and inhibiting a Forkhead transcription factor. *Cell* **96:** 857-868

Cahalan MD, Chandy KG (2009) The functional network of ion channels in T lymphocytes. *Immunological reviews* **231:** 59-87

Cai Z, Jitkaew S, Zhao J, Chiang HC, Choksi S, Liu J, Ward Y, Wu LG, Liu ZG (2014) Plasma membrane translocation of trimerized MLKL protein is required for TNF-induced necroptosis. *Nature cell biology* **16:** 55-65

Camidge DR (2008) Apomab: an agonist monoclonal antibody directed against Death Receptor 5/TRAIL-Receptor 2 for use in the treatment of solid tumors. *Expert opinion on biological therapy* **8:** 1167-1176

Caouette D, Dongmo C, Berube J, Fournier D, Daleau P (2003) Hydrogen peroxide modulates the Kv1.5 channel expressed in a mammalian cell line. *Naunyn-Schmiedeberg's archives of pharmacology* **368:** 479-486

Castedo M, Perfettini JL, Roumier T, Andreau K, Medema R, Kroemer G (2004a) Cell death by mitotic catastrophe: a molecular definition. *Oncogene* **23:** 2825-2837

Castedo M, Perfettini JL, Roumier T, Valent A, Raslova H, Yakushijin K, Horne D, Feunteun J, Lenoir G, Medema R, Vainchenker W, Kroemer G (2004b) Mitotic catastrophe constitutes a special case of apoptosis whose suppression entails aneuploidy. *Oncogene* **23:** 4362-4370

Cha SS, Kim MS, Choi YH, Sung BJ, Shin NK, Shin HC, Sung YC, Oh BH (1999a) 2.8 A resolution crystal structure of human TRAIL, a cytokine with selective antitumor activity. *Immunity* **11:** 253-261

Cha SS, Shin HC, Choi KY, Oh BH (1999b) Expression, purification and crystallization of recombinant human TRAIL. *Acta crystallographica Section D, Biological crystallography* **55:** 1101-1104

Chang L, Kamata H, Solinas G, Luo JL, Maeda S, Venuprasad K, Liu YC, Karin M (2006) The E3 ubiquitin ligase itch couples JNK activation to TNFalpha-induced cell death by inducing c-FLIP(L) turnover. *Cell* **124:** 601-613

Chang L, Karin M (2001) Mammalian MAP kinase signalling cascades. *Nature* **410:** 37-40

Chaudhary PM, Eby M, Jasmin A, Bookwalter A, Murray J, Hood L (1997) Death receptor 5, a new member of the TNFR family, and DR4 induce FADD-dependent apoptosis and activate the NF-kappaB pathway. *Immunity* **7:** 821-830

Chen JJ, Knudsen S, Mazin W, Dahlgaard J, Zhang B (2012) A 71-gene signature of TRAIL sensitivity in cancer cells. *Molecular cancer therapeutics* **11:** 34-44

Chen Y, Sanchez A, Rubio ME, Kohl T, Pardo LA, Stuhmer W (2011) Functional K(v)10.1 channels localize to the inner nuclear membrane. *PloS one* **6:** e19257

Cheng Y, Gulbins E, Siemen D (2011) Activation of the permeability transition pore by Bax via inhibition of the mitochondrial BK channel. *Cellular physiology and biochemistry : international journal of experimental cellular physiology, biochemistry, and pharmacology* **27:** 191-200

Chinnaiyan AM, O'Rourke K, Yu GL, Lyons RH, Garg M, Duan DR, Xing L, Gentz R, Ni J, Dixit VM (1996) Signal transduction by DR3, a death domain-containing receptor related to TNFR-1 and CD95. *Science* **274:** 990-992

Chinnaiyan AM, Prasad U, Shankar S, Hamstra DA, Shanaiah M, Chenevert TL, Ross BD, Rehemtulla A (2000) Combined effect of tumor necrosis factor-related apoptosis-inducing ligand and ionizing radiation in breast cancer therapy. *Proceedings of the National Academy of Sciences of the United States of America* **97:** 1754-1759

Chipuk JE, Moldoveanu T, Llambi F, Parsons MJ, Green DR (2010) The BCL-2 family reunion. *Molecular cell* **37:** 299-310

Cho YS, Challa S, Moquin D, Genga R, Ray TD, Guildford M, Chan FK (2009) Phosphorylation-driven assembly of the RIP1-RIP3 complex regulates programmed necrosis and virus-induced inflammation. *Cell* **137:** 1112-1123

Choi YE, Butterworth M, Malladi S, Duckett CS, Cohen GM, Bratton SB (2009) The E3 ubiquitin ligase cIAP1 binds and ubiquitinates caspase-3 and -7 via unique mechanisms at distinct steps in their processing. *The Journal of biological chemistry* **284:** 12772-12782

Clancy L, Mruk K, Archer K, Woelfel M, Mongkolsapaya J, Screaton G, Lenardo MJ, Chan FK (2005) Preligand assembly domain-mediated ligand-independent association between TRAIL receptor 4 (TR4) and TR2 regulates TRAIL-induced apoptosis. *Proceedings of the National Academy of Sciences of the United States of America* **102:** 18099-18104

Cookson BT, Brennan MA (2001) Pro-inflammatory programmed cell death. *Trends in microbiology* **9:** 113-114

Corazza N, Jakob S, Schaer C, Frese S, Keogh A, Stroka D, Kassahn D, Torgler R, Mueller C, Schneider P, Brunner T (2006) TRAIL receptor-mediated JNK activation and Bim phosphorylation critically regulate Fas-mediated liver damage and lethality. *The Journal of clinical investigation* **116:** 2493-2499

Cretney E, Takeda K, Yagita H, Glaccum M, Peschon JJ, Smyth MJ (2002) Increased susceptibility to tumor initiation and metastasis in TNF-related apoptosis-inducing ligand-deficient mice. *Journal of immunology* **168:** 1356-1361

Daniels RA, Turley H, Kimberley FC, Liu XS, Mongkolsapaya J, Ch'En P, Xu XN, Jin BQ, Pezzella F, Screaton GR (2005) Expression of TRAIL and TRAIL receptors in normal and malignant tissues. *Cell research* **15:** 430-438

Davis BK, Wen H, Ting JP (2011) The inflammasome NLRs in immunity, inflammation, and associated diseases. *Annual review of immunology* **29:** 707-735

Decaudin D, Marzo I, Brenner C, Kroemer G (1998) Mitochondria in chemotherapy-induced apoptosis: a prospective novel target of cancer therapy (review). *International journal of oncology* **12:** 141-152

Declercq W, Vanden Berghe T, Vandenabeele P (2009) RIP kinases at the crossroads of cell death and survival. *Cell* **138:** 229-232

Degli-Esposti MA, Dougall WC, Smolak PJ, Waugh JY, Smith CA, Goodwin RG (1997a) The novel receptor TRAIL-R4 induces NF-kappaB and protects against TRAIL-mediated apoptosis, yet retains an incomplete death domain. *Immunity* **7:** 813-820

Degli-Esposti MA, Smolak PJ, Walczak H, Waugh J, Huang CP, DuBose RF, Goodwin RG, Smith CA (1997b) Cloning and characterization of TRAIL-R3, a novel member of the emerging TRAIL receptor family. *The Journal of experimental medicine* **186:** 1165-1170

Delmas D, Rebe C, Micheau O, Athias A, Gambert P, Grazide S, Laurent G, Latruffe N, Solary E (2004) Redistribution of CD95, DR4 and DR5 in rafts accounts for the synergistic toxicity of resveratrol and death receptor ligands in colon carcinoma cells. *Oncogene* **23:** 8979-8986

Denecker G, Hoste E, Gilbert B, Hochepied T, Ovaere P, Lippens S, Van den Broecke C, Van Damme P, D'Herde K, Hachem JP, Borgonie G, Presland RB, Schoonjans L, Libert C, Vandekerckhove J, Gevaert K, Vandenabeele P, Declercq W (2007) Caspase-14 protects against epidermal UVB photodamage and water loss. *Nature cell biology* **9:** 666-674

Diaz-Uriarte R, Alvarez de Andres S (2006) Gene selection and classification of microarray data using random forest. *BMC bioinformatics* **7:** 3

Diehl GE, Yue HH, Hsieh K, Kuang AA, Ho M, Morici LA, Lenz LL, Cado D, Riley LW, Winoto A (2004) TRAIL-R as a negative regulator of innate immune cell responses. *Immunity* **21:** 877-889

Dirice E, Sanlioglu AD, Kahraman S, Ozturk S, Balci MK, Omer A, Griffith TS, Sanlioglu S (2009) Adenovirus-mediated TRAIL gene (Ad5hTRAIL) delivery into pancreatic islets prolongs normoglycemia in streptozotocin-induced diabetic rats. *Human gene therapy* **20:** 1177-1189

Douma S, Van Laar T, Zevenhoven J, Meuwissen R, Van Garderen E, Peeper DS (2004) Suppression of anoikis and induction of metastasis by the neurotrophic receptor TrkB. *Nature* **430:** 1034-1039

Druker BJ, Guilhot F, O'Brien SG, Gathmann I, Kantarjian H, Gattermann N, Deininger MW, Silver RT, Goldman JM, Stone RM, Cervantes F, Hochhaus A, Powell BL, Gabrilove JL, Rousselot P, Reiffers J, Cornelissen JJ, Hughes T, Agis H, Fischer T, Verhoef G, Shepherd J, Saglio G, Gratwohl A, Nielsen JL, Radich JP, Simonsson B, Taylor K, Baccarani M, So C, Letvak L, Larson RA, Investigators I (2006) Five-year follow-up of patients receiving imatinib for chronic myeloid leukemia. *The New England journal of medicine* **355:** 2408-2417

Eckelman BP, Salvesen GS (2006) The human anti-apoptotic proteins cIAP1 and cIAP2 bind but do not inhibit caspases. *The Journal of biological chemistry* **281:** 3254-3260

Eckelman BP, Salvesen GS, Scott FL (2006) Human inhibitor of apoptosis proteins: why XIAP is the black sheep of the family. *EMBO reports* **7:** 988-994

Ehrhardt H, Fulda S, Schmid I, Hiscott J, Debatin KM, Jeremias I (2003) TRAIL induced survival and proliferation in cancer cells resistant towards TRAIL-induced apoptosis mediated by NF-kappaB. *Oncogene* **22:** 3842-3852

Ehrlich S, Infante-Duarte C, Seeger B, Zipp F (2003) Regulation of soluble and surface-bound TRAIL in human T cells, B cells, and monocytes. *Cytokine* **24:** 244-253

Elrod JW, Molkentin JD (2013) Physiologic functions of cyclophilin D and the mitochondrial permeability transition pore. *Circulation journal : official journal of the Japanese Circulation Society* **77:** 1111-1122

Emery JG, McDonnell P, Burke MB, Deen KC, Lyn S, Silverman C, Dul E, Appelbaum ER, Eichman C, DiPrinzio R, Dodds RA, James IE, Rosenberg M, Lee JC, Young PR (1998) Osteoprotegerin is a receptor for the cytotoxic ligand TRAIL. *The Journal of biological chemistry* **273:** 14363-14367

Farooqi AA, Waseem S, Ashraf MS, Iqbal MJ, Bhatti S (2011) TRAIL and guardian angel of genome integrity: ATM boards TRAIL blazer. *Journal of cancer research and clinical oncology* **137:** 1283-1287

Fernandes-Alnemri T, Armstrong RC, Krebs J, Srinivasula SM, Wang L, Bullrich F, Fritz LC, Trapani JA, Tomaselli KJ, Litwack G, Alnemri ES (1996) In vitro activation of CPP32 and Mch3 by Mch4, a novel human apoptotic cysteine protease containing two FADD-like domains. *Proceedings of the National Academy of Sciences of the United States of America* **93:** 7464-7469

Fimia GM, Piacentini M (2010) Regulation of autophagy in mammals and its interplay with apoptosis. *Cellular and molecular life sciences : CMLS* **67:** 1581-1588

Fink SL, Cookson BT (2006) Caspase-1-dependent pore formation during pyroptosis leads to osmotic lysis of infected host macrophages. *Cellular microbiology* **8:** 1812-1825

Finnberg N, Gruber JJ, Fei P, Rudolph D, Bric A, Kim SH, Burns TF, Ajuha H, Page R, Wu GS, Chen Y, McKenna WG, Bernhard E, Lowe S, Mak T, El-Deiry WS (2005) DR5 knockout mice are compromised in radiation-induced apoptosis. *Molecular and cellular biology* **25:** 2000-2013

Fisher MJ, Virmani AK, Wu L, Aplenc R, Harper JC, Powell SM, Rebbeck TR, Sidransky D, Gazdar AF, El-Deiry WS (2001) Nucleotide substitution in the ectodomain of trail receptor DR4 is associated with lung cancer and head and neck cancer. *Clinical cancer research : an official journal of the American Association for Cancer Research* **7:** 1688-1697

Frisch SM (2008) Caspase-8: fly or die. *Cancer research* **68:** 4491-4493

Frisch SM, Francis H (1994) Disruption of epithelial cell-matrix interactions induces apoptosis. *The Journal of cell biology* **124:** 619-626

Frisch SM, Ruoslahti E (1997) Integrins and anoikis. *Current opinion in cell biology* **9:** 701-706

Fu J, Jin Y, Arend LJ (2003) Smac3, a novel Smac/DIABLO splicing variant, attenuates the stability and apoptosis-inhibiting activity of X-linked inhibitor of apoptosis protein. *The Journal of biological chemistry* **278:** 52660-52672

Fulda S, Meyer E, Debatin KM (2002) Inhibition of TRAIL-induced apoptosis by Bcl-2 overexpression. *Oncogene* **21:** 2283-2294

Fulda S, Vucic D (2012) Targeting IAP proteins for therapeutic intervention in cancer. *Nature reviews Drug discovery* **11:** 109-124

Gao Z, Tian Y, Wang J, Yin Q, Wu H, Li YM, Jiang X (2007) A dimeric Smac/diablo peptide directly relieves caspase-3 inhibition by XIAP. Dynamic and cooperative regulation of XIAP by Smac/Diablo. *The Journal of biological chemistry* **282:** 30718-30727

Garg G, Gibbs J, Belt B, Powell MA, Mutch DG, Goedegebuure P, Collins L, Piwnica-Worms D, Hawkins WG, Spitzer D (2014) Novel treatment option for MUC16-positive malignancies with the targeted TRAIL-based fusion protein Meso-TR3. *BMC cancer* **14:** 35

Gautier L, Cope L, Bolstad BM, Irizarry RA (2004) affy--analysis of Affymetrix GeneChip data at the probe level. *Bioinformatics* **20:** 307-315

Geman S. BE, Doursat R. (1992) Neural networks and the bias/variance dilemma. *Neural Computation* **4:** 1-58

Gentleman RC, Carey VJ, Bates DM, Bolstad B, Dettling M, Dudoit S, Ellis B, Gautier L, Ge Y, Gentry J, Hornik K, Hothorn T, Huber W, Iacus S, Irizarry R, Leisch F, Li C, Maechler M, Rossini AJ, Sawitzki G, Smith C, Smyth G, Tierney L, Yang JY, Zhang J (2004) Bioconductor: open software development for computational biology and bioinformatics. *Genome biology* **5:** R80

Gjorgieva D, Zaidman N, Bosnakovski D (2013) Mesenchymal stem cells for anti-cancer drug delivery. *Recent patents on anti-cancer drug discovery* **8:** 310-318

Glucksmann A (1951) Cell deaths in normal vertebrate ontogeny. *Biological reviews of the Cambridge Philosophical Society* **26:** 59-86

Goossens V, Stange G, Moens K, Pipeleers D, Grooten J (1999) Regulation of tumor necrosis factor-induced, mitochondria- and reactive oxygen species-dependent cell death by the electron flux through the electron transport chain complex I. *Antioxidants & redox signaling* **1:** 285-295

Green DR (2000) Apoptotic pathways: paper wraps stone blunts scissors. *Cell* **102:** 1-4

Green DR, Kroemer G (2004) The pathophysiology of mitochondrial cell death. *Science* **305:** 626-629

Gregory R. Warnes BB, Lodewijk Bonebakker, Robert, Gentleman WHAL, Thomas Lumley, Martin, Maechler AM, Steffen Moeller, Marc Schwartz and, Venables B (2014) gplots: Various R programming tools for

plotting data. R package version 2.13.0. *http://CRANR-projectorg/package=gplots*

Griffith TS, Kazama H, VanOosten RL, Earle JK, Jr., Herndon JM, Green DR, Ferguson TA (2007) Apoptotic cells induce tolerance by generating helpless CD8+ T cells that produce TRAIL. *Journal of immunology* **178:** 2679-2687

Grosse-Wilde A, Voloshanenko O, Bailey SL, Longton GM, Schaefer U, Csernok AI, Schutz G, Greiner EF, Kemp CJ, Walczak H (2008) TRAIL-R deficiency in mice enhances lymph node metastasis without affecting primary tumor development. *The Journal of clinical investigation* **118:** 100-110

Halaas O, Vik R, Ashkenazi A, Espevik T (2000) Lipopolysaccharide induces expression of APO2 ligand/TRAIL in human monocytes and macrophages. *Scandinavian journal of immunology* **51:** 244-250

Hanahan D, Weinberg RA (2011) Hallmarks of cancer: the next generation. *Cell* **144:** 646-674

He S, Wang L, Miao L, Wang T, Du F, Zhao L, Wang X (2009) Receptor interacting protein kinase-3 determines cellular necrotic response to TNF-alpha. *Cell* **137:** 1100-1111

Henson ES, Gibson EM, Villanueva J, Bristow NA, Haney N, Gibson SB (2003) Increased expression of Mcl-1 is responsible for the blockage of TRAIL-induced apoptosis mediated by EGF/ErbB1 signaling pathway. *Journal of cellular biochemistry* **89:** 1177-1192

Herbst RS, Eckhardt SG, Kurzrock R, Ebbinghaus S, O'Dwyer PJ, Gordon MS, Novotny W, Goldwasser MA, Tohnya TM, Lum BL, Ashkenazi A, Jubb AM, Mendelson DS (2010a) Phase I dose-escalation study of recombinant human Apo2L/TRAIL, a dual proapoptotic receptor agonist, in patients with advanced cancer. *Journal of clinical oncology : official journal of the American Society of Clinical Oncology* **28:** 2839-2846

Herbst RS, Kurzrock R, Hong DS, Valdivieso M, Hsu CP, Goyal L, Juan G, Hwang YC, Wong S, Hill JS, Friberg G, LoRusso PM (2010b) A first-in-human study of conatumumab in adult patients with advanced solid tumors. *Clinical cancer research : an official journal of the American Association for Cancer Research* **16:** 5883-5891

Hernandez A, Thomas R, Smith F, Sandberg J, Kim S, Chung DH, Evers BM (2001a) Butyrate sensitizes human colon cancer cells to TRAIL-mediated apoptosis. *Surgery* **130:** 265-272

Hernandez A, Wang QD, Schwartz SA, Evers BM (2001b) Sensitization of human colon cancer cells to TRAIL-mediated apoptosis. *Journal of gastrointestinal surgery : official journal of the Society for Surgery of the Alimentary Tract* **5:** 56-65

Hinz S, Trauzold A, Boenicke L, Sandberg C, Beckmann S, Bayer E, Walczak H, Kalthoff H, Ungefroren H (2000) Bcl-XL protects pancreatic adenocarcinoma cells against CD95- and TRAIL-receptor-mediated apoptosis. *Oncogene* **19:** 5477-5486

Hitomi J, Christofferson DE, Ng A, Yao J, Degterev A, Xavier RJ, Yuan J (2008) Identification of a molecular signaling network that regulates a cellular necrotic cell death pathway. *Cell* **135:** 1311-1323

Holler N, Zaru R, Micheau O, Thome M, Attinger A, Valitutti S, Bodmer JL, Schneider P, Seed B, Tschopp J (2000) Fas triggers an alternative, caspase-8-independent cell death pathway using the kinase RIP as effector molecule. *Nature immunology* **1:** 489-495

Horak P, Pils D, Kaider A, Pinter A, Elandt K, Sax C, Zielinski CC, Horvat R, Zeillinger R, Reinthaller A, Krainer M (2005) Perturbation of the tumor necrosis factor--related apoptosis-inducing ligand cascade in ovarian cancer: overexpression of FLIPL and deregulation of the functional receptors DR4 and DR5. *Clinical cancer research : an official journal of the American Association for Cancer Research* **11:** 8585-8591

Hoshi H, Sawada T, Uchida M, Iijima H, Kimura K, Hirakawa K, Wanibuchi H (2013) MUC5AC protects pancreatic cancer cells from TRAIL-induced death pathways. *International journal of oncology* **42:** 887-893

Hsu H, Huang J, Shu HB, Baichwal V, Goeddel DV (1996) TNF-dependent recruitment of the protein kinase RIP to the TNF receptor-1 signaling complex. *Immunity* **4:** 387-396

Hu CL, Zeng XM, Zhou MH, Shi YT, Cao H, Mei YA (2008a) Kv 1.1 is associated with neuronal apoptosis and modulated by protein kinase C in the rat cerebellar granule cell. *Journal of neurochemistry* **106:** 1125-1137

Hu MC, Lee DF, Xia W, Golfman LS, Ou-Yang F, Yang JY, Zou Y, Bao S, Hanada N, Saso H, Kobayashi R, Hung MC (2004) IkappaB kinase promotes tumorigenesis through inhibition of forkhead FOXO3a. *Cell* **117:** 225-237

Hu WH, Johnson H, Shu HB (1999) Tumor necrosis factor-related apoptosis-inducing ligand receptors signal NF-kappaB and JNK activation and apoptosis through distinct pathways. *The Journal of biological chemistry* **274:** 30603-30610

Hu X, Xu C, Cong Y (2008b) Kv1.3 channel as a promising therapeutic target for acquired aplastic anemia. *Medical hypotheses* **70:** 1072

Huang Y, Park YC, Rich RL, Segal D, Myszka DG, Wu H (2001) Structural basis of caspase inhibition by XIAP: differential roles of the linker versus the BIR domain. *Cell* **104:** 781-790

Hunter AM, LaCasse EC, Korneluk RG (2007) The inhibitors of apoptosis (IAPs) as cancer targets. *Apoptosis : an international journal on programmed cell death* **12:** 1543-1568

Hymowitz SG, Christinger HW, Fuh G, Ultsch M, O'Connell M, Kelley RF, Ashkenazi A, de Vos AM (1999) Triggering cell death: the crystal structure of Apo2L/TRAIL in a complex with death receptor 5. *Molecular cell* **4:** 563-571

Hymowitz SG, O'Connell MP, Ultsch MH, Hurst A, Totpal K, Ashkenazi A, de Vos AM, Kelley RF (2000) A unique zinc-binding site revealed by a high-resolution X-ray structure of homotrimeric Apo2L/TRAIL. *Biochemistry* **39:** 633-640

Irmler M, Thome M, Hahne M, Schneider P, Hofmann K, Steiner V, Bodmer JL, Schroter M, Burns K, Mattmann C, Rimoldi D, French LE, Tschopp J (1997) Inhibition of death receptor signals by cellular FLIP. *Nature* **388:** 190-195

Jang SH, Kang KS, Ryu PD, Lee SY (2009) Kv1.3 voltage-gated K(+) channel subunit as a potential diagnostic marker and therapeutic target for breast cancer. *BMB reports* **42:** 535-539

Jansen MP, Sieuwerts AM, Look MP, Ritstier K, Meijer-van Gelder ME, van Staveren IL, Klijn JG, Foekens JA, Berns EM (2007) HOXB13-to-IL17BR expression ratio is related with tumor aggressiveness and response to tamoxifen of recurrent breast cancer: a retrospective study. *Journal of clinical oncology : official journal of the American Society of Clinical Oncology* **25:** 662-668

Jehle J, Schweizer PA, Katus HA, Thomas D (2011) Novel roles for hERG K(+) channels in cell proliferation and apoptosis. *Cell death & disease* **2:** e193

Jin Z, McDonald ER, 3rd, Dicker DT, El-Deiry WS (2004) Deficient tumor necrosis factor-related apoptosis-inducing ligand (TRAIL) death receptor transport to the cell surface in human colon cancer cells selected for resistance to TRAIL-induced apoptosis. *The Journal of biological chemistry* **279:** 35829-35839

Jordan MA, Wendell K, Gardiner S, Derry WB, Copp H, Wilson L (1996) Mitotic block induced in HeLa cells by low concentrations of paclitaxel (Taxol) results in abnormal mitotic exit and apoptotic cell death. *Cancer research* **56:** 816-825

Jouan-Lanhouet S, Arshad MI, Piquet-Pellorce C, Martin-Chouly C, Le Moigne-Muller G, Van Herreweghe F, Takahashi N, Sergent O, Lagadic-Gossmann D, Vandenabeele P, Samson M, Dimanche-Boitrel MT (2012) TRAIL induces necroptosis involving RIPK1/RIPK3-dependent PARP-1 activation. *Cell death and differentiation* **19:** 2003-2014

Kalai M, Van Loo G, Vanden Berghe T, Meeus A, Burm W, Saelens X, Vandenabeele P (2002) Tipping the balance between necrosis and apoptosis in human and murine cells treated with interferon and dsRNA. *Cell death and differentiation* **9:** 981-994

Kandasamy K, Srinivasula SM, Alnemri ES, Thompson CB, Korsmeyer SJ, Bryant JL, Srivastava RK (2003) Involvement of proapoptotic molecules Bax and Bak in tumor necrosis factor-related apoptosis-inducing ligand (TRAIL)-induced mitochondrial disruption and apoptosis: differential regulation of cytochrome c and Smac/DIABLO release. *Cancer research* **63:** 1712-1721

Karacay B, Sanlioglu S, Griffith TS, Sandler A, Bonthius DJ (2004) Inhibition of the NF-kappaB pathway enhances TRAIL-mediated apoptosis in neuroblastoma cells. *Cancer gene therapy* **11:** 681-690

Kayagaki N, Yamaguchi N, Nakayama M, Takeda K, Akiba H, Tsutsui H, Okamura H, Nakanishi K, Okumura K, Yagita H (1999) Expression and function of TNF-related apoptosis-inducing ligand on murine activated NK cells. *Journal of immunology* **163:** 1906-1913

Kemp TJ, Elzey BD, Griffith TS (2003) Plasmacytoid dendritic cell-derived IFN-alpha induces TNF-related apoptosis-inducing ligand/Apo-2L-mediated antitumor activity by human monocytes following CpG oligodeoxynucleotide stimulation. *Journal of immunology* **171:** 212-218

Kim EH, Kim SU, Shin DY, Choi KS (2004) Roscovitine sensitizes glioma cells to TRAIL-mediated apoptosis by downregulation of survivin and XIAP. *Oncogene* **23:** 446-456

Kim YS, Morgan MJ, Choksi S, Liu ZG (2007) TNF-induced activation of the Nox1 NADPH oxidase and its role in the induction of necrotic cell death. *Molecular cell* **26:** 675-687

Kirshner JR, Karpova AY, Kops M, Howley PM (2005) Identification of TRAIL as an interferon regulatory factor 3 transcriptional target. *Journal of virology* **79:** 9320-9324

Kischkel FC, Lawrence DA, Chuntharapai A, Schow P, Kim KJ, Ashkenazi A (2000) Apo2L/TRAIL-dependent recruitment of endogenous FADD and caspase-8 to death receptors 4 and 5. *Immunity* **12:** 611-620

Koeberle PD, Wang Y, Schlichter LC (2010) Kv1.1 and Kv1.3 channels contribute to the degeneration of retinal ganglion cells after optic nerve transection in vivo. *Cell death and differentiation* **17:** 134-144

Koksal IT, Sanlioglu AD, Karacay B, Griffith TS, Sanlioglu S (2008) Tumor necrosis factor-related apoptosis inducing ligand-R4 decoy receptor expression is correlated with high Gleason scores, prostate-specific antigen recurrence, and decreased survival in patients with prostate carcinoma. *Urologic oncology* **26:** 158-165

Korsmeyer SJ, Wei MC, Saito M, Weiler S, Oh KJ, Schlesinger PH (2000) Pro-apoptotic cascade activates BID, which oligomerizes BAK or BAX into pores that result in the release of cytochrome c. *Cell death and differentiation* **7:** 1166-1173

Kreuz S, Siegmund D, Scheurich P, Wajant H (2001) NF-kappaB inducers upregulate cFLIP, a cycloheximide-sensitive inhibitor of death receptor signaling. *Molecular and cellular biology* **21:** 3964-3973

Krick S, Platoshyn O, McDaniel SS, Rubin LJ, Yuan JX (2001) Augmented K(+) currents and mitochondrial membrane depolarization in pulmonary artery myocyte apoptosis. *American journal of physiology Lung cellular and molecular physiology* **281:** L887-894

Kroemer G, Galluzzi L, Vandenabeele P, Abrams J, Alnemri ES, Baehrecke EH, Blagosklonny MV, El-Deiry WS, Golstein P, Green DR, Hengartner M, Knight RA, Kumar S, Lipton SA, Malorni W, Nunez G, Peter ME, Tschopp J, Yuan J, Piacentini M, Zhivotovsky B, Melino G, Nomenclature Committee on Cell D (2009) Classification of cell death: recommendations of the Nomenclature Committee on Cell Death 2009. *Cell death and differentiation* **16:** 3-11

Lalaoui N, Morle A, Merino D, Jacquemin G, Iessi E, Morizot A, Shirley S, Robert B, Solary E, Garrido C, Micheau O (2011) TRAIL-R4 promotes tumor growth and resistance to apoptosis in cervical carcinoma HeLa cells through AKT. *PloS one* **6:** e19679

Lam EW, Brosens JJ, Gomes AR, Koo CY (2013) Forkhead box proteins: tuning forks for transcriptional harmony. *Nature reviews Cancer* **13:** 482-495

Lamhamedi-Cherradi SE, Zheng S, Tisch RM, Chen YH (2003) Critical roles of tumor necrosis factor-related apoptosis-inducing ligand in type 1 diabetes. *Diabetes* **52:** 2274-2278

Lamkanfi M, Festjens N, Declercq W, Vanden Berghe T, Vandenabeele P (2007) Caspases in cell survival, proliferation and differentiation. *Cell death and differentiation* **14:** 44-55

Lang F, Foller M, Lang K, Lang P, Ritter M, Vereninov A, Szabo I, Huber SM, Gulbins E (2007) Cell volume regulatory ion channels in cell proliferation and cell death. *Methods in enzymology* **428:** 209-225

Lang F, Gulbins E, Szabo I, Lepple-Wienhues A, Huber SM, Duranton C, Lang KS, Lang PA, Wieder T (2004) Cell volume and the regulation of apoptotic cell death. *Journal of molecular recognition : JMR* **17:** 473-480

Lang F, Ritter M, Gamper N, Huber S, Fillon S, Tanneur V, Lepple-Wienhues A, Szabo I, Gulbins E (2000) Cell volume in the regulation of cell proliferation and apoptotic cell death. *Cellular physiology and biochemistry : international journal of experimental cellular physiology, biochemistry, and pharmacology* **10:** 417-428

Lannan E, Vandergaast R, Friesen PD (2007) Baculovirus caspase inhibitors P49 and P35 block virus-induced apoptosis downstream of effector caspase DrICE activation in Drosophila melanogaster cells. *Journal of virology* **81:** 9319-9330

Larranaga P, Calvo B, Santana R, Bielza C, Galdiano J, Inza I, Lozano JA, Armananzas R, Santafe G, Perez A, Robles V (2006) Machine learning in bioinformatics. *Briefings in bioinformatics* **7:** 86-112

Laster SM, Wood JG, Gooding LR (1988) Tumor necrosis factor can induce both apoptic and necrotic forms of cell lysis. *Journal of immunology* **141:** 2629-2634

Lastraioli E, Guasti L, Crociani O, Polvani S, Hofmann G, Witchel H, Bencini L, Calistri M, Messerini L, Scatizzi M, Moretti R, Wanke E, Olivotto M, Mugnai G, Arcangeli A (2004) herg1 gene and HERG1 protein are overexpressed in colorectal cancers and regulate cell invasion of tumor cells. *Cancer research* **64:** 606-611

Leanza L, Henry B, Sassi N, Zoratti M, Chandy KG, Gulbins E, Szabo I (2012a) Inhibitors of mitochondrial Kv1.3 channels induce Bax/Bak-independent death of cancer cells. *EMBO molecular medicine* **4:** 577-593

Leanza L, O'Reilly P, Doyle A, Venturini E, Zoratti M, Szegezdi E, Szabo I (2014) Correlation between Potassium Channel Expression and Sensitivity to Drug-

induced Cell Death in Tumor Cell Lines. *Current pharmaceutical design* **20:** 189-200

Leanza L, Zoratti M, Gulbins E, Szabo I (2012b) Induction of apoptosis in macrophages via Kv1.3 and Kv1.5 potassium channels. *Current medicinal chemistry* **19:** 5394-5404

LeBlanc HN, Ashkenazi A (2003) Apo2L/TRAIL and its death and decoy receptors. *Cell death and differentiation* **10:** 66-75

Lee MW, Park SC, Yang YG, Yim SO, Chae HS, Bach JH, Lee HJ, Kim KY, Lee WB, Kim SS (2002) The involvement of reactive oxygen species (ROS) and p38 mitogen-activated protein (MAP) kinase in TRAIL/Apo2L-induced apoptosis. *FEBS letters* **512:** 313-318

Leong S, Christopherson RI, Baxter RC (2007) Profiling of apoptotic changes in human breast cancer cells using SELDI-TOF mass spectrometry. *Cellular physiology and biochemistry : international journal of experimental cellular physiology, biochemistry, and pharmacology* **20:** 579-590

Leong S, Cohen RB, Gustafson DL, Langer CJ, Camidge DR, Padavic K, Gore L, Smith M, Chow LQ, von Mehren M, O'Bryant C, Hariharan S, Diab S, Fox NL, Miceli R, Eckhardt SG (2009) Mapatumumab, an antibody targeting TRAIL-R1, in combination with paclitaxel and carboplatin in patients with advanced solid malignancies: results of a phase I and pharmacokinetic study. *Journal of clinical oncology : official journal of the American Society of Clinical Oncology* **27:** 4413-4421

Leverkus M, Sprick MR, Wachter T, Denk A, Brocker EB, Walczak H, Neumann M (2003) TRAIL-induced apoptosis and gene induction in HaCaT keratinocytes: differential contribution of TRAIL receptors 1 and 2. *The Journal of investigative dermatology* **121:** 149-155

Li J, Yuan J (2008) Caspases in apoptosis and beyond. *Oncogene* **27:** 6194-6206

Li Q, Birkbak NJ, Gyorffy B, Szallasi Z, Eklund AC (2011) Jetset: selecting the optimal microarray probe set to represent a gene. *BMC bioinformatics* **12:** 474

Liu S, Yu Y, Zhang M, Wang W, Cao X (2001) The involvement of TNF-alpha-related apoptosis-inducing ligand in the enhanced cytotoxicity of IFN-beta-stimulated human dendritic cells to tumor cells. *Journal of immunology* **166:** 5407-5415

Lock RB, Stribinskiene L (1996) Dual modes of death induced by etoposide in human epithelial tumor cells allow Bcl-2 to inhibit apoptosis without affecting clonogenic survival. *Cancer research* **56:** 4006-4012

Lockshin RA, Williams CM (1965) Programmed Cell Death--I. Cytology of Degeneration in the Intersegmental Muscles of the Pernyi Silkmoth. *Journal of insect physiology* **11:** 123-133

Lorick KL, Jensen JP, Fang S, Ong AM, Hatakeyama S, Weissman AM (1999) RING fingers mediate ubiquitin-conjugating enzyme (E2)-dependent ubiquitination. *Proceedings of the National Academy of Sciences of the United States of America* **96:** 11364-11369

LoRusso P HD, Heath E, Kurzrock R, Wang D, Hsu M et al (2007) First-in-human study of AMG 655, a pro-apoptotic TRAIL receptor-2 agonist, in adult patients with advanced solid tumors. *Journal of clinical oncology : official journal of the American Society of Clinical Oncology*

Ma Y, Temkin V, Liu H, Pope RM (2005) NF-kappaB protects macrophages from lipopolysaccharide-induced cell death: the role of caspase 8 and receptor-interacting protein. *The Journal of biological chemistry* **280:** 41827-41834

Mahalingam D, Keane M, Pirianov G, Mehmet H, Samali A, Szegezdi E (2009) Differential activation of JNK1 isoforms by TRAIL receptors modulate apoptosis of colon cancer cell lines. *British journal of cancer* **100:** 1415-1424

Mahalingam D, Oldenhuis CN, Szegezdi E, Giles FJ, de Vries EG, de Jong S, Nawrocki ST (2011) Targeting TRAIL towards the clinic. *Current drug targets* **12:** 2079-2090

Marsters SA, Sheridan JP, Pitti RM, Huang A, Skubatch M, Baldwin D, Yuan J, Gurney A, Goddard AD, Godowski P, Ashkenazi A (1997) A novel receptor for Apo2L/TRAIL contains a truncated death domain. *Current biology : CB* **7:** 1003-1006

Martinez-Lorenzo MJ, Alava MA, Gamen S, Kim KJ, Chuntharapai A, Pineiro A, Naval J, Anel A (1998) Involvement of APO2 ligand/TRAIL in activation-induced death of Jurkat and human peripheral blood T cells. *European journal of immunology* **28:** 2714-2725

Matsuzaki H, Daitoku H, Hatta M, Tanaka K, Fukamizu A (2003) Insulin-induced phosphorylation of FKHR (Foxo1) targets to proteasomal degradation. *Proceedings of the National Academy of Sciences of the United States of America* **100:** 11285-11290

Matte-Martone C, Venkatesan S, Tan HS, Athanasiadis I, Chang J, Pavisic J, Shlomchik WD (2011) Graft-versus-leukemia (GVL) against mouse blast-crisis chronic myelogenous leukemia (BC-CML) and chronic-phase chronic myelogenous leukemia (CP-CML): shared mechanisms of T cell killing, but programmed death ligands render CP-CML and not BC-CML GVL resistant. *Journal of immunology* **187:** 1653-1663

McDonald ER, 3rd, El-Deiry WS (2004) Suppression of caspase-8- and -10-associated RING proteins results in sensitization to death ligands and inhibition of tumor cell growth. *Proceedings of the National Academy of Sciences of the United States of America* **101:** 6170-6175

McFerrin MB, Turner KL, Cuddapah VA, Sontheimer H (2012) Differential role of IK and BK potassium channels as mediators of intrinsic and extrinsic apoptotic cell death. *American journal of physiology Cell physiology* **303:** C1070-1078

Mellier G, Huang S, Shenoy K, Pervaiz S (2010) TRAILing death in cancer. *Molecular aspects of medicine* **31:** 93-112

Meredith JE, Jr., Fazeli B, Schwartz MA (1993) The extracellular matrix as a cell survival factor. *Molecular biology of the cell* **4:** 953-961

Merino D, Giam M, Hughes PD, Siggs OM, Heger K, O'Reilly LA, Adams JM, Strasser A, Lee EF, Fairlie WD, Bouillet P (2009) The role of BH3-only protein Bim extends beyond inhibiting Bcl-2-like prosurvival proteins. *The Journal of cell biology* **186:** 355-362

Merino D, Lalaoui N, Morizot A, Schneider P, Solary E, Micheau O (2006) Differential inhibition of TRAIL-mediated DR5-DISC formation by decoy receptors 1 and 2. *Molecular and cellular biology* **26:** 7046-7055

Merritt AJ, Allen TD, Potten CS, Hickman JA (1997) Apoptosis in small intestinal epithelial from p53-null mice: evidence for a delayed, p53-independent G2/M-associated cell death after gamma-irradiation. *Oncogene* **14:** 2759-2766

Micheau O (2003) Cellular FLICE-inhibitory protein: an attractive therapeutic target? *Expert opinion on therapeutic targets* **7:** 559-573

Micheau O, Thome M, Schneider P, Holler N, Tschopp J, Nicholson DW, Briand C, Grutter MG (2002) The long form of FLIP is an activator of caspase-8 at the Fas death-inducing signaling complex. *The Journal of biological chemistry* **277:** 45162-45171

Milani D, Zauli G, Rimondi E, Celeghini C, Marmiroli S, Narducci P, Capitani S, Secchiero P (2003) Tumour necrosis factor-related apoptosis-inducing ligand sequentially activates pro-survival and pro-apoptotic pathways in SK-N-MC neuronal cells. *Journal of neurochemistry* **86:** 126-135

Mitchell MJ, Wayne E, Rana K, Schaffer CB, King MR (2014) TRAIL-coated leukocytes that kill cancer cells in the circulation. *Proceedings of the National Academy of Sciences of the United States of America* **111:** 930-935

Mitsiades N, Mitsiades CS, Poulaki V, Chauhan D, Richardson PG, Hideshima T, Munshi N, Treon SP, Anderson KC (2002) Biologic sequelae of nuclear factor-kappaB blockade in multiple myeloma: therapeutic applications. *Blood* **99:** 4079-4086

Mongkolsapaya J, Cowper AE, Xu XN, Morris G, McMichael AJ, Bell JI, Screaton GR (1998) Lymphocyte inhibitor of TRAIL (TNF-related apoptosis-inducing ligand): a new receptor protecting lymphocytes from the death ligand TRAIL. *Journal of immunology* **160:** 3-6

Mongkolsapaya J, Grimes JM, Chen N, Xu XN, Stuart DI, Jones EY, Screaton GR (1999) Structure of the TRAIL-DR5 complex reveals mechanisms conferring specificity in apoptotic initiation. *Nature structural biology* **6:** 1048-1053

Montemurro F, Valabrega G, Aglietta M (2004) Trastuzumab-based combination therapy for breast cancer. *Expert opinion on pharmacotherapy* **5:** 81-96

Mucha SR, Rizzani A, Gerbes AL, Camaj P, Thasler WE, Bruns CJ, Eichhorst ST, Gallmeier E, Kolligs FT, Goke B, De Toni EN (2009) JNK inhibition sensitises hepatocellular carcinoma cells but not normal hepatocytes to the TNF-related apoptosis-inducing ligand. *Gut* **58:** 688-698

Muhlenbeck F, Haas E, Schwenzer R, Schubert G, Grell M, Smith C, Scheurich P, Wajant H (1998) TRAIL/Apo2L activates c-Jun NH2-terminal kinase (JNK) via caspase-dependent and caspase-independent pathways. *The Journal of biological chemistry* **273:** 33091-33098

Muppidi JR, Tschopp J, Siegel RM (2004) Life and death decisions: secondary complexes and lipid rafts in TNF receptor family signal transduction. *Immunity* **21:** 461-465

Nagata S (1997) Apoptosis by death factor. *Cell* **88:** 355-365

Nagata S, Golstein P (1995) The Fas death factor. *Science* **267:** 1449-1456

Nam JH, Shin DH, Zheng H, Lee DS, Park SJ, Park KS, Kim SJ (2011) Expression of TASK-2 and its upregulation by B cell receptor stimulation in WEHI-231 mouse immature B cells. *American journal of physiology Cell physiology* **300:** C1013-1022

Nicholson DW, Ali A, Thornberry NA, Vaillancourt JP, Ding CK, Gallant M, Gareau Y, Griffin PR, Labelle M, Lazebnik YA, et al. (1995) Identification and inhibition of the ICE/CED-3 protease necessary for mammalian apoptosis. *Nature* **376:** 37-43

Nishizuka S, Tamura G, Terashima M, Satodate R (1998) Loss of heterozygosity during the development and progression of differentiated adenocarcinoma of the stomach. *The Journal of pathology* **185:** 38-43

Olden JD, Lawler JJ, Poff NL (2008) Machine learning methods without tears: a primer for ecologists. *The Quarterly review of biology* **83:** 171-193

Otsuka T, Kohno T, Mori M, Noguchi M, Hirohashi S, Yokota J (1996) Deletion mapping of chromosome 2 in human lung carcinoma. *Genes, chromosomes & cancer* **16:** 113-119

Ousingsawat J, Spitzner M, Puntheeranurak S, Terracciano L, Tornillo L, Bubendorf L, Kunzelmann K, Schreiber R (2007) Expression of voltage-gated potassium channels in human and mouse colonic carcinoma. *Clinical cancer research : an official journal of the American Association for Cancer Research* **13:** 824-831

Pai SI, Wu GS, Ozoren N, Wu L, Jen J, Sidransky D, El-Deiry WS (1998) Rare loss-of-function mutation of a death receptor gene in head and neck cancer. *Cancer research* **58:** 3513-3518

Paik JH, Kollipara R, Chu G, Ji H, Xiao Y, Ding Z, Miao L, Tothova Z, Horner JW, Carrasco DR, Jiang S, Gilliland DG, Chin L, Wong WH, Castrillon DH, DePinho RA (2007) FoxOs are lineage-restricted redundant tumor suppressors and regulate endothelial cell homeostasis. *Cell* **128:** 309-323

Pan G, Ni J, Wei YF, Yu G, Gentz R, Dixit VM (1997a) An antagonist decoy receptor and a death domain-containing receptor for TRAIL. *Science* **277:** 815-818

Pan G, O'Rourke K, Chinnaiyan AM, Gentz R, Ebner R, Ni J, Dixit VM (1997b) The receptor for the cytotoxic ligand TRAIL. *Science* **276:** 111-113

Pannuzzo G, Cardile V, Costantino-Ceccarini E, Alvares E, Mazzone D, Perciavalle V (2010) A galactose-free diet enriched in soy isoflavones and antioxidants results in delayed onset of symptoms of Krabbe disease in twitcher mice. *Molecular genetics and metabolism* **100:** 234-240

Pardo LA (2004) Voltage-gated potassium channels in cell proliferation. *Physiology* **19:** 285-292

Park KJ, Lee CH, Kim A, Jeong KJ, Kim CH, Kim YS (2012) Death receptors 4 and 5 activate Nox1 NADPH oxidase through riboflavin kinase to induce reactive oxygen species-mediated apoptotic cell death. *The Journal of biological chemistry* **287:** 3313-3325

Park WS, Lee JH, Shin MS, Park JY, Kim HS, Lee JH, Kim YS, Lee SN, Xiao W, Park CH, Lee SH, Yoo NJ, Lee JY (2002) Inactivating mutations of the caspase-10 gene in gastric cancer. *Oncogene* **21:** 2919-2925

Partemi S, Cestele S, Pezzella M, Campuzano O, Paravidino R, Pascali VL, Zara F, Tassinari CA, Striano S, Oliva A, Brugada R, Mantegazza M, Striano P (2013) Loss-of-function KCNH2 mutation in a family with long QT syndrome, epilepsy, and sudden death. *Epilepsia* **54:** e112-116

Passante E, Wurstle ML, Hellwig CT, Leverkus M, Rehm M (2013) Systems analysis of apoptosis protein expression allows the case-specific prediction of cell death responsiveness of melanoma cells. *Cell death and differentiation* **20:** 1521-1531

Pedersen A, Wallgren M, Karlsson BG, Grobner G (2011) Expression and purification of full-length anti-apoptotic Bcl-2 using cell-free protein synthesis. *Protein expression and purification* **77:** 220-223

Perlstein B, Finniss SA, Miller C, Okhrimenko H, Kazimirsky G, Cazacu S, Lee HK, Lemke N, Brodie S, Umansky F, Rempel SA, Rosenblum M, Mikklesen T, Margel S, Brodie C (2013) TRAIL conjugated to nanoparticles exhibits increased anti-tumor activities in glioma cells and glioma stem cells in vitro and in vivo. *Neuro-oncology* **15:** 29-40

Peternel S, Prpic-Massari L, Manestar-Blazic T, Brajac I, Kastelan M (2011) Increased expression of TRAIL and its death receptors DR4 and DR5 in plaque psoriasis. *Archives of dermatological research* **303:** 389-397

Pitti RM, Marsters SA, Ruppert S, Donahue CJ, Moore A, Ashkenazi A (1996) Induction of apoptosis by Apo-2 ligand, a new member of the tumor necrosis factor cytokine family. *The Journal of biological chemistry* **271:** 12687-12690

Plantivaux A, Szegezdi E, Samali A, Egan L (2009) Is there a role for nuclear factor kappaB in tumor necrosis factor-related apoptosis-inducing ligand resistance? *Annals of the New York Academy of Sciences* **1171:** 38-49

Pongs O (1993) Structure-function studies on the pore of potassium channels. *The Journal of membrane biology* **136:** 1-8

Pop C, Salvesen GS (2009) Human caspases: activation, specificity, and regulation. *The Journal of biological chemistry* **284:** 21777-21781

Preussat K, Beetz C, Schrey M, Kraft R, Wolfl S, Kalff R, Patt S (2003) Expression of voltage-gated potassium channels Kv1.3 and Kv1.5 in human gliomas. *Neuroscience letters* **346:** 33-36

Psahoulia FH, Drosopoulos KG, Doubravska L, Andera L, Pintzas A (2007) Quercetin enhances TRAIL-mediated apoptosis in colon cancer cells by inducing the accumulation of death receptors in lipid rafts. *Molecular cancer therapeutics* **6:** 2591-2599

Ravi R, Bedi GC, Engstrom LW, Zeng Q, Mookerjee B, Gelinas C, Fuchs EJ, Bedi A (2001) Regulation of death receptor expression and TRAIL/Apo2L-induced apoptosis by NF-kappaB. *Nature cell biology* **3:** 409-416

Ray CA, Black RA, Kronheim SR, Greenstreet TA, Sleath PR, Salvesen GS, Pickup DJ (1992) Viral inhibition of inflammation: cowpox virus encodes an inhibitor of the interleukin-1 beta converting enzyme. *Cell* **69:** 597-604

Read SH, Baliga BC, Ekert PG, Vaux DL, Kumar S (2002) A novel Apaf-1-independent putative caspase-2 activation complex. *The Journal of cell biology* **159:** 739-745

Reddig PJ, Juliano RL (2005) Clinging to life: cell to matrix adhesion and cell survival. *Cancer metastasis reviews* **24:** 425-439

Reis CR, van der Sloot AM, Natoni A, Szegezdi E, Setroikromo R, Meijer M, Sjollema K, Stricher F, Cool RH, Samali A, Serrano L, Quax WJ (2010) Rapid and efficient cancer cell killing mediated by high-affinity death receptor homotrimerizing TRAIL variants. *Cell death & disease* **1:** e83

Remijsen Q, Goossens V, Grootjans S, Van den Haute C, Vanlangenakker N, Dondelinger Y, Roelandt R, Bruggeman I, Goncalves A, Bertrand MJ, Baekelandt V, Takahashi N, Berghe TV, Vandenabeele P (2014) Depletion of RIPK3 or MLKL blocks TNF-driven necroptosis and switches towards a delayed RIPK1 kinase-dependent apoptosis. *Cell death & disease* **5:** e1004

Remillard CV, Yuan JX (2004) Activation of K+ channels: an essential pathway in programmed cell death. *American journal of physiology Lung cellular and molecular physiology* **286:** L49-67

Riccioni R, Pasquini L, Mariani G, Saulle E, Rossini A, Diverio D, Pelosi E, Vitale A, Chierichini A, Cedrone M, Foa R, Lo Coco F, Peschle C, Testa U (2005) TRAIL decoy receptors mediate resistance of acute myeloid leukemia cells to TRAIL. *Haematologica* **90:** 612-624

Riedl SJ, Renatus M, Schwarzenbacher R, Zhou Q, Sun C, Fesik SW, Liddington RC, Salvesen GS (2001) Structural basis for the inhibition of caspase-3 by XIAP. *Cell* **104:** 791-800

Rosenblatt F (1958) The perceptron: a probabilistic model for information storage and organization in the brain. *Psychological review* **65:** 386-408

Rossin A, Derouet M, Abdel-Sater F, Hueber AO (2009) Palmitoylation of the TRAIL receptor DR4 confers an efficient TRAIL-induced cell death signalling. *The Biochemical journal* **419:** 185-192, 182 p following 192

Roth W, Stenner-Liewen F, Pawlowski K, Godzik A, Reed JC (2002) Identification and characterization of DEDD2, a death effector domain-containing protein. *The Journal of biological chemistry* **277:** 7501-7508

Rumelhart D. E. HGE, Williams R. J. (1986) Learning representations by back-propagating error. *Nature* **323:** 533-536

Safa AR (2012) c-FLIP, a master anti-apoptotic regulator. *Experimental oncology* **34:** 176-184

Saltz. (2009) Safety and efficacy of AMG 655 plus modified FOLFOX6 (mFOLFOX6) and bevacizumab (B) for the first-line treatment of patients with metastatic colorectal cancer (mCRC). *Journal of clinical oncology : official journal of the American Society of Clinical Oncology*

Sanlioglu AD, Dirice E, Aydin C, Erin N, Koksoy S, Sanlioglu S (2005) Surface TRAIL decoy receptor-4 expression is correlated with TRAIL resistance in MCF7 breast cancer cells. *BMC cancer* **5:** 54

Sasaki S, Nakamura T, Arakawa H, Mori M, Watanabe T, Nagawa H, Croce CM (2002) Isolation and characterization of a novel gene, hRFI, preferentially expressed in esophageal cancer. *Oncogene* **21:** 5024-5030

SB. K (2007) Supervised Machine Learning: A review of classification techniques. *Proceedings of the 2007 Conference on Emerging Artificial Intelligence Applications in Computer Engineering* **IOS Press**

Schneider P, Bodmer JL, Thome M, Hofmann K, Holler N, Tschopp J (1997a) Characterization of two receptors for TRAIL. *FEBS letters* **416:** 329-334

Schneider P, Thome M, Burns K, Bodmer JL, Hofmann K, Kataoka T, Holler N, Tschopp J (1997b) TRAIL receptors 1 (DR4) and 2 (DR5) signal FADD-dependent apoptosis and activate NF-kappaB. *Immunity* **7:** 831-836

Schuler S, Fritsche P, Diersch S, Arlt A, Schmid RM, Saur D, Schneider G (2010) HDAC2 attenuates TRAIL-induced apoptosis of pancreatic cancer cells. *Molecular cancer* **9:** 80

Schulze-Osthoff K, Bakker AC, Vanhaesebroeck B, Beyaert R, Jacob WA, Fiers W (1992) Cytotoxic activity of tumor necrosis factor is mediated by early damage of mitochondrial functions. Evidence for the involvement of mitochondrial radical generation. *The Journal of biological chemistry* **267:** 5317-5323

Scott FL, Denault JB, Riedl SJ, Shin H, Renatus M, Salvesen GS (2005) XIAP inhibits caspase-3 and -7 using two binding sites: evolutionarily conserved mechanism of IAPs. *The EMBO journal* **24:** 645-655

Sedger LM, Glaccum MB, Schuh JC, Kanaly ST, Williamson E, Kayagaki N, Yun T, Smolak P, Le T, Goodwin R, Gliniak B (2002) Characterization of the in vivo function of TNF-alpha-related apoptosis-inducing ligand, TRAIL/Apo2L, using TRAIL/Apo2L gene-deficient mice. *European journal of immunology* **32:** 2246-2254

Sessler T, Healy S, Samali A, Szegezdi E (2013) Structural determinants of DISC function: new insights into death receptor-mediated apoptosis signalling. *Pharmacology & therapeutics* **140:** 186-199

She QB, Chandarlapaty S, Ye Q, Lobo J, Haskell KM, Leander KR, DeFeo-Jones D, Huber HE, Rosen N (2008) Breast tumor cells with PI3K mutation or HER2 amplification are selectively addicted to Akt signaling. *PloS one* **3:** e3065

Shen QJ, Zhao YM, Cao DX, Wang XL (2009) Contribution of Kv channel subunits to glutamate-induced apoptosis in cultured rat hippocampal neurons. *Journal of neuroscience research* **87:** 3153-3160

Sheridan JP, Marsters SA, Pitti RM, Gurney A, Skubatch M, Baldwin D, Ramakrishnan L, Gray CL, Baker K, Wood WI, Goddard AD, Godowski P, Ashkenazi A (1997) Control of TRAIL-induced apoptosis by a family of signaling and decoy receptors. *Science* **277:** 818-821

Shimizu S, Kanaseki T, Mizushima N, Mizuta T, Arakawa-Kobayashi S, Thompson CB, Tsujimoto Y (2004) Role of Bcl-2 family proteins in a non-apoptotic programmed cell death dependent on autophagy genes. *Nature cell biology* **6:** 1221-1228

Shiozaki EN, Chai J, Rigotti DJ, Riedl SJ, Li P, Srinivasula SM, Alnemri ES, Fairman R, Shi Y (2003) Mechanism of XIAP-mediated inhibition of caspase-9. *Molecular cell* **11:** 519-527

Shiozaki EN, Chai J, Shi Y (2002) Oligomerization and activation of caspase-9, induced by Apaf-1 CARD. *Proceedings of the National Academy of Sciences of the United States of America* **99:** 4197-4202

Slamon DJ, Clark GM, Wong SG, Levin WJ, Ullrich A, McGuire WL (1987) Human breast cancer: correlation of relapse and survival with amplification of the HER-2/neu oncogene. *Science* **235:** 177-182

Slamon DJ, Godolphin W, Jones LA, Holt JA, Wong SG, Keith DE, Levin WJ, Stuart SG, Udove J, Ullrich A, et al. (1989) Studies of the HER-2/neu proto-oncogene in human breast and ovarian cancer. *Science* **244:** 707-712

Sommer C, Gerlich DW (2013) Machine learning in cell biology - teaching computers to recognize phenotypes. *Journal of cell science* **126:** 5529-5539

Son JK, Varadarajan S, Bratton SB (2010) TRAIL-activated stress kinases suppress apoptosis through transcriptional upregulation of MCL-1. *Cell death and differentiation* **17:** 1288-1301

Song JH, Tse MC, Bellail A, Phuphanich S, Khuri F, Kneteman NM, Hao C (2007) Lipid rafts and nonrafts mediate tumor necrosis factor related apoptosis-inducing ligand induced apoptotic and nonapoptotic signals in non small cell lung carcinoma cells. *Cancer research* **67:** 6946-6955

Song K, Chen Y, Goke R, Wilmen A, Seidel C, Goke A, Hilliard B, Chen Y (2000) Tumor necrosis factor-related apoptosis-inducing ligand (TRAIL) is an inhibitor of autoimmune inflammation and cell cycle progression. *The Journal of experimental medicine* **191:** 1095-1104

Soria JC, Mark Z, Zatloukal P, Szima B, Albert I, Juhasz E, Pujol JL, Kozielski J, Baker N, Smethurst D, Hei YJ, Ashkenazi A, Stern H, Amler L, Pan Y, Blackhall F (2011) Randomized phase II study of dulanermin in combination with paclitaxel, carboplatin, and bevacizumab in advanced non-small-cell lung cancer. *Journal of clinical oncology : official journal of the American Society of Clinical Oncology* **29:** 4442-4451

Sperandio S, de Belle I, Bredesen DE (2000) An alternative, nonapoptotic form of programmed cell death. *Proceedings of the National Academy of Sciences of the United States of America* **97:** 14376-14381

Sreekumar A, Nyati MK, Varambally S, Barrette TR, Ghosh D, Lawrence TS, Chinnaiyan AM (2001) Profiling of cancer cells using protein microarrays: discovery of novel radiation-regulated proteins. *Cancer research* **61:** 7585-7593

Srinivasula SM, Hegde R, Saleh A, Datta P, Shiozaki E, Chai J, Lee RA, Robbins PD, Fernandes-Alnemri T, Shi Y, Alnemri ES (2001) A conserved XIAP-interaction motif in caspase-9 and Smac/DIABLO regulates caspase activity and apoptosis. *Nature* **410:** 112-116

Stern HM, Padilla M, Wagner K, Amler L, Ashkenazi A (2010) Development of immunohistochemistry assays to assess GALNT14 and FUT3/6 in clinical trials of dulanermin and drozitumab. *Clinical cancer research : an official journal of the American Association for Cancer Research* **16:** 1587-1596

Stolpmann K, Brinkmann J, Salzmann S, Genkinger D, Fritsche E, Hutzler C, Wajant H, Luch A, Henkler F (2012) Activation of the aryl hydrocarbon receptor sensitises human keratinocytes for CD95L- and TRAIL-induced apoptosis. *Cell death & disease* **3:** e388

Storey NM, Gomez-Angelats M, Bortner CD, Armstrong DL, Cidlowski JA (2003) Stimulation of Kv1.3 potassium channels by death receptors during apoptosis in Jurkat T lymphocytes. *The Journal of biological chemistry* **278:** 33319-33326

Stuhmer W, Alves F, Hartung F, Zientkowska M, Pardo LA (2006) Potassium channels as tumour markers. *FEBS letters* **580:** 2850-2852

Suzuki Y, Nakabayashi Y, Nakata K, Reed JC, Takahashi R (2001) X-linked inhibitor of apoptosis protein (XIAP) inhibits caspase-3 and -7 in distinct modes. *The Journal of biological chemistry* **276:** 27058-27063

Szabo I, Bock J, Grassme H, Soddemann M, Wilker B, Lang F, Zoratti M, Gulbins E (2008) Mitochondrial potassium channel Kv1.3 mediates Bax-induced apoptosis in lymphocytes. *Proceedings of the National Academy of Sciences of the United States of America* **105:** 14861-14866

Szabo I, Bock J, Jekle A, Soddemann M, Adams C, Lang F, Zoratti M, Gulbins E (2005) A novel potassium channel in lymphocyte mitochondria. *The Journal of biological chemistry* **280:** 12790-12798

Szabo I, Gulbins E, Apfel H, Zhang X, Barth P, Busch AE, Schlottmann K, Pongs O, Lang F (1996) Tyrosine phosphorylation-dependent suppression of a voltage-gated K+ channel in T lymphocytes upon Fas stimulation. *The Journal of biological chemistry* **271:** 20465-20469

Szabo I, Soddemann M, Leanza L, Zoratti M, Gulbins E (2011) Single-point mutations of a lysine residue change function of Bax and Bcl-xL expressed in Bax- and Bak-less mouse embryonic fibroblasts: novel insights into the molecular mechanisms of Bax-induced apoptosis. *Cell death and differentiation* **18:** 427-438

Szabo I, Zoratti M, Gulbins E (2010) Contribution of voltage-gated potassium channels to the regulation of apoptosis. *FEBS letters* **584:** 2049-2056

Szegezdi E, Reis CR, van der Sloot AM, Natoni A, O'Reilly A, Reeve J, Cool RH, O'Dwyer M, Knapper S, Serrano L, Quax WJ, Samali A (2011) Targeting AML through DR4 with a novel variant of rhTRAIL. *Journal of cellular and molecular medicine* **15:** 2216-2231

Takeda K, Hayakawa Y, Smyth MJ, Kayagaki N, Yamaguchi N, Kakuta S, Iwakura Y, Yagita H, Okumura K (2001a) Involvement of tumor necrosis factor-related apoptosis-inducing ligand in surveillance of tumor metastasis by liver natural killer cells. *Nature medicine* **7:** 94-100

Takeda K, Smyth MJ, Cretney E, Hayakawa Y, Yamaguchi N, Yagita H, Okumura K (2001b) Involvement of tumor necrosis factor-related apoptosis-inducing ligand in NK cell-mediated and IFN-gamma-dependent suppression of subcutaneous tumor growth. *Cellular immunology* **214:** 194-200

Tarca AL, Carey VJ, Chen XW, Romero R, Draghici S (2007) Machine learning and its applications to biology. *PLoS computational biology* **3:** e116

Tata JR (1966) Requirement for RNA and protein synthesis for induced regression of the tadpole tail in organ culture. *Developmental biology* **13:** 77-94

Thompson CB (1995) Apoptosis in the pathogenesis and treatment of disease. *Science* **267:** 1456-1462

Timmer JC, Salvesen GS (2007) Caspase substrates. *Cell death and differentiation* **14:** 66-72

Tinel A, Tschopp J (2004) The PIDDosome, a protein complex implicated in activation of caspase-2 in response to genotoxic stress. *Science* **304:** 843-846

Ting JP, Lovering RC, Alnemri ES, Bertin J, Boss JM, Davis BK, Flavell RA, Girardin SE, Godzik A, Harton JA, Hoffman HM, Hugot JP, Inohara N, Mackenzie A, Maltais LJ, Nunez G, Ogura Y, Otten LA, Philpott D, Reed JC, Reith W, Schreiber S, Steimle V, Ward PA (2008) The NLR gene family: a standard nomenclature. *Immunity* **28:** 285-287

Toole MJ, Kidwell KM, Van Poznak C (2014) Oncotype dx results in multiple primary breast cancers. *Breast cancer : basic and clinical research* **8:** 1-6

Truneh A, Sharma S, Silverman C, Khandekar S, Reddy MP, Deen KC, McLaughlin MM, Srinivasula SM, Livi GP, Marshall LA, Alnemri ES, Williams WV, Doyle ML (2000) Temperature-sensitive differential affinity of TRAIL for its receptors. DR5 is the highest affinity receptor. *The Journal of biological chemistry* **275:** 23319-23325

Vaculova A, Hofmanova J, Soucek K, Kozubik A (2006) Different modulation of TRAIL-induced apoptosis by inhibition of pro-survival pathways in TRAIL-sensitive and TRAIL-resistant colon cancer cells. *FEBS letters* **580:** 6565-6569

Valencia-Cruz G, Shabala L, Delgado-Enciso I, Shabala S, Bonales-Alatorre E, Pottosin, II, Dobrovinskaya OR (2009) K(bg) and Kv1.3 channels mediate potassium efflux in the early phase of apoptosis in Jurkat T lymphocytes. *American journal of physiology Cell physiology* **297:** C1544-1553

Vanlangenakker N, Vanden Berghe T, Krysko DV, Festjens N, Vandenabeele P (2008) Molecular mechanisms and pathophysiology of necrotic cell death. *Current molecular medicine* **8:** 207-220

Varfolomeev E, Maecker H, Sharp D, Lawrence D, Renz M, Vucic D, Ashkenazi A (2005) Molecular determinants of kinase pathway activation by Apo2 ligand/tumor necrosis factor-related apoptosis-inducing ligand. *The Journal of biological chemistry* **280:** 40599-40608

Varfolomeev E, Vucic D (2008) (Un)expected roles of c-IAPs in apoptotic and NFkappaB signaling pathways. *Cell cycle* **7:** 1511-1521

Vaux DL, Silke J (2003) Mammalian mitochondrial IAP binding proteins. *Biochemical and biophysical research communications* **304:** 499-504

Ventura JJ, Hubner A, Zhang C, Flavell RA, Shokat KM, Davis RJ (2006) Chemical genetic analysis of the time course of signal transduction by JNK. *Molecular cell* **21:** 701-710

Vercammen D, Beyaert R, Denecker G, Goossens V, Van Loo G, Declercq W, Grooten J, Fiers W, Vandenabeele P (1998a) Inhibition of caspases increases the

sensitivity of L929 cells to necrosis mediated by tumor necrosis factor. *The Journal of experimental medicine* **187:** 1477-1485

Vercammen D, Brouckaert G, Denecker G, Van de Craen M, Declercq W, Fiers W, Vandenabeele P (1998b) Dual signaling of the Fas receptor: initiation of both apoptotic and necrotic cell death pathways. *The Journal of experimental medicine* **188:** 919-930

Von Pawel J HJ, Spigel DR, Dediu M, Reck M, Cebotaru CL (2010) A randomized phase II trial of mapatumumab, a TRAIL-R1 agonist monoclonal antibody, in combination with carboplatin and paclitaxel in patients with advanced NSCLC. *Journal of clinical oncology : official journal of the American Society of Clinical Oncology*

Voortman J, Resende TP, Abou El Hassan MA, Giaccone G, Kruyt FA (2007) TRAIL therapy in non-small cell lung cancer cells: sensitization to death receptor-mediated apoptosis by proteasome inhibitor bortezomib. *Molecular cancer therapeutics* **6:** 2103-2112

Wagner KW, Punnoose EA, Januario T, Lawrence DA, Pitti RM, Lancaster K, Lee D, von Goetz M, Yee SF, Totpal K, Huw L, Katta V, Cavet G, Hymowitz SG, Amler L, Ashkenazi A (2007) Death-receptor O-glycosylation controls tumor-cell sensitivity to the proapoptotic ligand Apo2L/TRAIL. *Nature medicine* **13:** 1070-1077

Wajant H, Moosmayer D, Wuest T, Bartke T, Gerlach E, Schonherr U, Peters N, Scheurich P, Pfizenmaier K (2001) Differential activation of TRAIL-R1 and -2 by soluble and membrane TRAIL allows selective surface antigen-directed activation of TRAIL-R2 by a soluble TRAIL derivative. *Oncogene* **20:** 4101-4106

Wakelee HA, Patnaik A, Sikic BI, Mita M, Fox NL, Miceli R, Ullrich SJ, Fisher GA, Tolcher AW (2010) Phase I and pharmacokinetic study of lexatumumab (HGS-ETR2) given every 2 weeks in patients with advanced solid tumors. *Annals of oncology : official journal of the European Society for Medical Oncology / ESMO* **21:** 376-381

Walczak H, Degli-Esposti MA, Johnson RS, Smolak PJ, Waugh JY, Boiani N, Timour MS, Gerhart MJ, Schooley KA, Smith CA, Goodwin RG, Rauch CT (1997) TRAIL-R2: a novel apoptosis-mediating receptor for TRAIL. *The EMBO journal* **16:** 5386-5397

Walczak H, Miller RE, Ariail K, Gliniak B, Griffith TS, Kubin M, Chin W, Jones J, Woodward A, Le T, Smith C, Smolak P, Goodwin RG, Rauch CT, Schuh JC, Lynch DH (1999) Tumoricidal activity of tumor necrosis factor-related apoptosis-inducing ligand in vivo. *Nature medicine* **5:** 157-163

Wang H, Zhang Y, Cao L, Han H, Wang J, Yang B, Nattel S, Wang Z (2002) HERG K+ channel, a regulator of tumor cell apoptosis and proliferation. *Cancer research* **62:** 4843-4848

Wang X, Xiao AY, Ichinose T, Yu SP (2000) Effects of tetraethylammonium analogs on apoptosis and membrane currents in cultured cortical neurons. *The Journal of pharmacology and experimental therapeutics* **295:** 524-530

Wang Z (2004) Roles of K+ channels in regulating tumour cell proliferation and apoptosis. *Pflugers Archiv : European journal of physiology* **448:** 274-286

Wei L, Yu SP, Gottron F, Snider BJ, Zipfel GJ, Choi DW (2003) Potassium channel blockers attenuate hypoxia- and ischemia-induced neuronal death in vitro and in vivo. *Stroke; a journal of cerebral circulation* **34:** 1281-1286

Weldon CB, Parker AP, Patten D, Elliott S, Tang Y, Frigo DE, Dugan CM, Coakley EL, Butler NN, Clayton JL, Alam J, Curiel TJ, Beckman BS, Jaffe BM, Burow ME (2004) Sensitization of apoptotically-resistant breast carcinoma cells to TNF and TRAIL by inhibition of p38 mitogen-activated protein kinase signaling. *International journal of oncology* **24:** 1473-1480

Werneburg NW, Guicciardi ME, Bronk SF, Kaufmann SH, Gores GJ (2007) Tumor necrosis factor-related apoptosis-inducing ligand activates a lysosomal pathway of apoptosis that is regulated by Bcl-2 proteins. *The Journal of biological chemistry* **282:** 28960-28970

Werner H, Bruchim I (2012) IGF-1 and BRCA1 signalling pathways in familial cancer. *The lancet oncology* **13:** e537-544

Wiener ALaM (2002) Classification and Regression by randomForest. *R News* **2:** 18-22

Wilbaux M, Henin E, Oza A, Colomban O, Pujade-Lauraine E, Freyer G, Tod M, You B (2014) Prediction of tumour response induced by chemotherapy using modelling of CA-125 kinetics in recurrent ovarian cancer patients. *British journal of cancer*

Wiley SR, Schooley K, Smolak PJ, Din WS, Huang CP, Nicholl JK, Sutherland GR, Smith TD, Rauch C, Smith CA, et al. (1995) Identification and characterization of a new member of the TNF family that induces apoptosis. *Immunity* **3:** 673-682

Wong WW, Gentle IE, Nachbur U, Anderton H, Vaux DL, Silke J (2010) RIPK1 is not essential for TNFR1-induced activation of NF-kappaB. *Cell death and differentiation* **17:** 482-487

Wong WW, Puthalakath H (2008) Bcl-2 family proteins: the sentinels of the mitochondrial apoptosis pathway. *IUBMB life* **60:** 390-397

Wu GS, Burns TF, McDonald ER, 3rd, Jiang W, Meng R, Krantz ID, Kao G, Gan DD, Zhou JY, Muschel R, Hamilton SR, Spinner NB, Markowitz S, Wu G, el-Deiry WS (1997) KILLER/DR5 is a DNA damage-inducible p53-regulated death receptor gene. *Nature genetics* **17:** 141-143

Wulff H, Castle NA, Pardo LA (2009) Voltage-gated potassium channels as therapeutic targets. *Nature reviews Drug discovery* **8:** 982-1001

Wyllie AH, Kerr JF, Currie AR (1980) Cell death: the significance of apoptosis. *International review of cytology* **68:** 251-306

Xu J, Zhou JY, Wei WZ, Wu GS (2010) Activation of the Akt survival pathway contributes to TRAIL resistance in cancer cells. *PloS one* **5:** e10226

Yang JY, Zong CS, Xia W, Yamaguchi H, Ding Q, Xie X, Lang JY, Lai CC, Chang CJ, Huang WC, Huang H, Kuo HP, Lee DF, Li LY, Lien HC, Cheng X, Chang KJ, Hsiao CD, Tsai FJ, Tsai CH, Sahin AA, Muller WJ, Mills GB, Yu D, Hortobagyi GN, Hung MC (2008) ERK promotes tumorigenesis by inhibiting FOXO3a via MDM2-mediated degradation. *Nature cell biology* **10:** 138-148

Yao X, Kwan HY (1999) Activity of voltage-gated K+ channels is associated with cell proliferation and Ca2+ influx in carcinoma cells of colon cancer. *Life sciences* **65:** 55-62

Yee L BH, Kozloff M, Wainberg Z, Pao M, Skettino S (2009) Phase Ib study of recombinant human Apo2L/TRAIL plus irinotecan and cetuximab or FOLFIRI in metastatic colorectal cancer (mCRC) patients (pts): preliminary results. *J Clin*

Oncol Rep

Yu L, Alva A, Su H, Dutt P, Freundt E, Welsh S, Baehrecke EH, Lenardo MJ (2004) Regulation of an ATG7-beclin 1 program of autophagic cell death by caspase-8. *Science* **304:** 1500-1502

Yu SP (2003) Regulation and critical role of potassium homeostasis in apoptosis. *Progress in neurobiology* **70:** 363-386

Yu SP, Yeh CH, Sensi SL, Gwag BJ, Canzoniero LM, Farhangrazi ZS, Ying HS, Tian M, Dugan LL, Choi DW (1997) Mediation of neuronal apoptosis by enhancement of outward potassium current. *Science* **278:** 114-117

Yuan J, Kroemer G (2010) Alternative cell death mechanisms in development and beyond. *Genes & development* **24:** 2592-2602

Yuan J, Shaham S, Ledoux S, Ellis HM, Horvitz HR (1993) The C. elegans cell death gene ced-3 encodes a protein similar to mammalian interleukin-1 beta-converting enzyme. *Cell* **75:** 641-652

Yuan J, Yankner BA (2000) Apoptosis in the nervous system. *Nature* **407:** 802-809

Yuan XJ, Wang J, Juhaszova M, Gaine SP, Rubin LJ (1998) Attenuated K+ channel gene transcription in primary pulmonary hypertension. *Lancet* **351:** 726-727

Yue HH, Diehl GE, Winoto A (2005) Loss of TRAIL-R does not affect thymic or intestinal tumor development in p53 and adenomatous polyposis coli mutant mice. *Cell death and differentiation* **12:** 94-97

Zauli G, Sancilio S, Cataldi A, Sabatini N, Bosco D, Di Pietro R (2005) PI-3K/Akt and NF-kappaB/IkappaBalpha pathways are activated in Jurkat T cells in response to TRAIL treatment. *Journal of cellular physiology* **202:** 900-911

Zerafa N, Westwood JA, Cretney E, Mitchell S, Waring P, Iezzi M, Smyth MJ (2005) Cutting edge: TRAIL deficiency accelerates hematological malignancies. *Journal of immunology* **175:** 5586-5590

Zhang X, Tang N, Hadden TJ, Rishi AK (2011) Akt, FoxO and regulation of apoptosis. *Biochimica et biophysica acta* **1813:** 1978-1986

Zhang XD, Borrow JM, Zhang XY, Nguyen T, Hersey P (2003) Activation of ERK1/2 protects melanoma cells from TRAIL-induced apoptosis by inhibiting Smac/DIABLO release from mitochondria. *Oncogene* **22:** 2869-2881

Zheng SJ, Jiang J, Shen H, Chen YH (2004) Reduced apoptosis and ameliorated listeriosis in TRAIL-null mice. *Journal of immunology* **173:** 5652-5658

Zitzmann K, de Toni E, von Ruden J, Brand S, Goke B, Laubender RP, Auernhammer CJ (2011) The novel Raf inhibitor Raf265 decreases Bcl-2 levels and confers TRAIL-sensitivity to neuroendocrine tumour cells. *Endocrine-related cancer* **18:** 277-285